

THE CONTRIBUTION OF MECHANICAL EFFECTS TO VENTRICULAR
ARRHYTHMIAS DURING ACUTE REGIONAL ISCHEMIA

by

Tarek I. Lawen

Submitted in partial fulfilment of requirements

for the degree of Master of Science

at

Dalhousie University

Halifax, Nova Scotia

July 2015

© Copyright by Tarek I. Lawen, 2015

TABLE OF CONTENTS

List of Figures.....	vi
Abstract.....	viii
List of Abbreviations Used.....	ix
Acknowledgements.....	x
Chapter 1: Introduction.....	1
1.1. Acute Regional Ischemia and Sudden Cardiac Death.....	1
1.1.1. Mechanisms of sudden cardiac death.....	2
1.1.2. Role of acute regional ischemia in sudden cardiac death.....	3
1.2. Acute Regional Ischemia and Altered Electro-Mechanical Activity.....	3
1.2.1. Changes in ion concentrations and currents, action potential morphology, and tissue activation.....	4
1.2.1.1. Hyperkalemia.....	4
(A) Mechanisms for hyperkalemia.....	5
(B) Effects of hyperkalemia on ion channel activity.....	6
(C) Effects of hyperkalemia on cardiac action potential.....	6
1.2.1.2. Acidosis.....	6
(A) Mechanisms for acidosis.....	7
(B) Effects of acidosis on ion channel activity.....	7
(C) Effects of acidosis on cardiac action potential.....	8
1.2.1.3. Increased $[Na^+]_i$	8
(A) Mechanisms for increased $[Na^+]_i$	8
(B) Effects of increased $[Na^+]_i$ on ion channel activity.....	9

(C) Effects of increased $[Na^+]_i$ on cardiac action potential.....	9
1.2.1.4. Increased cytoplasmic Ca^{2+}	9
(A) Mechanisms for increased cytoplasmic Ca^{2+}	10
(B) Effects of increased cytoplasmic Ca^{2+} on cardiac action potential.....	11
1.2.2. Changes in mechanical function.....	11
1.2.2.1. Mechanisms for changes in mechanical function.....	12
1.2.2.2. Heterogenous mechanical function during ischemia.....	12
1.3. Acute Regional Ischemia and Arrhythmias.....	13
1.3.1. Arrhythmic triggers and substrates.....	14
1.3.1.1. Ectopic triggers.....	14
1.3.1.2. Substrates for reentry.....	15
1.3.2. Phase 1a arrhythmias.....	16
1.3.3. Phase 1b arrhythmias.....	17
1.4. Mechano-Electric Coupling and Arrhythmias.....	18
1.4.1. Effects of mechano-electric coupling on ventricular electrophysiology.....	22
1.4.2. Evidence for a role of mechano-electric coupling in ventricular arrhythmia.....	23
1.5. Mechano-Electric Coupling, Acute Regional Ischemia and Arrhythmias.....	24
1.5.1. Experimental evidence for mechanically-induced phase 1b arrhythmias:	
Coronel <i>et al.</i>	25
1.5.2. Computational evidence for mechanically-induced phase 1b arrhythmias:	
Jie <i>et al.</i>	29
1.6. Objectives.....	32
Chapter 2: Methods.....	33

2.1. Choice of Experimental Animal.....	33
2.2. Heart Isolation and Langendorff-Perfusion.....	33
2.3. Instrumentation of the Isolated Heart.....	34
2.4. Voltage Optical Mapping.....	35
2.5. Experimental Protocol.....	39
2.6. Experimental Groups.....	40
2.7. Optical Mapping Analysis.....	40
2.8. Quantification of Arrhythmias.....	41
2.9. Measurement of Ischemic Volume and Cell Necrosis.....	42
2.10. Local Perfusion Experiments.....	42
Chapter 3: Results.....	44
3.1. Aim 1: Small Animal Isolated Heart Model of Acute Regional Ischemia.....	44
3.1.1. Hemodynamic and tissue effects of coronary artery ligation.....	44
3.1.2. Electrophysiological effects of coronary artery ligation.....	48
3.2. Aim 2: The Importance of Ventricular Load and Contraction for Arrhythmogenesis during Acute Regional Ischemia in the Isolated Rabbit Heart.....	55
3.2.1. Effects of coronary artery ligation across the experimental groups.....	55
3.2.2. Incidence of arrhythmias across the experimental groups.....	55
3.2.3. Origin of ischemia-induced PVE in the Loaded isolated rabbit heart.....	59
3.3. Aim 3: Effects of Independent Changes in Regional Mechanical Activity.....	63
Chapter 4: Discussion.....	66
4.1. Overview of Key Findings.....	66
4.2. Choice of Experimental Model.....	67

4.2.1. Rabbit versus other small animal models.....	67
4.2.2. Physiological pacing rate and ischemic volume-based exclusion criteria.....	69
4.3. Electrophysiological Effects of Regional Ischemia.....	70
4.4. Incidence of Arrhythmias.....	71
4.5. Origin of Arrhythmias.....	71
4.6. Necessity <i>versus</i> Sufficiency of Mechanical Effects in Arrhythmia Induction.....	73
4.7. Mechanisms Underlying the Mechanical Contribution to Arrhythmias during Acute Regional Ischemia.....	74
4.7.1. SAC _{NS}	74
4.7.2. Stretch-induced changes of intracellular Ca ²⁺ -handling.....	76
(A) Non-uniform contraction and Ca ²⁺ waves.....	77
(B) Stretch and reactive oxygen species-induced Ca ²⁺ -release.....	78
(C) Inhibition of arrhythmias by Ca ²⁺ chelators.....	79
(D) Inhibition of arrhythmias by Na ⁺ /Ca ²⁺ -exchanger antagonists.....	79
4.7.3. Effects on metabolism.....	80
4.8. Conclusion & Future Directions.....	81
References.....	83
Appendix: Copyright Permissions.....	117

LIST OF FIGURES

Figure 1.1: Diagram of mechano-electric coupling.....	21
Figure 1.2: Average incidence of arrhythmias through 60 min ischemia.....	27
Figure 1.3: Isochronal mapping of ectopic beats.....	28
Figure 1.4: Computational simulation of mechanically-induced arrhythmias.....	31
Figure 2.1: Langendorff-perfused isolated rabbit heart.....	37
Figure 2.2: Schematic of experimental setup.....	38
Figure 3.1: Example of experimental tracing in Loaded heart.....	45
Figure 3.2: Assessing ischemic area using fluorescent microspheres.....	46
Figure 3.3: Assessing myocardial necrosis using TTC staining.....	47
Figure 3.4: Epicardial activation maps of anterior left ventricle.....	49
Figure 3.5: Epicardial APD ₈₀ maps of anterior left ventricle.....	50
Figure 3.6: Average APD ₈₀ values across the ischemic border and with time of ischemia.....	52
Figure 3.7: Summary of ischemic effects on APD ₈₀ across the ischemic border and with time of ischemia.....	53
Figure 3.8: Summary of ischemic effects on dF_n/dt_{max} across the ischemic border and with time of ischemia.....	54
Figure 3.9: Average ischemic volume and coronary flow reduction after coronary artery ligation.....	56
Figure 3.10: Representative example of ECG and LVP traces during arrhythmia.....	57
Figure 3.11: Average incidence of arrhythmias during 60 min of ischemia.....	58
Figure 3.12: Total average incidence of arrhythmias during 60 min of ischemia	

across groups.....61

Figure 3.13: Voltage-optical mapping of epicardial activation sequence.....62

Figure 3.14: Assessing locally-perfused area using fluorescent microspheres.....64

Figure 3.15: Activation maps example of ventricular pressures and
hemodynamics in locally-perfused heart.....65

ABSTRACT

Arrhythmias during acute regional ischemia can cause sudden cardiac death. Our goal was to investigate the mechanical contribution to ventricular arrhythmias in this setting. Experiments were conducted in Langendorff-perfused rabbit hearts. The anterior branch of the left circumflex coronary artery was ligated for 60 min in three groups: (i) physiologically-loaded left ventricle (Loaded); (ii) unloaded left ventricle (Unloaded); and (iii) physiologically-loaded, non-contracting left ventricle (Non-contracting). Loaded hearts had a significantly higher incidence of arrhythmias than Unloaded and Non-contracting hearts, peaking at 30-35 min, with activation often arising from the ischemic border. This suggests mechanical effects during ischemia are necessary for ventricular arrhythmias. To investigate whether altered mechanics are sufficient for arrhythmia induction, hearts were locally perfused with blebbistatin to cause regional loss of contraction. This did not result in arrhythmias, suggesting that mechanical effects are necessary, but not sufficient, for ventricular arrhythmias during acute regional ischemia in isolated rabbit hearts.

LIST OF ABBREVIATIONS USED

ADP	Adenosine Diphosphate
APD ₈₀	Action Potential Duration at 80% Repolarization
ANOVA	Analysis of Variance
AP	Action Potential
ATP	Adenosine Triphosphate
DAD	Delayed Afterdepolarization
dF _n /dt _{max}	Maximum Rate of Membrane Potential Change (nominal units of normalized fluorescence per ms)
EAD	Early Afterdepolarization
ECG	Electrocardiogram
fNADH	NADH Fluorescence
Gd ³⁺	Gadolinium
GsMTx-4	<i>Grammostola spatulata</i> Mechanotoxin-4
MEC	Mechano-Electric Coupling
NADH	Nicotinamide Adenine Dinucleotide
P _i	Phosphate
PVE	Premature Ventricular Excitation
ROS	Reactive Oxygen Species
RyR	Ryanodine Receptor
SAC _{NS}	Cation-Nonselective Stretch-Activated Channel
SAC _K	Potassium-Selective Stretch-Activated Channel
SCD	Sudden Cardiac Death
SERCA	SR Ca ²⁺ -ATPase
SR	Sarcoplasmic Reticulum
TRPC	Transient Receptor Potential Channel
VT	Ventricular Tachyarrhythmia

ACKNOWLEDGEMENTS

Words cannot express my sincere gratitude for my supervisor, mentor and instructor, Dr. Alex Quinn. You have been a constant source of knowledge and inspiration for me in the last few years. You trusted me as your student and as such, I worked in an environment conducive to my independent learning and academic growth. You empower me as a student and for that I am forever grateful to you. I thank you for your patience, your encouragement and for providing me with this opportunity.

I would also like to extend my deepest gratitude to Peter Baumeister, without whom I truly would not be where I am today. You selflessly and significantly contributed to the success of my project and I only wish I could thank you more. You have taught me to work tirelessly and passionately. Thank you for being a friend inside and outside of the lab.

A sincere and special thank you to Rick Livingston for his extensive assistance with my project and for always contributing to a healthy and positive work environment. I would also like to thank the members of my supervisory committee, Dr. Robert Rose, Dr. Stacy O'Blenes and Dr. Xianping Dong for their constructive input, guidance and support throughout my Master's work.

I would also like to acknowledge the important work done by the animal care technicians, who prioritize animal welfare as they ensure the smooth operation of the animal house. Without their training in animal care and handling, my project would not have been possible.

Finally, I would like to thank the Canadian Institute of Health Research, Nova Scotia Health Research Fund and Heart & Stroke Foundation for their generous funding and support.

CHAPTER 1

Introduction

1.1 Acute Regional Ischemia and Sudden Cardiac Death

One Canadian dies every 7 min from heart disease, and it remains the leading cause of death in our country. 30% of all deaths in Canada are attributed to cardiovascular disease (Statistics Canada 2011c). In addition to its terrible emotional and social toll, our nation suffers economically, with over \$20 billion lost annually from our economy in an effort to combat cardiac pathologies (Conference Board of Canada 2011).

Management of cardiovascular disease has steadily improved in recent decades, in large part due to basic science research and innovations in medical technologies and therapies. In the majority of cases, death from a cardiac event is due to the disruption of the normal electrical rhythm of the heart, such that there is loss of its pumping function. Aberrant cardiac electrical rhythms are known as ‘arrhythmias’ and they underlie one of the most common cardiovascular-related deaths in the western world: sudden cardiac death (SCD) (Janse 2003). SCD describes the abrupt and unexpected natural death from a cardiac cause that occurs within a very short time frame in an individual with no prior history of cardiac pathology (Zipes *et al.* 1998; Suvarna 2013). In other words, SCD is the abrupt loss of the pumping function of the heart, which causes a person to quickly lose consciousness and, if left untreated, will lead to death within min. SCD is often a fatal manifestation of undiagnosed coronary heart disease (Zipes *et al.* 1998), and accounts for over 40,000 annual Canadian fatalities (Statistics Canada 2011c).

1.1.1. Mechanisms of sudden cardiac death

Elucidating the underlying etiology of SCD can be quite difficult as 40% of deaths occur out-of-hospital and unwitnessed (Janse 2003; de Vreede Swagemakers *et al.* 1997).

Nonetheless, post-mortem examinations indicate that 80% of SCD victims manifest pre-existing coronary artery disease and its consequent pathologies (*i.e.*, acute myocardial ischemia or post-infarct scarring) (Rubart & Zipes 2005).

The most common electrophysiological events leading to SCD are ventricular tachycardia (abnormal acceleration of ventricular rate and pattern of activation) degenerating into ventricular fibrillation, during which the chaotic and uncoordinated contraction of the ventricles ('fibrillation') fail to effectively eject blood, quickly leading to death (Janse 2003; Rubart & Zipes 2005). It is estimated that ventricular fibrillation causes one-third of sudden cardiac deaths (Cobb *et al.* 2002).

There are many mechanisms through which a tachyarrhythmia may establish itself within the myocardium. The most likely cause of ventricular tachyarrhythmias (VTs) is development and sustenance of a 'reentrant' electrical wave, which describes a continuous wave of excitation that does not extinguish itself, but instead becomes a self-sustaining circuit of excitation (Doddall & Ideker 2014). Interruption of this reentrant circuit may re-synchronize the myocardium, such that the tachyarrhythmia ceases and normal rhythm is reestablished. However, it is possible that break of the reentrant circuit may lead to increasingly chaotic excitation, degenerating into potentially lethal ventricular fibrillation (Doddall & Ideker 2014).

1.1.2. Role of acute regional ischemia in sudden cardiac death

As mentioned before, 80% of SCD victims are found to exhibit preexisting coronary artery disease (Rubart & Zipes 2005). The most common consequence of this pathology is the accumulation of atherosclerotic plaque within the coronary arteries, leading to a drastic reduction in the delivery of oxygen and nutrients to an area of the myocardium, causing a mismatch between oxygen supply and demand at the tissue level known as ‘ischemia’. Ischemia may be chronic, however, considering that sudden cardiac death often occurs within an hour of the onset of symptoms, an acute ischemic insult in many cases most likely precipitates the fatal event (Janse 2003).

Moreover, atherosclerotic blockage of a major coronary artery supplying a region of the myocardium is sufficient to cause the lethal acute ‘regional’ ischemic attack underlying SCD (Myerburg 2014). Thus, events associated with acute regional ischemia, and specifically how they induce lethal ventricular arrhythmias, are of considerable clinical importance. Yet, the nature of the immediate precipitating event that triggers these fatal arrhythmias during acute regional ischemia in an otherwise stable patient remains a major unanswered question.

1.2 Acute Regional Ischemia and Altered Electro-Mechanical Activity

As mentioned before, acute regional ischemia occurs when there is an occlusion of a coronary artery, causing a significant reduction in the supply of oxygen- and nutrient-rich blood to a region of myocardium. There is compelling evidence that acute myocardial ischemia is one of the most important causes of ventricular arrhythmias in humans (Janse & Wit 1989).

An ischemic attack has profound effects on the electrophysiological properties of cardiac cells, as well as on cardiac mechanics, all of which may contribute to the development of deadly ventricular arrhythmias (Carmeliet 1999).

1.2.1 Changes in ion concentrations and currents, action potential morphology and tissue activation

Cessation of coronary blood flow causes a block of oxidative metabolism, a drop in ATP production, altered distribution of ions such as K^+ , Na^+ , Ca^{2+} and H^+ , as well as reduced washout of metabolites and waste. Ultimately, these changes have profound electrophysiological consequences at the subcellular and tissue levels. To thoroughly understand how these alterations occur, it is best to understand the mechanism for altered subcellular ion distribution, how this influences ion channel activity, and ultimately affects action potential morphology and tissue-level electrophysiology.

1.2.1.1 Hyperkalemia

Under aerobic conditions, $[K^+]_i$ is high and $[K^+]_o$ is low. Any passive potassium efflux is compensated by active reuptake of potassium *via* the Na^+/K^+ -ATPase. During ischemia, this dynamic equilibrium ceases and extracellular K^+ accumulates, a condition known as hyperkalemia.

During ischemia, $[K^+]_o$ increases in two distinct phases. Immediately after occlusion of a coronary artery, extracellular K^+ accumulates rapidly until reaching a plateau at around 10 min post-occlusion. This is followed by a second slower increase in $[K^+]_o$ between 15 to 30 min post-occlusion (Wilde & Aksnes 1995). $[K^+]_o$ is highest in the center of the ischemic area, compared to either the border zone or healthy myocardium. Transmural

heterogeneity also exists, as extracellular K^+ accumulation is higher in the subepicardium than in the subendocardium (Schaapherder *et al.* 1990).

(A) *Mechanisms for hyperkalemia*

Three main factors contribute to extracellular accumulation of K^+ :

1. Shrinkage of the extracellular space:

Water is osmotically taken up by cells during ischemia due to the increase of osmotically active solutes in the intracellular space. As a result, the extracellular space is restricted as its volume decreases (Tranum-Jensen *et al.* 1981). Small decreases in the extracellular volume will amplify effects of an increased $[K]_o$.

2. Decreased active K^+ influx:

A reduction in Na^+/K^+ -pump activity causes a decreased active K^+ influx (Kléber 1983). Only a moderate inhibition of the pump is needed to increase extracellular K^+ . Ischemic conditions moderately inhibit Na^+/K^+ -pump function by increasing oxygen free radicals (Shattock & Matsuura 1993) and decreasing metabolic energy needed to fuel the ATPase (Glitsch & Tappe, 1995). The fall in $[ATP]$ is not the main reason for decreased pump function, but instead it is the increased $[ADP]$ and $[P_i]$ that decrease ATP hydrolysis.

3. Increased passive K^+ efflux:

There is also an increased passive K^+ efflux during ischemia. Some K^+ leaves the cell *via* the KCl cotransporter, which is stimulated by an increased cell volume as occurs during ischemia (Yan *et al.* 1995). Another channel responsible for K^+ efflux is the ATP-

inactivated K^+ channel, which increases K^+ conductance as $[ATP]$ falls (as it does during ischemia) (Friedrich *et al.* 1990).

(B) Effects of hyperkalemia on ion channel activity

The effect that increased $[K^+]_o$ has on other channels is mainly through its depolarization of the cell membrane (Carmeliet 1999). At first hyperkalemia-induced depolarization of the membrane causes an increase in cell excitability, but once enhanced, hyperkalemia causes decreased excitability, increased refractoriness, and conduction slowing or block (Kléber *et al.* 1986) by causing a partial or complete inactivation of the fast Na^+ channel, as well as slowed recovery from normal inactivation.

(C) Effects of hyperkalemia on the cardiac action potential

At the cell level, hyperkalemia causes membrane depolarization and a reduction in action potential amplitude, upstroke velocity, and duration (Dominguez & Fozzard 1970). The decrease in action potential amplitude and upstroke velocity is mainly due to the depolarized membrane caused by hyperkalemia and the consequent inactivation of Na^+ channels and decreased Na^+ conductance (Dominguez & Fozzard 1970). The decrease in action potential duration on the other hand is due to increased K^+ efflux from the cell *via* I_{K1} and I_{Kr} (Kléber *et al.* 1986). Membrane depolarization prolongs the recovery from inactivation of Na^+ channels and this results in the development of post-repolarization refractoriness (Janse & Wit 1989).

1.2.1.2 Acidosis

Under normal perfusion and oxygenation, the pH of the intracellular milieu is slightly more acidic than the extracellular pH. During ischemia, a lack of CO_2 washout, combined

with increased production of protons causes both the intracellular and extracellular pH to shift in the acidic direction (Clarke *et al.* 1993). In aerobic conditions, the constant production of protons is compensated by CO₂ elimination, Na⁺/H⁺ exchange and Na⁺-HCO₃ co-transport (Kaila & Vaughan-Jones 1987). The latter two mechanisms are tightly coupled to Na⁺/K⁺-ATPase activity. In ischemic conditions, reduced CO₂ elimination and the functional depression of the Na⁺/K⁺-ATPase contribute to the increased proton concentration and thus the fall in pH.

(A) Mechanisms for acidosis

There are two main mechanisms by which intracellular proton concentration is increased:

1. Anaerobic cell respiration:

Anaerobic catabolism of glucose results in a net H⁺ production. During ischemia, ATP production shifts from mitochondrial pathways to fermentation pathways in the cytoplasm. Fermentation is followed by an obligatory rise in protons (Allen *et al.* 1985).

2. Insufficient proton removal:

Under normal conditions, a large amount of acidic content is removed by CO₂ elimination *via* simple diffusion. In ischemic conditions, glycolytic pathways form acidic end-products, which increase intracellular proton production. The lack of CO₂ washout causes a drop in intracellular pH (Watson *et al.* 1984).

(B) Effects of acidosis on ion channel activity

Most plasma membrane currents are inhibited by acidosis. Increased acidity causes a major shift in ion channel activation-inactivation kinetics, ion conductance, and

permeability (Xiao *et al.* 1995; Prod'hom *et al.* 1989). Among the major channels and currents inhibited by acidosis are: I_{Na} , $I_{Ca,L}$, I_{Kr} , I_{K1} , and the Na^+/Ca^+ -exchanger (Doering & Lederer 1993; Philipson *et al.* 1982). Thus acidosis will lead to depressed influx of Na^+ and Ca^+ and efflux of K^+ . Acidosis also has an inhibitory effect on gap junctions and may facilitate their closure, slowing conduction or causing block (Noma & Tsuboi 1987).

(C) Effects of acidosis on the cardiac action potential

At the cell level, acidotic effects translate into a depolarized membrane, a reduction in upstroke velocity, decreased action potential duration, and increased refractoriness (Coraboeuf & Coulombe 1980).

1.2.1.3 Increased $[Na^+]_i$

Under normal aerobic conditions, the cell actively maintains a very low $[Na^+]_i$ and a very high $[Na^+]_o$. This dynamic imbalance is mostly due to the function of the Na^+/K^+ -ATPase (Carmeliet 1999).

(A) Mechanisms for increased $[Na^+]_i$

During ischemia, there is a substantial increase in $[Na^+]_i$ caused by:

1. A reduced active efflux of Na^+ :

A reduced outward movement of Na^+ occurs due to inhibition of the Na^+/K^+ -ATPase during ischemia, which can be attributed to a change in the $[ATP]$, $[ADP]$ and $[P_i]$ (Donoso *et al.* 1992). An increased oxidative stress due to the buildup of free oxygen radicals will also depress pump function (Shattock & Matsuura 1993).

2. An increased passive influx of Na^+ :

Inward leak of Na^+ occurs *via* carriers and channels. An important contributor is the Na^+/H^+ -exchanger, which extrudes accumulated protons in exchange of an influx of Na^+ . Thus, acidosis causes an increased $[\text{Na}^+]_i$ through the action of this exchanger (Anderson *et al.* 1991; Pike *et al.* 1993). Inward movement of Na^+ may also occur *via* non-selective cation channels. Non-selective cation channels have been shown to open *via* stretch (Craelius *et al.* 1988), free oxygen radical buildup (Jabr & Cole 1993), and increased intracellular Ca^{2+} (Ehara *et al.* 1988), all changes which occur during early ischemia.

(B) Effects of increased $[\text{Na}^+]_i$ on ion channel activity

The rise in $[\text{Na}^+]_i$ causes the $\text{Na}^+/\text{Ca}^{2+}$ -exchanger to work in the reverse mode and thus causes extrusion of Na^+ for an influx of Ca^{2+} . Thus, increased intracellular Na^+ has been shown to increase the frequency of spontaneous Ca^{2+} release (Diaz *et al.* 1996).

(C) Effects of increased $[\text{Na}^+]_i$ on the cardiac action potential

Increased intracellular Na^+ leads to increased Ca^{2+} influx *via* the reverse mode of $\text{Na}^+/\text{Ca}^{2+}$ -exchanger and thus causes spontaneous release of Ca^{2+} from the sarcoplasmic reticulum (SR). This Ca^{2+} release can lead to depolarization of the membrane and early (EAD) or delayed afterdepolarizations (DAD).

1.2.1.4 Increased cytoplasmic Ca^{2+}

Under normal aerobic conditions, Ca^{2+} concentrations are different in the cytosol, mitochondria, sarcoplasmic reticulum, and nucleus (Piper *et al.* 1993). In each compartment, Ca^{2+} plays a different role. The SR is the main reservoir of intracellular Ca^{2+} in the cardiomyocyte. Proper excitation-contraction coupling depends on a rapid release of Ca^{2+} from the SR, so that free Ca^{2+} may activate myofilaments and cause

contraction. Thus, during diastole (ventricular relaxation), free cytoplasmic Ca^{2+} is very low. Whereas during systole (ventricular contraction), free cytoplasmic Ca^{2+} dramatically increases (ter Keurs 2011).

(A) Mechanisms for increased cytoplasmic Ca^{2+}

During ischemia, cytoplasmic Ca^{2+} becomes elevated. This is mainly due to:

1. Displacement of Ca^{2+} from cytoplasmic binding sites by H^+ :

This occurs early in ischemia, as the intracellular milieu becomes more acidic. Studies have shown that cytoplasmic Ca^{2+} is increased with decreased pH, independent of SR calcium release (Gambassi *et al.* 1993).

2. Increased inward leak through the plasma membrane:

Background channels carrying Ca^{2+} into the cell are activated by radicals and become very active during ischemia (Trafford *et al.* 1997; Kabr & Cole 1995). Inward leak of Ca^{2+} also occurs *via* non-selective cation channels, which are activated by ischemic conditions (Friel & Bean 1988), mechanical stretch (Craelius *et al.* 1988) and increased cytoplasmic Ca^{2+} (Colquhoun *et al.* 1981).

3. Decreased activity of the $\text{Na}^+/\text{Ca}^{2+}$ -exchanger:

This exchanger is the most important mechanism by which Ca^{2+} is removed from the cytoplasm. It is responsible for approximately 70% of Ca^{2+} extrusion (LaMont & Eisner 1996). During ischemia, the $\text{Na}^+/\text{Ca}^{2+}$ -exchanger is less efficient due to the increased $[\text{Na}^+]_i$ and $[\text{H}^+]_i$. Increased $[\text{Na}^+]_i$ promotes the reverse mode of the $\text{Na}^+/\text{Ca}^{2+}$ -exchanger and will thus increase cytoplasmic Ca^{2+} (Haigney *et al.* 1994).

4. Decreased reuptake of Ca^{2+} into the SR:

During ischemia, less Ca^{2+} is stored in the SR. This is due to decreased function of the SR Ca^{2+} -ATPase (SERCA) which works to pump cytoplasmic calcium back into the SR. This effect is mainly due to the drastic reduction in intracellular [ATP] needed to fuel the pump (Griese *et al.* 1988).

(B) *Effects of increased cytoplasmic Ca^{2+} on the cardiac action potential*

Increased cytoplasmic Ca^{2+} facilitates inactivation of $I_{\text{Ca,L}}$ (McDonald *et al.* 1994). As such, enhanced intracellular Ca^{2+} will cause a shortening of the action potential. If calcium levels are heightened the point of Ca^{2+} overload, EADs and DADs may result (Kihara *et al.* 1989). The mechanism underlying an EAD or DAD in this setting is Ca^{2+} -induced Ca^{2+} release from the SR, which induces an inward depolarizing current across the membrane. This depolarizing current is mainly through the $\text{Na}^+/\text{Ca}^{2+}$ -exchanger (Han & Ferrier 1995). Calcium overload also causes closure of gap junctions and thus a reduction in conduction velocity and potential block (De Mello 1975).

1.2.2. Changes in mechanical function

As mentioned before, acute ischemia inhibits oxidative metabolism and thus causes a drop in [ATP] and a simultaneous increase in [ADP] and [P_i]. Ischemia-induced Ca^{2+} overload causes mitochondrial dysfunction, which precipitates the alterations in [ATP] and [ADP]. These subcellular biochemical changes have profound effects on myocardial mechanical function. In general, acutely ischemic myocardium suffers abrupt alterations in transmural fiber strain and decreased fractional shortening during systole (Langer *et al.* 2007).

1.2.2.1. Mechanisms for changes in mechanical function

The main mechanical dysfunctions that occur during ischemia are:

1. Loss of contractility:

Ischemia causes an increase in cytoplasmic Ca^{2+} during diastole and systole. The elevated levels of cytoplasmic Ca^{2+} cause a reduced SR release of calcium, which ultimately leads to a lower activation of myofilaments and thus reduced contraction (Allen & Orchard 1987). Thus, early in ischemia, the under-perfused myocardium suffers a loss of contractility.

2. Rigor contracture:

As ischemia progresses, cytoplasmic Ca^{2+} continues to increase and this causes mitochondrial dysfunction, such that ATP synthase no longer efficiently generates ATP. This, in combination with reduced oxidative metabolism due to hypoxic conditions, causes a decrease in intracellular [ATP] (Carmeliet 1999). Free ATP molecules are required for proper sarcomeric cross-bridge cycling. Therefore, as ATP levels fall, the myosin heads continue binding the active sites of actin proteins *via* ADP and the muscle fiber is unable to relax.

1.2.2.2. Heterogeneous mechanical function during ischemia

As myocytes within the ischemic region begin to have depressed contractility, they become elongated by the actively contracting viable cells surrounding the ischemic tissue. This type of stretch is characterized by an increase in the longitudinal dimension and decrease in the transversal direction (Carmeliet 1999). Therefore, during systolic

shortening of healthy myocardium, there is a paradoxical segment lengthening of the ischemic tissue or at the ischemic border zone (Barrabes *et al.* 2002). Thus, a gradient of contractility is established during acute regional ischemia, where healthy myocardium is mechanically intact and ischemic tissue is mechanically depressed. Consequently, the region between non-contractile ischemic and contractile healthy tissue (*i.e.*, the ischemic border zone) experiences stretch (Allen & Orchard, 1987).

1.3. Acute Regional Ischemia and Arrhythmias

As described above, acute regional ischemia has profound effects on subcellular ion concentrations, ion channel activity, and the cardiac action potential. These changes translate into altered electrical activity at the tissue-level, which can lead to deadly arrhythmias. Ischemia is a dynamic process however, such that these effects progress with time after coronary artery occlusion (Carmeliet 1999). As a result, two distinct phases of arrhythmias have been observed during an acute ischemic attack (phase 1a and 1b) (Smith *et al.* 1995). It is known that the nature of phase 1a and phase 1b arrhythmias are distinctly different, but the mechanisms for either phase of arrhythmias are not completely understood.

Before distinguishing between phase 1a and 1b arrhythmias, it is important to understand the general prerequisites required for the initiation and maintenance of VTs, including ventricular tachycardia and fibrillation. For VTs to occur, two primary conditions need to co-exist: an ectopic focus (trigger) and a stable circuit for reentry (substrate) (Doddall & Ideker 2014).

1.3.1. Arrhythmic triggers and substrates

1.3.1.1 Ectopic triggers

Arrhythmic triggers are ectopic foci that initiate aberrant electrical activity. Triggers are caused either by: (i) abnormal automaticity within the ventricular myocardium or the Purkinje network; or (ii) triggered activity such as premature myocyte depolarization.

1) Abnormal automaticity:

Embryonically, the majority of pre-cursor cardiomyocytes have automaticity and can self-sufficiently diastolically depolarize their membrane *via* I_f (the ‘pacemaker’ current) (Ophthof 2007). As cardiac tissue differentiates, only certain cell-types retain their automaticity, such as sinoatrial node cells, atrioventricular nodal cells, and Purkinje cells (Callewart *et al.* 1984). However, in pathological conditions, some cell may dedifferentiate and regain their automaticity. In certain pathologies, ventricular myocytes may regain automaticity and automatic activity of the atrioventricular node, Purkinje or ventricular cells may cause ectopic foci within the ventricular myocardium.

2) Triggered activity:

There are two types of triggered activity: EADs and DADs. In both cases, early depolarization of the membrane occurs during the plateau or repolarization phases of the cardiac action potential. If this abnormal secondary depolarization occurs during the plateau/early repolarization phase, it is termed an EAD. If the depolarization occurs during late repolarizations, it is a DAD. Mechanistically, both types of activity are thought to be Ca^{2+} -related, *via* early activation of $I_{Ca,L}$, SR Ca^{2+} release, or Ca^{2+} overload activating the Na^+/Ca^{2+} -exchanger (Ming *et al.* 1994). Increased cytoplasmic Ca^{2+} causes

the Na⁺/Ca²⁺-exchanger to extrude 1 Ca²⁺ in exchange for 3 Na⁺ entering the cell. As such, the exchanger is electrogenic and causes depolarization, which can lead to ectopic excitation.

1.3.1.2 Substrates for reentry

Once an ectopic focus is established, a stable functional or anatomical circuit is required to sustain VTs. The stabilizing circuit is considered a substrate and will facilitate the establishment of sustained reentry. Reentry occurs when a wave of excitation follows a circumferential path and is able to re-excite repolarized tissue such that it becomes a self-sustaining circular wave of excitation (Doddall & Ideker 2014). The existence of reentry is dependent on the fulfillment of two conditions: (i) a region of unidirectional block is required whereby an excitation wave is blocked in the anterograde direction but freely passes in the retrograde direction (Quan & Rudy 1990) and (ii) conduction velocity needs to be slow enough and refractory period short enough such that the excitation wave avoids encountering refractory tissue (Carmeliet & Vereecke 2002). If either conduction velocity is too fast, or refractory period too long, the reentrant wave will extinguish itself. Furthermore, a reentrant wave follows a circuit that can be defined by: (i) an anatomical core of inexcitability; or (ii) a functional core of reduced excitability.

1) Anatomical substrate:

In this case, the wave of excitation follows a circular path around an anatomical obstacle that remains inexcitable. Examples of this are post-infarct scars or the right ventricular outflow tract, both of which have dramatically altered excitability and are known to act as substrates for reentrant arrhythmias (Carmeliet & Vereecke 2002).

2) Functional substrate:

Reentrant arrhythmias can also occur without a fixed anatomical substrate (Allessie *et al.* 1977). In “leading circle reentry”, the center of the circle is inexcitable since it is continuously depolarized by centripetal waves originating from the circular excitation. This type of reentrant wave will travel along a functional circuit determined by its wavelength and the electrical properties of the myocardium. Other forms of functional reentry occur when remodeling of gap junctions (during healing of an infarct) causes the myocardium to become inhomogeneously anisotropic. Normally, the myocardium is uniformly anisotropic such that conduction is faster in the longitudinal than in the transverse direction. Uniform anisotropy allows conduction to travel in an organized manner. With remodeling of gap junctions and non-uniform anisotropy, the excitation wave can circulate around a functional line of block and cause “anisotropic reentry”.

1.3.2. Phase 1a arrhythmias

The first wave of ventricular arrhythmias (phase 1a) occurs between 2 and 10 min after complete coronary artery occlusion (Knopf *et al.* 1988). Phase 1a arrhythmias are characteristically of the ventricular tachycardia type and rarely degrade into ventricular fibrillation, and thus mortality during phase 1a is relatively low.

In the period preceding the onset of phase 1a arrhythmias, conduction is slowed in the subepicardial region. Conduction slowing is related to the rise in extracellular K^+ , which causes depolarization of the resting membrane potential and inactivation of Na^+ channels, resulting in decreased upstroke velocity (Pogwizd & Corr 1987). Phase 1a VTs are often

preceded by T-wave alternans, a beat-to-beat variation in the amplitude and shape of the T wave in the electrocardiogram (Coronel *et al.* 1991; Tan *et al.* 1991).

Epicardial mapping studies have demonstrated that once established, phase 1a arrhythmias are 'reentrant' in nature (Pogwizd & Corr 1987). This is supported by electrocardiogram recordings identifying continuous electrical activity between QRS complexes known as 'diastolic bridging', indicative of reentrant arrhythmias (Kiyosue *et al.* 1984).

During phase 1a there is increased dispersion of refractoriness, which is an important factor in establishing unidirectional block to allow reentry to occur. While repolarization is accelerated in the center of the ischemic region; decreasing action potential duration, effective refractory period (ERP) is increased as post-repolarization refractoriness emerges due to hyperkalemia and acidosis. At the border between ischemic and healthy myocardium, however, action potential duration and ERP both shorten. Thus, ERP is increased in the ischemic zone but decreased at the border zone, establishing dispersion in refractoriness, which creates favourable conditions for unidirectional conduction block and reentry.

1.3.3. Phase 1b arrhythmias

Following the phase 1a, there is a short window of relative quiescence where the incidence of arrhythmias is quite low. The second wave of arrhythmias (phase 1b) occurs between 20 and 30 min post-occlusion. Studies suggest that phase 1b arrhythmias are more likely to evolve into VF. Therefore, mortality during phase 1b is higher than it is during phase 1a (Coronel *et al.* 2002). The mechanisms of 1b-type arrhythmias is less

well known. The onset of these delayed arrhythmias are thought to be dependent on an increase in gap junction resistance (closure of gap junctions), a second phase of K^+ increase (Kléber 1983) and accompanying depolarization, worsening of Ca^{2+} overload, and a massive release of endogenous catecholamines (Smith *et al.* 1995).

Studies suggest that arrhythmias seen during phase 1b are non-reentrant in nature, due to the absence of diastolic bridging and completely normal local electrocardiograms (Kaplinsky *et al.* 1979). A thorough mechanistic understanding of this phase of arrhythmias remains elusive.

One potential mechanism, based on recent and compelling evidence, is that changes in myocardial mechanics during ischemia may play an important role in the onset of the phase 1b arrhythmias (Coronel *et al.* 2002). As mentioned previously, ischemia causes a depression in myocardial contractility and contracture rigor. This establishes heterogeneity in mechanics between healthy and ischemic tissue and it has been suggested that this may lead to lethal ventricular arrhythmias by feedback of mechanical effects onto cardiac electrical activity, through a process known as mechano-electric feedback, or more recently mechano-electric coupling (MEC).

1.4. Mechano-Electric Coupling and Arrhythmias

As Figure 1.1 depicts, cardiac mechanics and electrophysiology are intimately linked. This year is the centenary mark of Dr. Bainbridge's pioneering observation that right atrial distension was linked to heart rate in dogs (Bainbridge 1915). Since then, mechanical influences on cardiac electrical activity have been shown clinically and experimentally from the cell to whole organism.

Experimentally, stretch has been shown to increase diastolic depolarization and increase firing rate of sinoatrial nodal cells and tissue and isolated Purkinje fibers (Deck 1964). In fact, it was Ursula Ravens who first used the term mechano-electric feedback (“mechano-elektrische rückkoppelung”) when she demonstrated a positive chronotropic effect of stretch in Purkinje fibers isolated from rhesus monkeys (Kaufmann & Theophile 1967). Today, this is more generally referred to as cardiac mechano-electric coupling (MEC) and comprises an emerging field of cardiovascular research (Kohl *et al.* 2011).

The existence of MEC in human has been shown by various groups, for instance by a decrease in ventricular action potential duration with increased left ventricular pressure (Taggart *et al.* 1988) or during balloon valvuloplasty (Levine *et al.* 1988). A more mechanistic understanding of MEC was first provided through single-channel recordings of stretch-activated ion currents in rat ventricular myocytes (Craelius *et al.* 1988), followed by cloning of mechano-sensitive ion channels in *E. coli* (Sukharev *et al.* 1994). Pharmacological inhibitors of MEC have been identified, which have further provided insight into the role that stretch-activated currents might play in various cardiac pathologies. Early pharmacological studies used gadolinium to block stretch-activated alterations in electrophysiology in the isolated heart (Hansen *et al.* 1991; Bode *et al.* 2000; Kamkin *et al.* 2000), but this has since been replaced by higher-specificity blockers of MEC such as streptomycin and *Grammostola spatulata* mechanotoxin-4 (GsMTx-4), which blocks stretch-induced atrial fibrillation (this is thoroughly reviewed by Caldwell *et al.* 1998 and Reed *et al.* 2014). The molecular identity of cardiac stretch-activated channels, however, still remains elusive. Candidates include transient receptor potential channels (TRPC) (Morato *et al.* 2005) and piezo channels, despite piezo’s apparently

negligible expression in cardiac tissue (Coste *et al.* 2010). MEC may also act through other mechanisms, especially effects on intracellular Ca^{2+} handling, as stretch has been shown to induce spontaneous SR Ca^{2+} release due to ryanodine receptor (RyR) mechano-sensitivity (Iribe & Kohl 2008) and Ca^{2+} surges due to release of Ca^{2+} during relaxation of stretched myofilaments (ter Keurs *et al.* 2008).

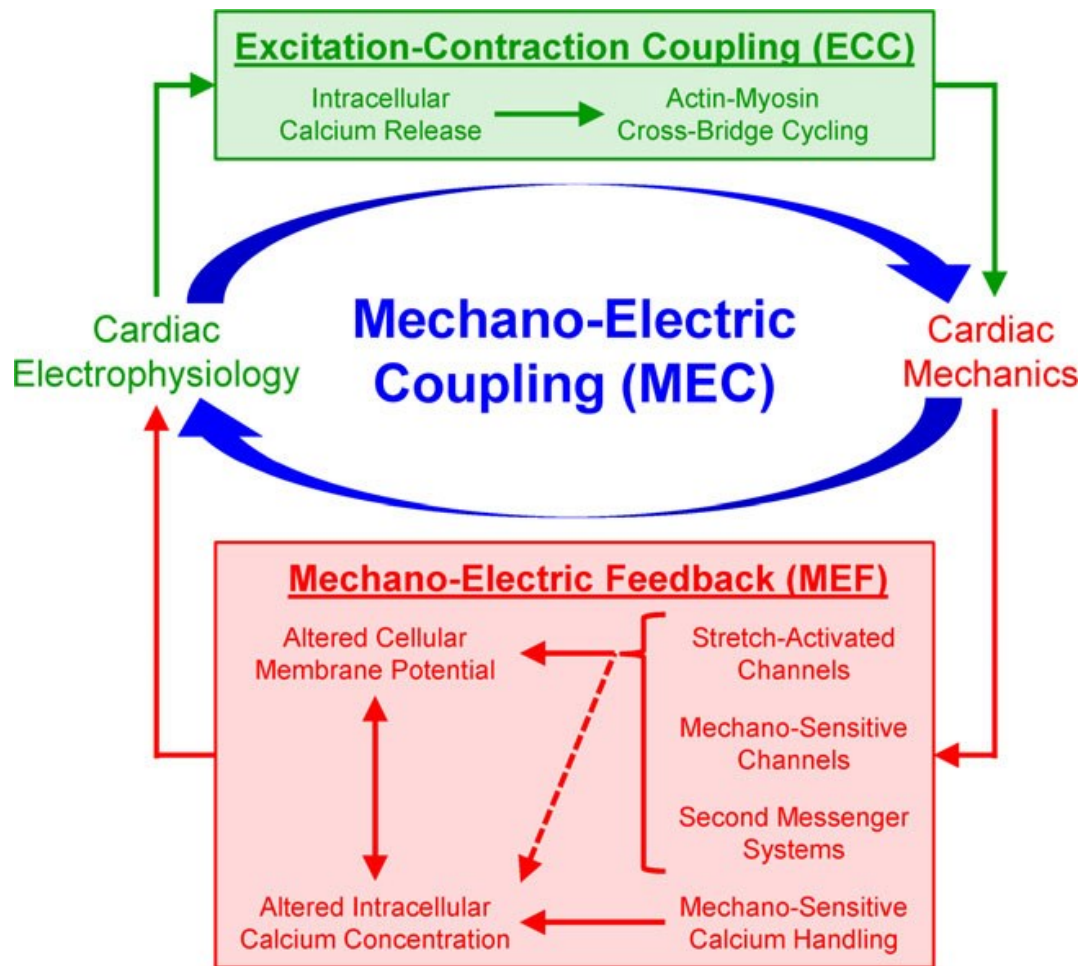


Figure 1.1. *Diagram of mechano-electric coupling.* Schematic illustration of the “mechano-electric coupling” (MEC) concept, illustrating the interdependence of cardiac mechanics and electrophysiology. The feed-forward arm (green) shows how cardiac electrophysiology, through excitation-contraction coupling, causes cardiac contraction. This process requires transsarcolemmal Ca^{2+} influx, which increases intracellular Ca^{2+} levels thereby initiating actin-myosin cross-bridge cycling. Alterations in the heart’s mechanical environment – whether through stretch, deformation of the sarcolemma etc. – can feedback (red) and alter tissue-level electrophysiology. The mechano-electric feedback may occur through mechanical-induction of stretch-activated channels, mechano-sensitive ion currents, activation of secondary messenger systems or alterations in intracellular Ca^{2+} handling. (Used with permission from Quinn 2014).

1.4.1. Effects of mechano-electric coupling on ventricular electrophysiology

When considering mechanical modulation of cardiac electrophysiology, it is important to distinguish between systolic and diastolic stretch-effects. In general, it has been shown that diastolic stretch depolarizes ventricular myocytes (Franz 1995), which can lead to EAD- or DAD-like activity (Kohl 2009). Systolic stretch, however, has a more complex influence on membrane potential, which depends on its specific timing. During early repolarization, systolic stretch will enhance repolarizing currents and thus shorten action potential duration (White *et al.* 1993), while stretch during late repolarization causes action potential prolongation *via* a depolarizing current (Franz 1995).

This behavior can be explained by stretch-activated ion channels, of which there are cation-nonspecific channels (SAC_{NS}) and potassium-selective channels (SAC_K) (Kohl *et al.* 1999). The reversal potential for SAC_{NS} is midway between resting membrane potential and the action potential plateau (values between 0 and -50 mV have been measured experimentally) (Ruknudin *et al.* 1993). Thus, during diastole, opening of SAC_{NS} will depolarize a cell, whereas during systole, opening of SAC_{NS} will affect the rate of repolarization, causing either repolarization or depolarization, depending on the phase of the action potential.

The reversal potential of SAC_K, on the other hand, is very close to the resting membrane potential of ventricular myocytes (vanWagoner 1993). Systolic activation of SAC_K will enhance repolarization of membrane potential, whereas diastolic activation will have very little effect, or may cause slight hyperpolarization (Nakagawa *et al.* 1988), although with physiologic levels of stretch diastolic depolarization occurs, suggesting a predominant role for SAC_{NS} (Nakagawa *et al.* 1988).

1.4.2. Evidence for a role of mechano-electric coupling in ventricular arrhythmias

There is both clinical and experimental evidence implicating MEC in the generation of ventricular arrhythmias.

Clinically, the most striking example is the temporary arrest of established VTs with the Valsalva maneuver, by which exhaling against a closed airway increases intrathoracic pressure, which causes a reduction in ventricular volume due to decreased venous return (Taggart & Sutton 2011). Importantly, this also occurs in the denervated heart of transplant patients (Ambrosi *et al.* 1995; Taggart *et al.* 1992), highlighting that MEC effects are intrinsic to the myocardium and do not require autonomic innervation.

Mechanically-induced VTs are also commonly observed during intracardiac catheterization by mechanical stimulation the myocardium (Bohm *et al.* 2002; Lee *et al.* 2009; Lindsay *et al.* 2006), and with non-traumatic impacts to the precordium (*i.e.*, *Commotio cordis*) (Cayla *et al.* 2007).

In isolated heart experiments, increasing intraventricular volume in a pulsatile fashion has been shown to dramatically alter tissue-level electrical activity. If supra-threshold intraventricular volume pulses are applied during diastole, they cause transmembrane depolarization and premature excitation (Franz *et al.* 1989), while if applied during early repolarization (a period of enhanced heterogeneity of repolarization across the tissue), ventricular tachycardia (Hansen *et al.* 1990; Stacy *et al.* 1992) and fibrillation can occur (Bode *et al.* 2006; Seo *et al.* 2010). These effects of transient ventricular stretch have been shown to be enhanced by acute regional ischemia (Parker *et al.* 2004), which, as

described above, is a setting where heterogeneous changes in cardiac mechanics have been implicated in arrhythmogenesis.

1.5. Mechano-Electric Coupling, Acute Regional Ischemia, and Arrhythmias

Ventricular arrhythmias resulting from acute myocardial ischemia are a major cause of sudden cardiac death (Janse & Wit 1989). Contraction of ischemic tissue is reduced early in ischemia, resulting in dyssynchronous contraction followed by akinesis, both of which result in regions of local stretch. In particular, the ischemic region first becomes less contractile and then begins to stiffen during phase 1b of ischemia (Silverman & Stern 1994). When this occurs, a region of stretch is established at the interface between healthy and ischemic myocardium ('ischemic border zone'), whereby the healthy contractile muscle begins to pull against the stiffening, non-contractile ischemic tissue (Coronel *et al.* 2011).

Non-uniformity of ventricular contraction is associated with a high susceptibility to VTs (Quinn 2014) and is one of the largest predictors of sudden cardiac death (Taggart & Sutton 1999). Furthermore, in patients there is a strong correlation between the presence of regional wall motion abnormalities and the occurrence of arrhythmias (Janse & Wit 1989; Califf *et al.* 1978; Siogas *et al.* 1998; Opthof *et al.* 2012). Similarly, the magnitude of border zone stretch (Hirche *et al.* 1987) and the degree of dilation of an ischemic region are strong predictors of VF probability (Barrabes *et al.* 2002).

As such, MEC has been suggested to play a role in arrhythmogenesis in acute regional ischemia, especially during phase 1b (Janse 2003).

1.5.1 Experimental evidence for mechanically-induced phase 1b arrhythmias: Coronel et al.

The best experimental evidence supporting the contribution of MEC in phase 1b arrhythmias comes from a ischemia study by Coronel et al. using the in situ and isolated pig heart (Coronel *et al.* 2002). In their model they ligated the left anterior descending coronary artery, generating an anteroapical region of ischemia on the left ventricle, which was maintained for 60 min while measuring the incidence of arrhythmias and epicardial activation with a grid of contact electrodes. They tested three experimental groups: the *in situ* heart, the isolated non-working heart, with an empty left ventricle, and the isolated working heart, with the left ventricle loaded by a fluid-filled balloon.

As is depicted in Figure 1.2, it was shown that the *in situ* heart had a very high incidence of arrhythmias during 60 min of acute regional ischemia, with the highest incidence occurring between 15-35 min (phase 1b). The arrhythmias included single premature ventricular excitations, ventricular tachycardia, and fibrillation. Conversely, the unloaded heart, which contracted against no ventricular preload or afterload, had a significantly reduced number of arrhythmias throughout the 60 min. Strikingly, in isolated hearts that were physiologically loaded, the incidence of arrhythmias was significantly increased as compared to unloaded hearts, while similar to *in situ* hearts, and also showed a peak in arrhythmias between 15-35 min. Further, the severity of arrhythmias was significantly greater in the *in situ* and loaded groups compared to the unloaded group.

These results suggest a necessary contribution of mechanical effects to arrhythmogenesis during acute regional ischemia.

In a second set of experiments, isolated loaded hearts were subjected to augmented ventricular contraction resulting from a diastolic pause. It was assumed that the stronger, post-pause contraction would lead to increased stretch at the ischemic border zone. It was found that these “potentiated beats” often led to premature ventricular excitations. Moreover, as shown in Figure 1.3, epicardial contact mapping showed that many of these premature ventricular excitations originated within 1 cm of the ischemic border zone, the region previously shown to have enhanced stretch, further supporting the potential importance of mechanics for phase 1b arrhythmias.

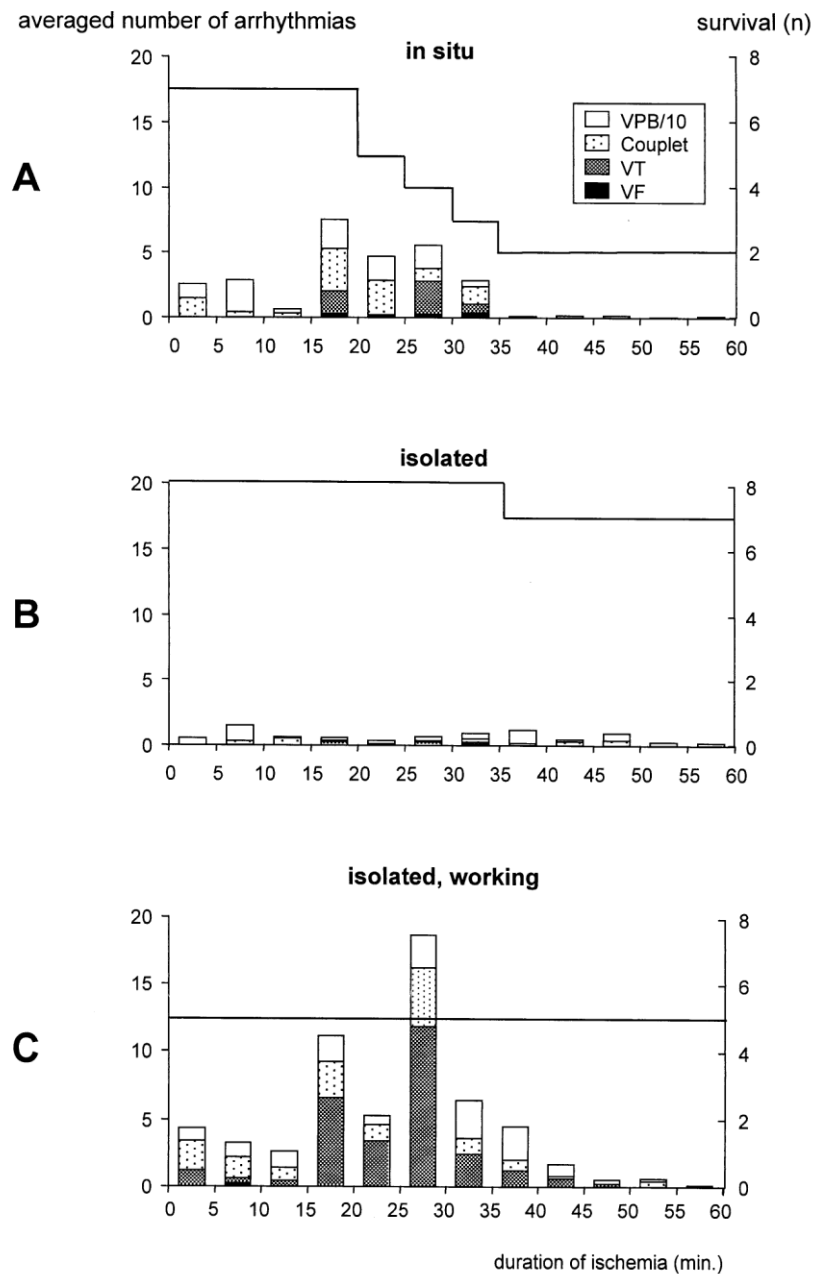


Figure 1.2. Average incidence of arrhythmias through 60 min ischemia. The number of spontaneous arrhythmias during the first hour after occlusion were tabulated in the three experimental groups of swine hearts: (A) *in situ*; (B) isolated and unloaded ventricle (*isolated*); and (C) isolated and physiologically loaded ventricle (*isolated, working*). The incidence and severity of ventricular arrhythmias were significantly greater in both the *in situ* and *isolated, working* hearts than in the *isolated* hearts, with a peak incidence at 30-35 min post-coronary artery occlusion (phase 1b arrhythmias). The types of arrhythmias observed were ventricular premature beats (VPBs), two consecutive VPBs (couplet), ventricular tachycardia defined as three or more VPBs (VT) and ventricular fibrillation (VF).

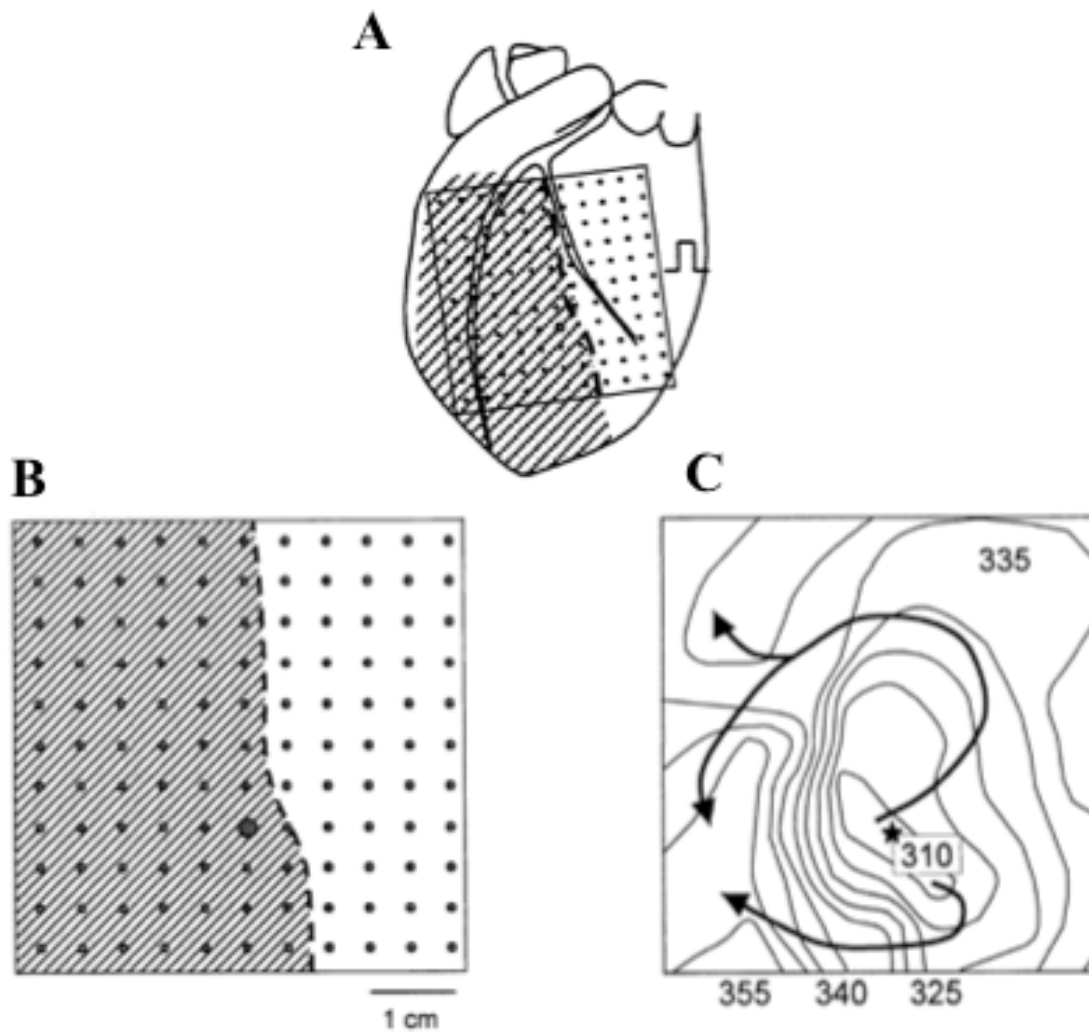


Figure 1.3. *Isochronal mapping of ectopic beats.* To investigate the focal origin of the arrhythmias seen, isochronal maps were made using 121 silver electrodes arranged on a 11x11 silicone matrix, as seen in **Panel A**. Half the matrix was positioned over the prospective ischemic area (shaded zone). In **Panel B**, the circle represents the site of focal origin of the ventricular ectopy. Thus, the ectopic origin was commonly located near the ischemic border (between ischemic and healthy myocardium). Isochronal mapping, as done in **Panel C**, shows how the ectopic focus (asterisk) originates at the ischemic border and devolves into ventricular fibrillation. (Used with permission from Coronel *et al.* 2002).

1.5.2 Computational evidence for mechanically-induced phase 1b arrhythmias: Jie et al.

While the above study by Coronel et al. provides compelling evidence for a role of stretch in phase 1b arrhythmias during acute regional ischemia, ischemia is a complex process and it is difficult to differentiate between the potential contributions of changes in mechanics *versus* independent alterations in ion concentrations, ion channel activity, and action potential morphology. For this, computational modeling is a powerful tool, as factors that cannot be independently controlled in the experimental setting can be *in silico*.

For this, Jie et al. created an anatomically-based, electro-mechanically coupled, three-dimensional computational model of the rabbit ventricles as shown in Figure 1.4 (Jie et al. 2010). The major changes in mechanics and ion concentrations and ion channel activity seen with ischemia were simulated, with MEC incorporated in the model by the inclusion of SAC_{NS}, whose activation was dependent on local strain. With this model, they were able to investigate the independent contributions of ischemia-induced mechanical effects and effects on ion concentrations, ion channel activity, and action potential morphology in the induction of arrhythmias during acute regional ischemia.

In the full model, ischemia caused premature excitation at the ischemic border zone, which, combined with conduction slowing, resulted in conduction block, reentry and ventricular tachycardia. To investigate the role of changes in ion concentrations, ion channel activity, and action potential morphology only, stretch-activate channels were omitted from the model. This eliminated the previously observed premature excitation and conduction slowing, thus reentry also did not occur, suggesting that altered

subcellular electrophysiology alone is not sufficient to initiate arrhythmias during ischemia.

To then investigate the role of changes in mechanics only, stretch-activated channels were re-introduced into the model, while ischemic alterations in ion concentrations, ion channel activity, and action potential morphology were omitted. It was found that ischemia-induced changes in contraction alone resulted in stretch-induced premature excitation and conduction slowing, but that this still did not result in reentrant arrhythmias. This suggests that mechanical-effects of acute regional ischemia are in fact sufficient for the induction of premature excitation, and while they are not sufficient for the induction of reentry, they are a necessary contributor, interacting with changes in ion concentrations, ion channel activity, and action potential morphology to cause deadly reentrant arrhythmias.

Of course, with the use of computational models one must be careful not to fall into the plausibility trap, by which a quantitatively plausible explanation is taken as proof (Quinn & Kohl 2011). While this study supported the finding of Coronel et al., that mechanics are important for ischemia-induced arrhythmias, and extended this work to generate a novel hypothesis, that mechanical effects are sufficient for premature excitation during acute regional ischemia, and necessary but not sufficient for reentry, this remains to be experimentally tested. In addition, as with any computational or experimental model, this study is not without limitations, the most important being neglect of other MEC mechanisms, especially effects on intracellular Ca^{2+} handling.

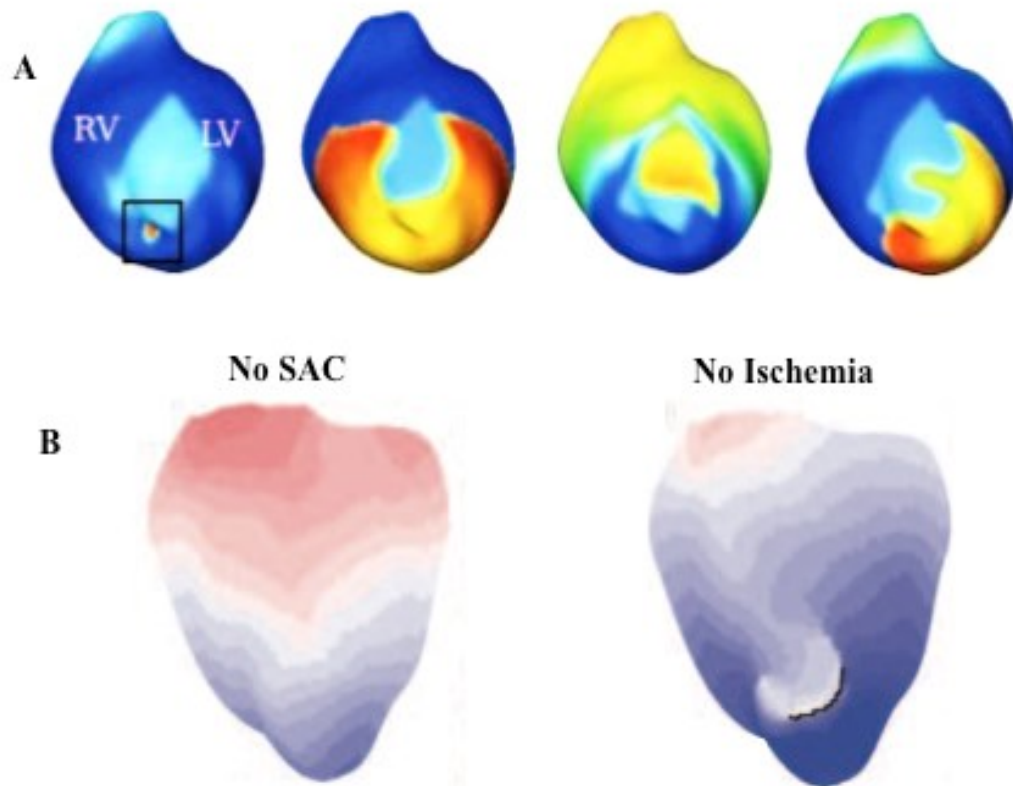


Figure 1.4. *Computational simulation of mechanically-induced arrhythmias.* A three-dimensional electromechanical computational simulation of the beating rabbit ventricles was developed to study mechanically-induced arrhythmias during acute regional ischemia. Dynamic mechano-electric feedback was represented in the model via stretch activated channels (SAC), the conductance of which was dependent on local strain rate (i.e. membrane stretch or deformation). **Panel A** shows the evolution of a mechanically induced ventricular ectopy into a subsequent reentrant arrhythmia during acute regional ischemia. The ectopy originated from the epicardial ischemic border (black rectangle on first inset), a region of strain. To dissect how electrophysiological and mechanical factors each contribute to arrhythmogenesis, two more models were used as shown in **Panel B**. The ‘No SAC’ model had all the electrophysiological changes of ischemia but without stretch effects via SAC. The ‘No Ischemia’ model had SAC involvement but without the ischemia-induced electrophysiological changes. ‘No SAC’ had no conduction block whatsoever. ‘No Ischemia’ had slowed conduction and block. However, no reentrant arrhythmia resulted from either of the additional models suggesting that arrhythmogenesis requires the involvement of mechanical and electrophysiological changes. (Used with permission from Jie *et al.* 2010).

1.6. Objectives

Thus, there exists substantial evidence that mechanical effects contribute to arrhythmias during acute regional ischemia. However, whether altered mechanics are sufficient for the induction of arrhythmias, and the mechanisms by which they contribute to arrhythmogenesis are unknown. It is thought that altered mechanics may indeed be sufficient for premature excitation, and observed MEC-effects on transmembrane voltage and intracellular calcium may be involved, but this is yet to be experimentally investigated. For this, a relevant small animal model of acute regional ischemia, which shows a contribution of mechanics to arrhythmias is needed.

The overarching hypothesis of this project was that mechanical effects are necessary and sufficient for the induction of ventricular arrhythmias during acute regional ischemia in the isolated rabbit heart. To address this hypothesis, my specific aims were to:

1. Develop a small animal isolated heart model of acute regional ischemia in which ventricular load and contraction can be varied;
2. Establish the importance of ventricular load and contraction for arrhythmogenesis during acute regional ischemia in this experimental model; and
3. Determine whether changes in regional mechanical activity alone, without accompanying changes in ion channel activity that occur with ischemia, are sufficient for the induction of arrhythmias.

CHAPTER 2

Methods

2.1. Choice of Experimental Animal

Female New Zealand white rabbits (2.1 ± 0.1 kg) were used for this study. Rabbits were chosen as they are the most suitable small animal model for the proposed work. Rabbit cardiac electrophysiology is more similar to human than that of small rodents (Nattel *et al.* 2008; Bers 2002; Nerbonne 2000). As well, arrhythmogenic wave patterns are dramatically affected by the ratio of effective heart size to excitation wavelength; it has been shown that the ratio of rabbit heart size to wavelength is more similar to human than even dog or pig (Panfilov 2006). The pathophysiology of ischemia and response to pharmacological intervention in rabbit heart is also more similar to human than other small animal models (Harken *et al.* 1981). Thus, the rabbit a highly relevant model for the study of cardiovascular disease and arrhythmogenesis (Janse *et al.* 1998; Lawrence *et al.* 2008). Moreover, rabbit coronary artery architecture shares many similarities with human (Burton *et a.* 2011), with the added benefit of having very low collateral coronary circulation (Maxwell *et al.* 1987), which allows for a consistently well demarcated ischemic zone upon ligation of a coronary artery (Toyo-oka *et al.* 1984).

2.2. Heart isolation and Langendorff-Perfusion

Animals were euthanised in the animal housing facility by intravenous injection of sodium pentobarbital (140 mg/kg) *via* the marginal ear vein, as approved by the University Committee on Laboratory Animals. Successful euthanasia was verified by a lack of pupillary reflex, response to toe pinch, and palpable heartbeat. Thoracotomy was

performed and the heart was quickly excised, the aorta cannulated ($1:50 \pm 0:38$ min from excision), and retrogradely perfused at a rate of 20 mL/min with Krebs-Heinselet solution (containing [in mM]: 120 NaCl; 4.7 KCl; 24 NaHCO₃; 1.4 NaH₂PO₄; 1.0 MgCl₂, 1.8 CaCl₂; 10 Glucose; osmolality: 301 ± 1 mOsm/kg; pH: 7.38 ± 0.01) bubbled with carbogen (95% O₂, 5% CO₂) on a portable perfusion apparatus. The heart was cleaned of extraneous tissue (lung, thymus, pericardium, and vessels) and the proximal pulmonary artery opened to allow coronary effluent to exit the right ventricle.

This method of retrograde heart perfusion adheres closely to the techniques established by Oscar Langendorff in 1895 (Langendorff 1895). With the perfusion buffer flowing down the aorta, contrary to normal physiologic flow, the aortic valve is closed under pressure. With a column of perfusion buffer within the aorta, the coronary arterial vasculature is filled *via* the two aortic sinuses (left and right). Perfusion fills the arterial beds and is drawn away *via* coronary veins to all be collected by the coronary sinus in the right atrium, located superior to the tricuspid valve on the posterior atrial wall (Bell *et al.* 2011).

2.3. Instrumentation of the Isolated Heart

The heart was transported on the portable perfusion apparatus to the laboratory and transferred to a more extensive perfusion system. A 3-0 silk suture was passed under the anterior branch of the left circumflex coronary artery close to the base of the left ventricle and threaded through a Rummel tourniquet.

A small incision was made in the left atrium and a 15 mm long drain made from an 18G intravenous cannula was passed across the mitral valve into the left ventricle and pushed

transmurally through the apex to allow outflow of coronary return from the Thebesian veins. A deflated custom-made pre-strained polyethylene balloon was similarly inserted into the left ventricle and its tip anchored through the apical drain. The atrium was tied to the balloon inflow/outflow cannula with a silk ligature to secure the base of the balloon inside the ventricle. The intraventricular balloon was connected to a vertical column of water, which allowed passive beat-by-beat filling of the balloon to the appropriate preload, or end-diastolic pressure, controlled by altering the height of the column and measured with an inline pressure transducer. The rate of filling of the balloon, along with the afterload, or peak systolic pressure of the left ventricle was adjusted by restricting balloon inflow/outflow with a screw clamp.

Pacing electrodes were placed at the right atrial appendage for control of heart rate and at the base of the left ventricle for programmed ventricular stimulation. Global electrical activity was monitored using surface ECG electrodes placed at the right atrium and right ventricular apex. An image of the isolated heart preparation is shown in Figure 2.1.

2.4. Voltage Optical Mapping

After instrumentation, hearts were loaded with a voltage-sensitive dye (di-4-ANBDQPP) (Matiukas *et al.* 2007) by direct injection into the aortic cannula (20 μ L bolus of 27.3 mM solution in medical grade ethanol, delivered in 0.4 μ L increments over 2.5 min). As Figure 2.2 shows, the dye was excited using two red light emitting diodes with a band-pass filter (640 ± 10 nm). Excitation of the dye causes it to emit fluorescence, whose spectrum shifts with changes in membrane potential (Lee *et al.* 2011). Fluorescence was

collected at 500 frames/sec by a 350×512 pixel sCMOS camera ($100 \mu\text{m}/\text{pixel}$) through a 17 mm high-speed lens and long-pass filter ($>670 \text{ nm}$).

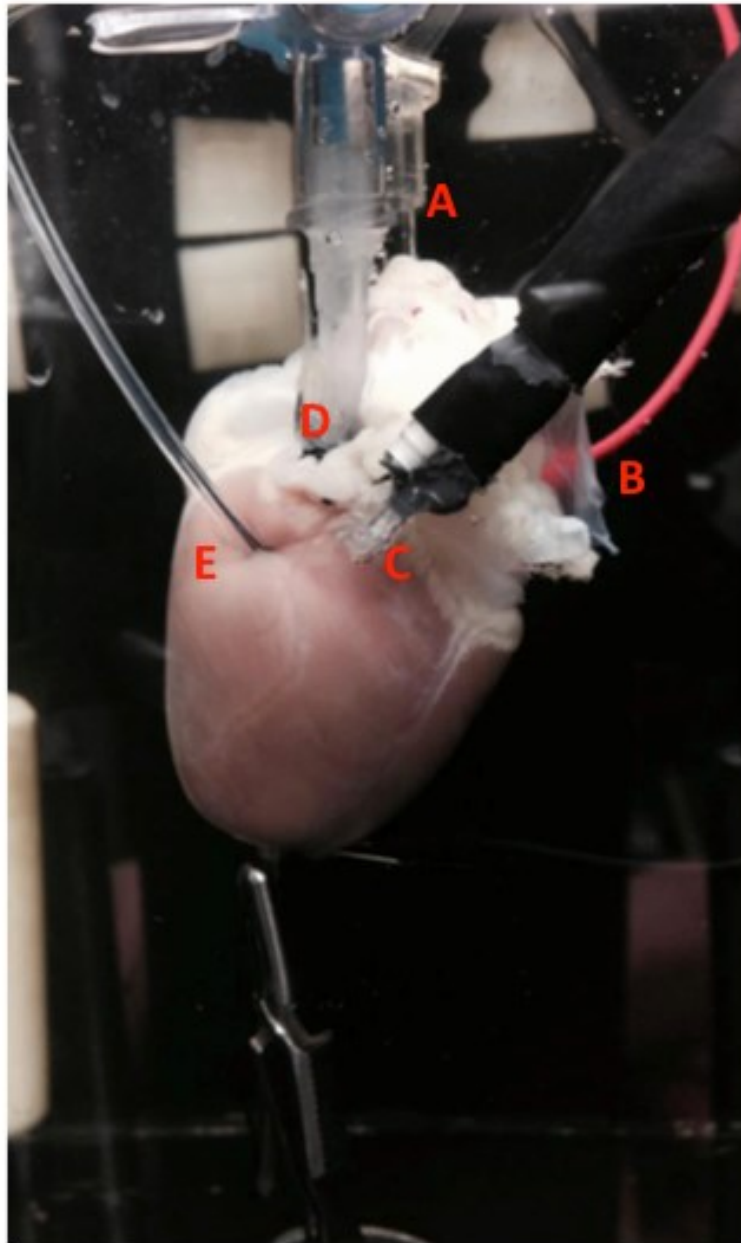


Figure 2.1. *Langendorff-perfused isolated rabbit heart.* Isolated rabbit hearts were placed in an environmentally-controlled chamber to maintain ambient temperature at 37° C for the duration of the experiment. (A) Hearts were retrogradely perfused at a constant pressure of 80 mmHg via cannulation of the aorta. (B) Heart rate was maintained at 4 Hz via right atrial pacing. Additionally, (C) programmed premature left ventricular excitation stimuli were delivered through a contact pacing electrode. (D) The left ventricle was loaded with a fluid-filled custom made polyethylene balloon. (E) A silk suture was passed under the anterior branch of the left circumflex nearest to the base of the heart and subsequently filed into a Rummel tourniquet.

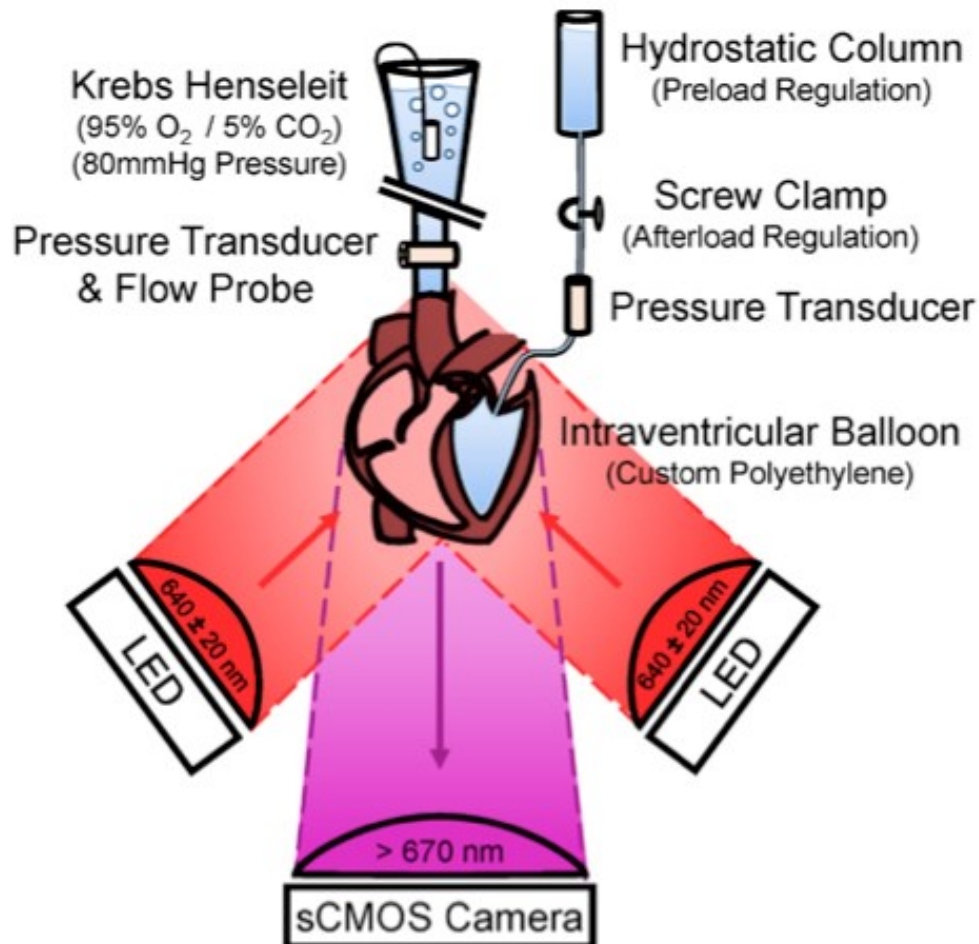


Figure 2.2. *Schematic of experimental setup.* Canulation of the aorta allowed retrograde perfusion at constant pressure of 80 mmHg with Krebs-Henseleit physiologic buffer, which is oxygenated with a carbogen mixture (95% O₂ / 5% CO₂). Coronary flow is measured using a flow probe. Left ventricular pressure was established with a custom polyethylene intraventricular balloon connected to a vertical hydrostatic column. Diastolic pressure was controlled by the height of the vertical column; systolic pressure was controlled by screw clamp occlusion of the column to establish afterload. To record spatiotemporally resolved epicardial electrophysiology, a voltage-sensitive dye (di-4-ANBDDQPQ) was perfused into the tissue. Excitation with red LED lights (640 ± 20 nm) causes the dye to fluoresce with a near infrared wavelength. Epicardial fluorescence is recorded using a sCMOS camera with a 670 nm longpass filter. (Figure created by Peter A. Baumeister).

2.5. Experimental Protocol

Hearts were placed in a temperature-controlled imaging chamber filled with Krebs-Heinselet solution that was bubbled with 95% N₂ / 5% CO₂. This maintained solution pH, while removing oxygen and preventing oxygen diffusion into epicardial tissue, which would result in a subepicardial layer of healthy tissue during acute regional ischemia. Perfusion was switched from constant flow to constant pressure with a pressure head of 80 mmHg and right atrial pacing was commenced at 4 Hz.

Following a 10-minute stabilization period, baseline optical mapping recordings were acquired. The instrumented coronary artery was then ligated by tightening and clamping the tourniquet, producing an antero-apical ischemic region in the left ventricle. The ECG, ventricular pressure, perfusion pressure, and coronary flow were recorded using a PowerLab analog-to-digital converter for 60 min of ischemia, followed by 30 min of reperfusion by releasing the ligation. Optical mapping recordings were obtained for 15 sec every min over the 90 min period.

At the end of the experiment, the tourniquet was retightened and 3 - 8 μm green polystyrene divinylbenzene fluorescent microspheres (1.25 mg/mL) were injected into the aortic cannula and imaged to demarcate perfused tissue and the ischemic border (excitation = 380 nm, emission = 531 ± 11 nm). The atria were then removed and the ventricles partly frozen (-20° C freezer for 1 hour), cut into 2 mm thick slices, stained with 2,3,5-triphenyltetrazolium chloride (which is enzymatically reduced to a red formazan product by dehydrogenases, most abundant in mitochondria, such that stain intensity correlates with mitochondrial functional activity) for 20 min, and stored in

formalin for subsequent analysis of ischemic volume and cell necrosis (Ytrehus *et al.* 1994).

2.6. Experimental Groups

We investigated three experimental groups to study the contribution of ventricular load or contraction to the onset of arrhythmias during acute regional ischemia.

Loaded (n=10): The left ventricle was physiologically loaded with the intraventricular balloon to an end-diastolic pressure of ~5 mmHg (5.9 ± 0.9 mmHg) with a resulting systolic pressure of 74.3 ± 3.7 mmHg.

Unloaded (n=10): The left ventricle was left unloaded by leaving the intraventricular balloon empty.

Non-Contracting (n=10): The left ventricle was physiologically loaded with an intraventricular balloon as in the *Loaded* group and then excitation-contraction uncoupled with 8 μ M blebbistatin (a myosin-II inhibitor) to block contraction without affecting electrical activity.

2.7. Optical Mapping Analysis

To assess the effects of ischemia in our experimental model we analyzed the maximum rate of membrane potential change (dF_n/dt_{\max} , in nominal units of normalized fluorescence per ms; ‘upstroke velocity’) and action potential duration at 80% repolarization (APD₈₀, difference between the time of membrane potential restoration to 80% of resting values and the time of activation, set as the time of dF_n/dt_{\max}) and

averaged values at regions across the ischemic border (the line separating healthy myocardium from ischemic tissue).

Custom programs in Matlab were used for this analysis. Optical mapping data was first filtered with a 10x10 spatial filter. The ischemic border was manually traced from the image acquired post microsphere injection and superimposed on the optical mapping images. A straight line of 1x1 mm regions is drawn across the ischemic border, with one region directly on top of the ischemic border and 5 regions extending 5 mm into both the healthy and ischemic myocardium. The fluorescent signals were averaged within each region of interest, filtered with a 60 Hz low-pass temporal filter, inverted (dye fluorescence decreases with an increase in voltage with the excitation wavelength used in this study), and normalized. Values of dF_n/dt_{\max} and APD_{80} were calculated for each action potential and averaged across nine consecutive beats. Values are presented as mean \pm SEM. Comparison of values with time across the ischemic border was analysed by two-way ANOVA with Tukey *post-hoc* tests and a significance value of $p < 0.05$ using SPSS.

2.8. Quantification of Arrhythmias

The data acquisition and analysis software LabChart was used for the identification and diagnosis of arrhythmias. Arrhythmias were defined according to the criteria established by Coronel et al. (Coronel *et al.* 2002) to allow direct comparison with previous results. Premature ventricular excitation (PVE) was defined as a single premature QRS complex. A couplet was defined as two successive PVEs. A run of 3 or more PVEs was defined as a VT. The incidence of ectopy over the 60 min of ischemia was tabulated in 5 min bins. Comparison of total average arrhythmia incidence across the groups was analysed by one-way ANOVA with Tukey *post-hoc* tests and a significance value of $p < 0.05$ using SPSS.

2.9. Measurement of Ischemic Volume and Cell Necrosis

Ventricular sections loaded with fluorescent microspheres and stained with 3,5-triphenyltetrazolium chloride were placed on a black plate and covered with glass with 2 mm spacers. Images were taken of microsphere distribution in each slice (excitation = 380 nm, emission = 531 ± 11 nm), to determine the ischemic region, defined as the area without microspheres. The total ischemic volume was calculated by manual planimetry of each slice (Nakano *et al.* 2002), and hearts with ischemic volumes $<25\%$ were excluded. 3,5-triphenyltetrazolium chloride staining was manually assessed under white light. Comparison of ischemic volume and reduction in coronary flow were analysed by one-way ANOVA with Tukey *post-hoc* tests and a significance value of $p < 0.05$ using SPSS.

2.10. Local Perfusion Experiments

An additional set of experiments ($n = 5$) was performed to assess whether changes in regional mechanical activity alone are sufficient for arrhythmia induction. This was accomplished by cannulating (rather than ligating) the anterior branch of the left circumflex coronary artery with a 27G needle, so that it could be independently perfused. Upon local cannulation, global coronary flow was reduced to 80% of its pre-cannulation value (based on the average observed drop in coronary flow with ligation) and local perfusion was set at 40% of pre-cannulation global coronary flow (to ensure adequate flow to the locally perfused region). Local cannulation was followed by a 30 min stabilization period, after which 8 μM blebbistatin was added to the perfusate for 60 min to cause a regional loss of contraction.

At the end of the experiment 3 - 8 μm green polystyrene divinylbenzene fluorescent microspheres (1.25 mg/mL) were perfused through the cannulated coronary artery and imaged as in the previous experiments to demarcate the locally perfused tissue. The atria were then removed and the ventricles partly frozen (-20°C freezer for 1 hour), cut into 2 mm thick slices and stored in formalin for subsequent analysis of locally perfused volume as in the previous experiments.

Chapter 3

Results

3.1. Aim 1: Small Animal Isolated Heart Model of Acute Regional Ischemia

3.1.1 Hemodynamic and tissue effects of coronary artery ligation

Figure 3.1 shows a representative example of the change in hemodynamics with ligation of the anterior branch of the left circumflex coronary artery in a heart from the Loaded group. Ligation caused an increase in perfusion pressure and a decrease in total coronary flow, which decreased an average of $18.6 \pm 1.8\%$ across all hearts. This was generally associated with a decrease in peak left ventricular pressure and an increase in left ventricular end-diastolic pressure in the Loaded group.

Figure 3.2 shows a representative example of the epicardial and transmural distribution in the myocardium of fluorescent microspheres injected at the end of an experiment. The microspheres clearly demarcate the ischemic and healthy regions, with an average ischemic volume of $39.1 \pm 1.7\%$ of the total volume of the ventricles across all hearts.

Figure 3.3 shows a representative example of 2,3,5-triphenyltetrazolium chloride staining. In general staining was uniformly red and showed no difference across all ventricular slices, indicating a lack of cell necrosis with 60 min of coronary artery ligation.

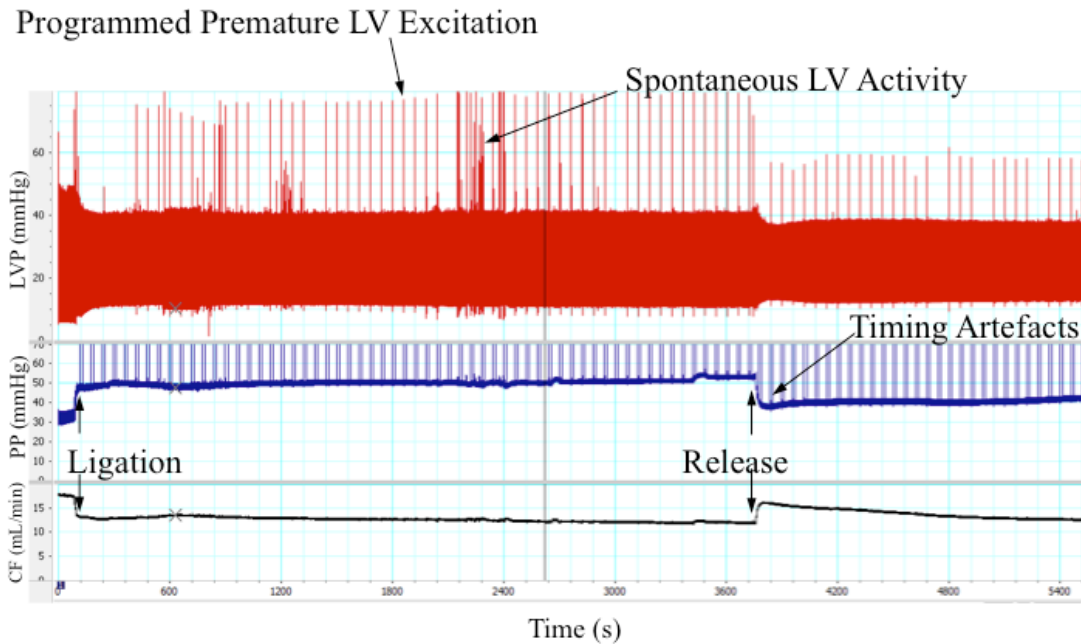


Figure 3.1. Example of experimental tracing in Loaded heart. Example of experimental tracing of left ventricular pressure (LVP), total perfusion pressure (PP) and total coronary flow (CF) in a *Loaded* heart over 60 min of acute regional ischemia following coronary artery ligation (indicated by arrows). The recurrent vertical spikes seen in this tracing are due to programmed premature left ventricular excitations delivered every minute throughout ischemia. Note that spontaneous left ventricular activity represents arrhythmic activity.

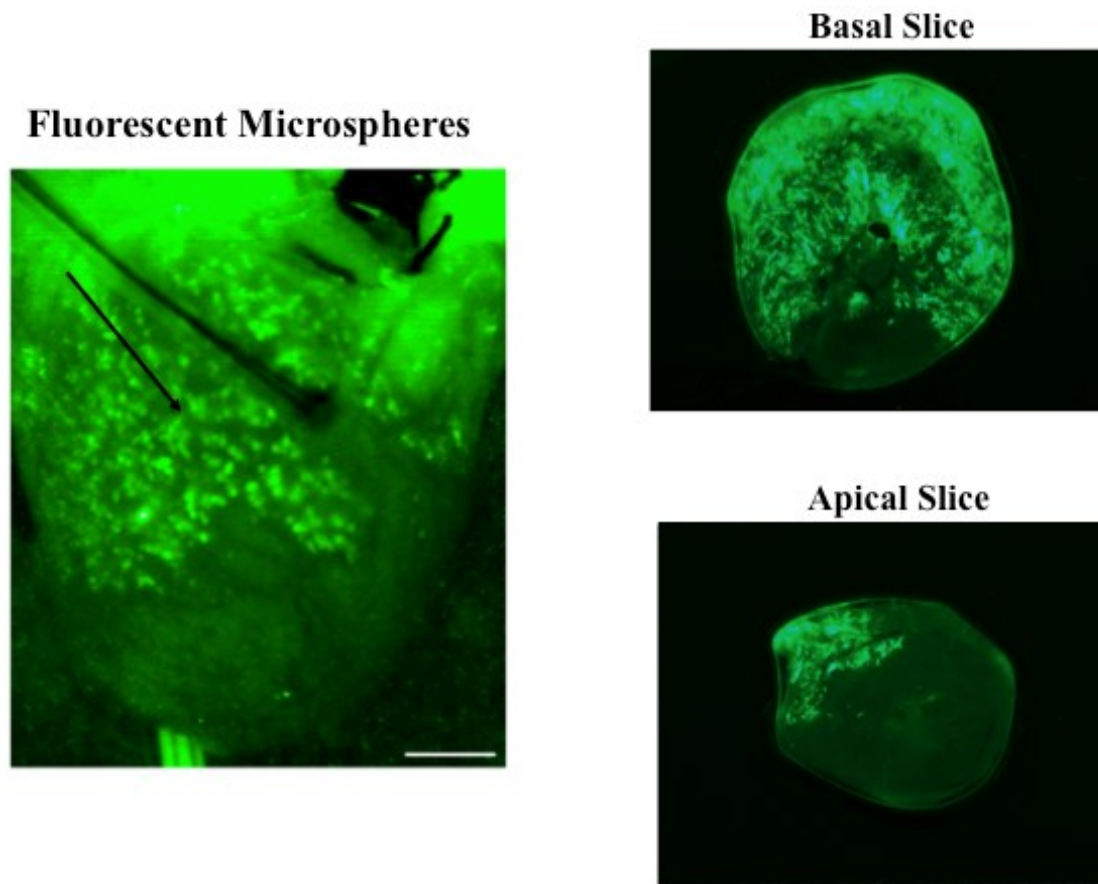
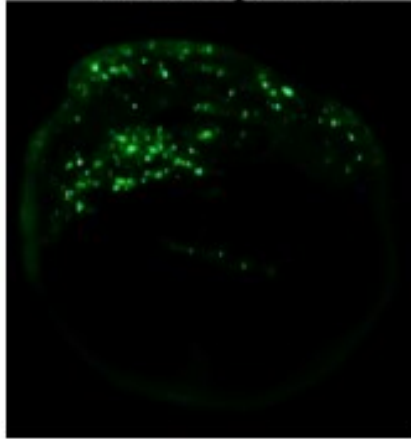


Figure 3.2. *Assessing ischemic area using fluorescent microspheres.* Transmural microsphere distribution in a basal and apical transverse section of the ventricles, showing the antero-apical location of the ischemic region.

Microspheres



TTC Staining



Figure 3.3. *Assessing myocardial necrosis using TTC staining.* The top panel shows transmural microsphere distribution in a transverse section of the ventricles, showing an ischemic region. The bottom panel shows TTC staining of the same ventricular slice. TTC stains deep red in viable tissue.

3.1.2 Electrophysiological effects of coronary artery ligation

Using our optical mapping data, we were able to analyze changes in epicardial action potential upstroke, action potential duration, and activation pattern caused by coronary artery ligation across the myocardium over the 60 min of ischemia. These values were only measured in the Non-contracting group, however, as motion artefacts associated with contraction preclude these measurements in contracting hearts.

Figure 3.4 depicts representative maps of activation time across the anterior left ventricular epicardial surface for unpaced pre-ligation, paced pre-ligation (atrially paced at 4 Hz) and after 30 min of ischemia. This shows that in the healthy heart activation begins at the mid-anterior left ventricle and progresses rapidly in a generally homogenous fashion through the myocardium. As well, atrial pacing does not alter the sequence of activation as can be seen. In contrast, after 30 min of ischemia, activation is drastically slowed in ischemic region, as indicated by crowding of the isochronal lines and longer activation times.

Figure 3.5 depicts representative maps of APD_{80} across the anterior left ventricular epicardial surface for unpaced pre-ligation, paced pre-ligation (atrially paced at 4 Hz) and after 30 min of ischemia. This shows that in the healthy heart APD_{80} is largely homogenous across the myocardium. As well, atrial pacing does not alter the homogeneity of APDs across the surface of the ventricle. In contrast, after 30 min of ischemia, APD_{80} is drastically reduced in the ischemic region.

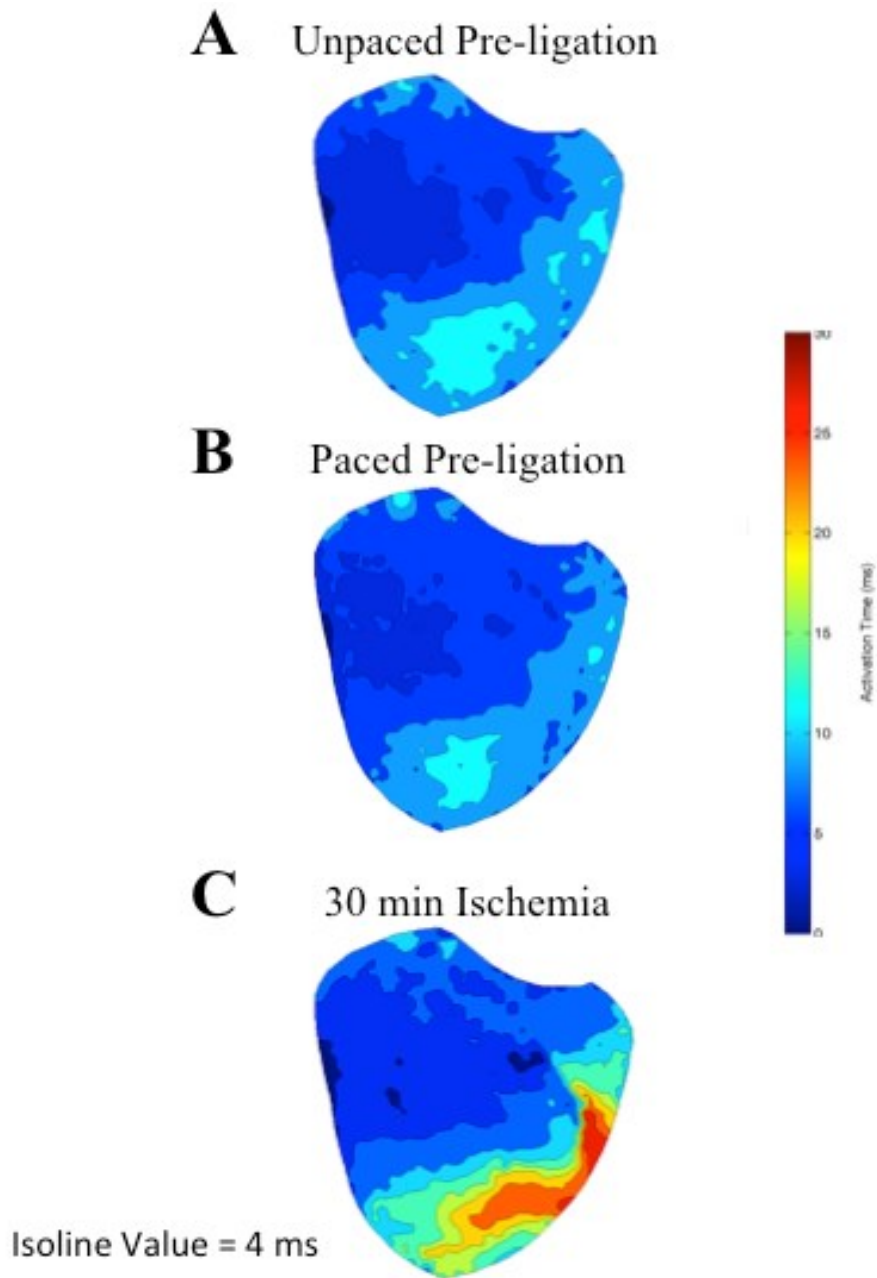
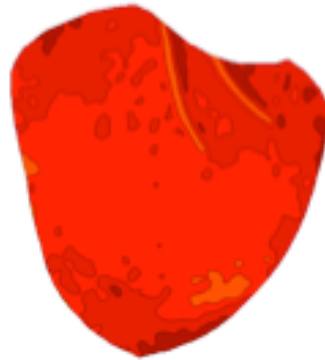
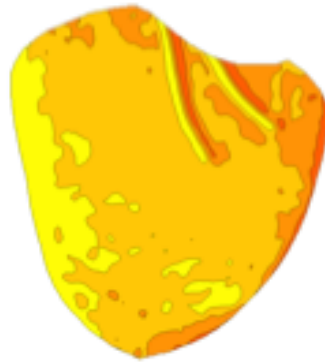


Figure 3.4. *Epicardial activation maps of anterior left ventricle.* Representative optical mapping-derived epicardial activation maps were made to assess altered patterns of conduction with ischemia in (A) unpaced pre-ligation, (B) pre-ligation atrially paced at 4 Hz and (C) after 30 min of ischemia. 0 ms represents earliest activation (deep blue). Isochrones represent 4 ms steps.

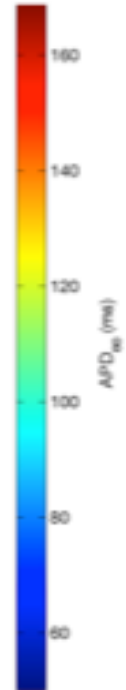
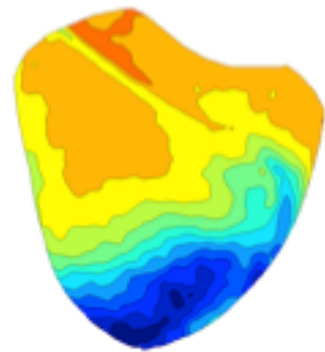
A Unpaced Pre-ligation



B Paced Pre-ligation



C 30 min Ischemia



Isoline Value = 10 ms

Figure 3.5. *Epicardial APD₈₀ maps of anterior left ventricle.* Representative optical mapping-derived epicardial APD₈₀ maps were made to assess alterations between (A) unpaced pre-ligation, (B) pre-ligation atrially paced at 4 Hz and (C) after 30 min of ischemia. Isochrones represent 10 ms steps.

In order to quantify the effects of ischemia over 60 min of coronary artery ligation, we conducted a more thorough analysis of effects across the ischemic border.

Figure 3.6 depicts the average value of APD_{80} across the ischemic border for various time points after coronary artery ligation. This shows that in pre-ligation, there was no variation in APD_{80} across the ischemic border, but immediately after ligation APD_{80} began to decrease in the ischemic region, progressively shortening through time until 30 min after ligation, at which point values stabilized.

Figure 3.7 presents a summary of the effects of time of ligation on the distribution of APD_{80} across the ischemic border, expressed as a percentage of the most healthy region in pre-ligation as well as a statistical comparison of values at the most healthy and ischemic regions. There was a significant difference in APD_{80} with both region and time, as assessed by two-way ANOVA. Specifically, there was an average a $33 \pm 3\%$ decrease of APD_{80} in the most ischemic region compared to pre-ligation after 30 min of ischemia.

Figure 3.8 presents a summary of the effects of time of ligation on the distribution of dF_n/dt_{max} across the ischemic border, expressed as a percentage of the most healthy region in pre-ligation, as well as a statistical comparison of values at the most healthy and ischemic regions. As was the case for APD_{80} , in pre-ligation there was no variation in dF_n/dt_{max} across the ischemic border, but immediately after ligation dF_n/dt_{max} began to decrease in the ischemic region, progressively decreasing through time until 30 min after ligation, at which point values stabilized. The decrease in dF_n/dt_{max} was also significant with both region and time, with an average reduction of $29 \pm 5\%$ in the most ischemic region compared to pre-ligation after 30 min of ischemia.

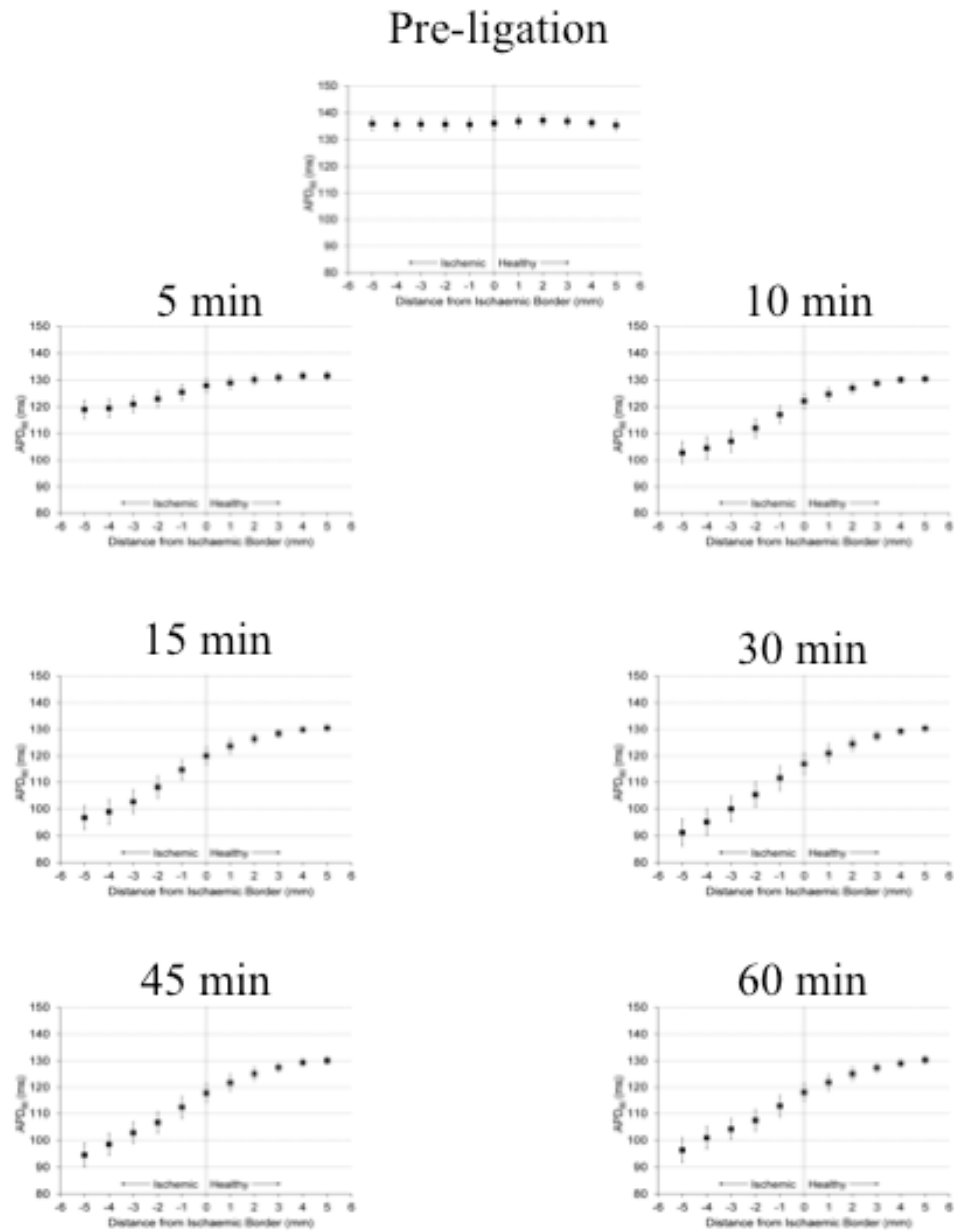


Figure 3.6. Average APD_{80} values across ischemic border at various time points. These graphs show average APD_{80} as a function of distance from the ischemic border. In terms of distance, positive values are for the healthy side of the border, whereas negative values are for the ischemic side of the border. Average APD_{80} values were calculated in regions of interest spanning the ischemic border, 5 mm into healthy tissue and 5 mm into ischemic tissue. This was completed for pre-ligation, as well as six time point after coronary artery occlusion: 5, 10, 15, 30, 45 and 60 min into ischemia.

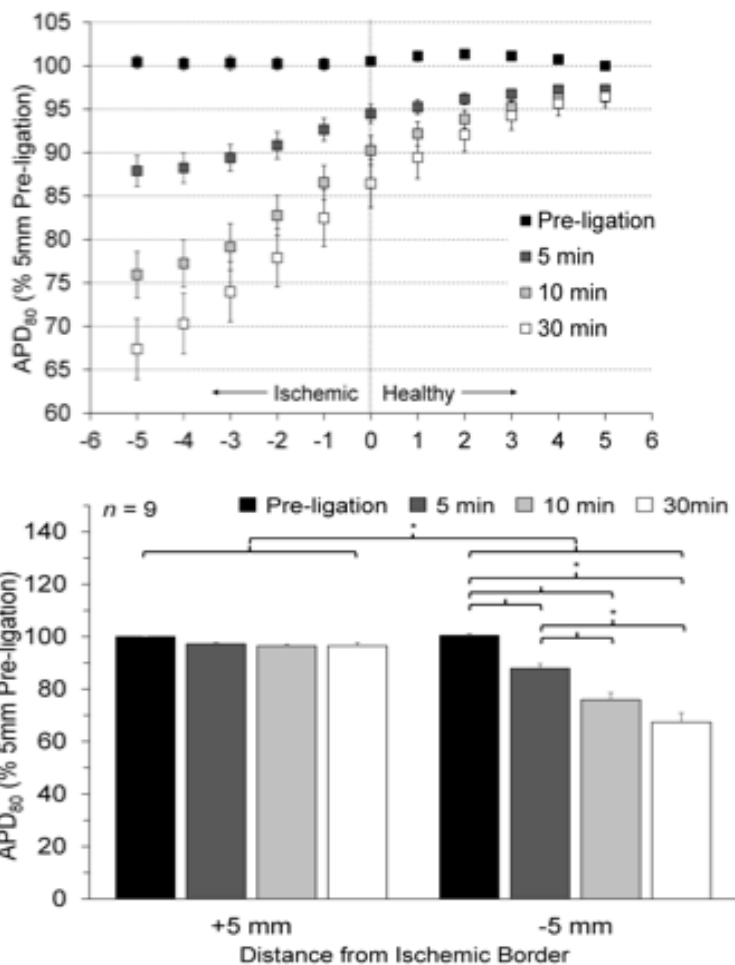


Figure 3.7. Summary of ischemic effects on APD₈₀ across the ischemic border and with time of ischemia. The top panel shows APD₈₀ as a function of distance from the ischemic border for varying times of ischemia. The bottom panel shows APD₈₀ for the most healthy (+5 mm) and most ischemic (-5 mm) regions for varying times of ischemia. * indicates p < 0.05 by two-way ANOVA with Tukey *post-hoc* tests. In both panels, APD₈₀ values are expressed as a percentage of the most healthy region of interest from pre-ligation heart, averaged across the hearts.

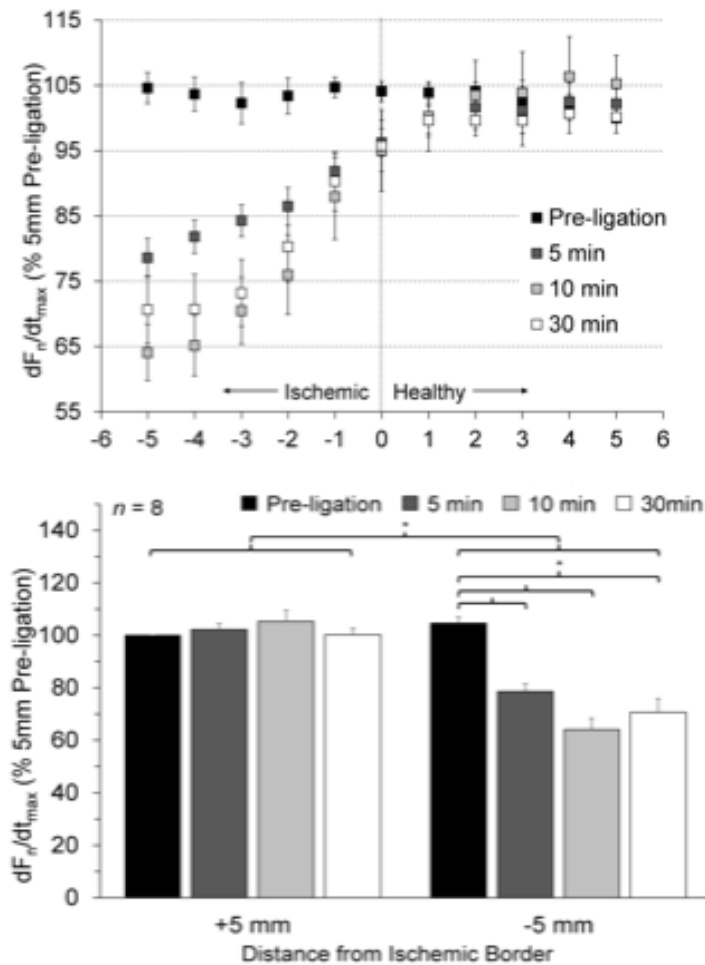


Figure 3.8. Summary of ischemic effects on dF_n/dt_{max} across ischemic border and with time of ischemia. The top panel shows dF_n/dt_{max} as a function of distance from the ischemic border for varying times of ischemia. The bottom panel shows dF_n/dt_{max} for the most healthy (+5 mm) and most ischemic (-5 mm) regions for varying times of ischemia. * indicates $p < 0.05$ by two-way ANOVA with Tukey *post-hoc* tests. In both panels, dF_n/dt_{max} values are expressed as a percentage of the most healthy region of interest from pre-ligation heart, averaged across the hearts.

3.2. Aim 2: The Importance of Ventricular Load and Contraction for

Arrhythmogenesis during Acute Regional Ischemia in the Isolated Rabbit Heart

3.2.1 Effects of coronary artery ligation across the experimental groups

Figure 3.9 shows the average percentage decrease in total coronary flow and average percentage decrease in total perfused ventricular volume (which represents the ischemic volume) with coronary artery ligation across the three experimental groups. After ligation, coronary flow decreased $19.0 \pm 1.9\%$ in the Loaded group, $22.4 \pm 3.8\%$ in the Unloaded group, and $14.5 \pm 2.8\%$ in the Non-contracting group. Total perfused ventricular volume decreased $37.6 \pm 3.2\%$ in Loaded group, $43.3 \pm 2.9\%$ in Unloaded group, and $36.3 \pm 2.8\%$ in the Non-contracting group. Both the reduction in coronary flow and total perfused ventricular volume were not significantly different across the groups.

3.2.2 Incidence of arrhythmias across the experimental groups

Figure 3.10 shows representative examples of the ECG and left ventricular pressure traces during a PVE and a VT in the Loaded group.

Figure 3.11 presents the average incidence of arrhythmias over 60 min of ischemia in the three groups. The loaded group had a high incidence of arrhythmias with two peaks, between 15-20 min of ischemia and between 30-35 min of ischemia. The Unloaded and Non-contracting groups, on the other hand, had few arrhythmias over the 60 min.

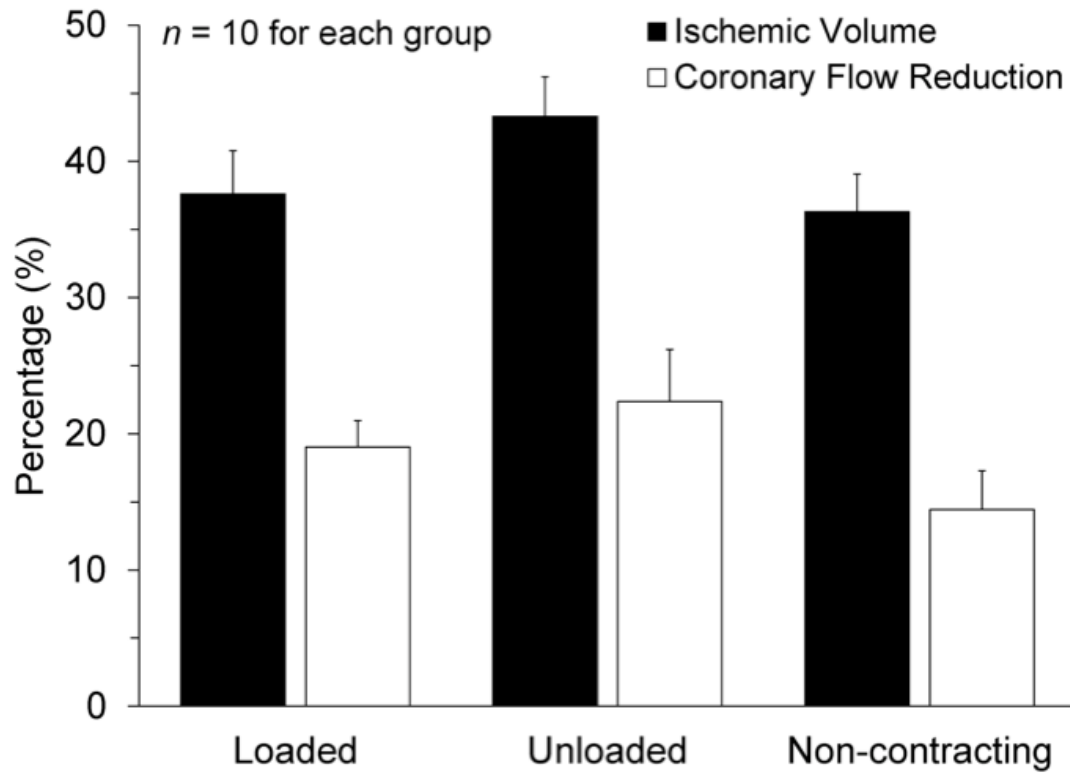


Figure 3.9. Average ischemic volume and coronary flow reduction after coronary artery ligation. A comparison of ischemic volume (black bars) and coronary flow reduction (white bars) across all three experimental groups: physiologically-loaded (Loaded), unloaded left ventricle (Unloaded) and physiologically-loaded, non-contracting (Non-contracting).

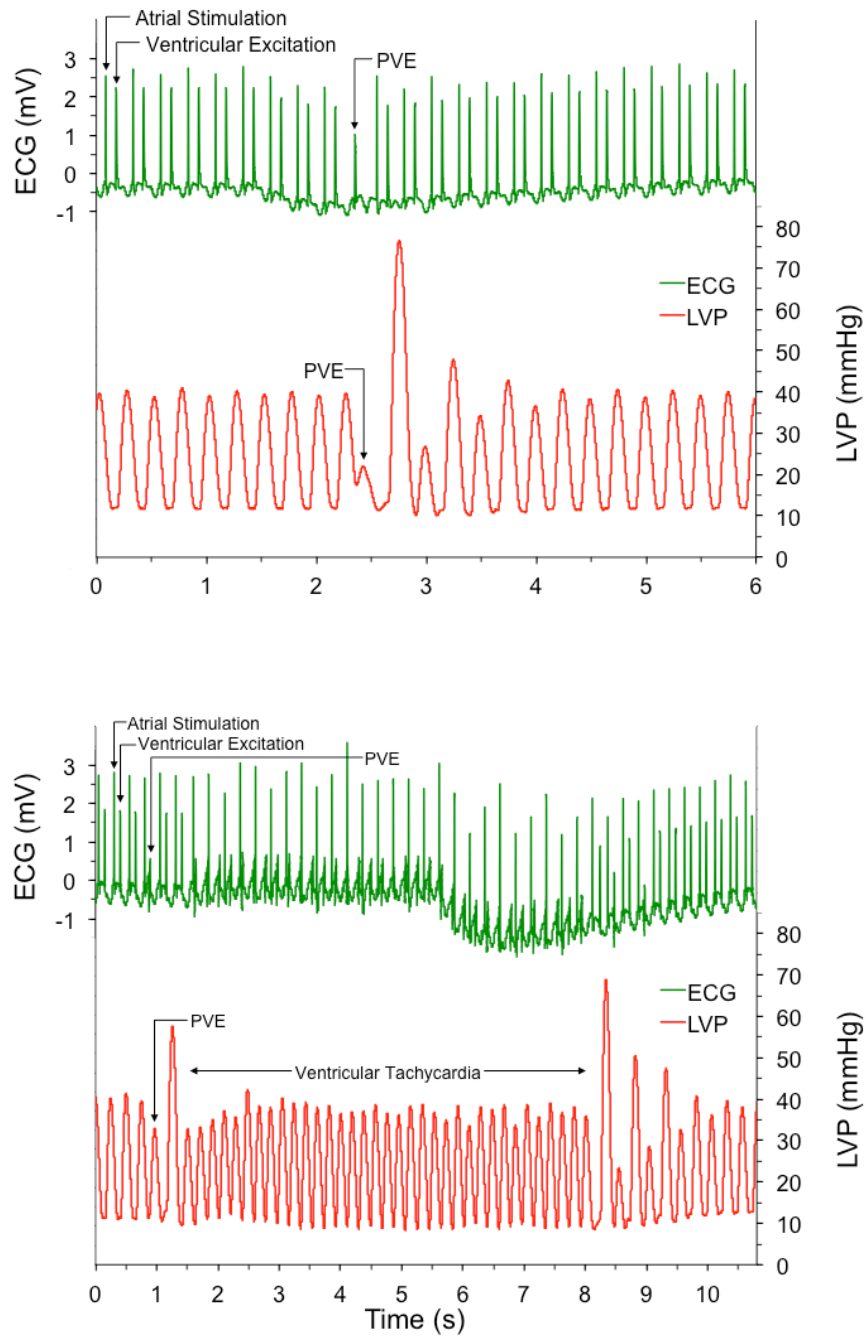


Figure 3.10. Representative example of ECG and LVP traces during arrhythmia. The ECG is shown in the green tracing and left ventricular pressure (LVP) is shown in the red tracing. Atrial stimulation is maintained via atrial pacing at 4 Hz throughout the experiment. The top panel shows an example of a *premature ventricular excitation* (PVE) and the bottom panel shows an example of a short run of ventricular tachycardia (VT).

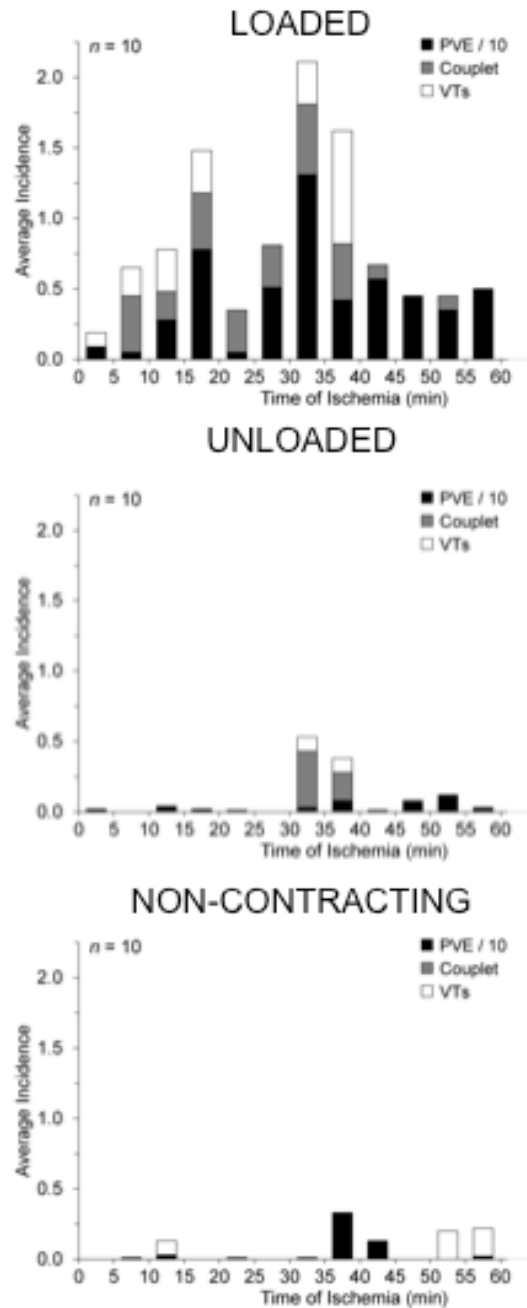


Figure 3.11. Average incidence of arrhythmias during 60 min of ischemia. The average incidence of various arrhythmias in all three experimental groups during 60 min of regional ischemia. Arrhythmia incidence is binned per 5 min. PVE/10 (black bars; premature ventricular excitations divided by 10); couplet (grey bars; two successive PVEs); VTs (white bars; ventricular tachycardia defined as three or more PVEs).

Figure 3.12 presents a statistical comparison of the total average incidence of arrhythmias over 60 min of ischemia between the three groups. There were a significantly greater average number of PVEs and couplets in the Loaded group compared to the Unloaded and Non-contracting groups during ischemia, as assessed by one-way ANOVA.

Specifically, the Loaded group had on average 53.6 ± 22.1 PVEs and 2.7 ± 0.9 couplets, compared to 4.4 ± 1.9 PVEs and 0.6 ± 0.4 couplets in the Unloaded group and 5.4 ± 4.5 PVEs and no couplets in the Non-contracting group. While there was a trend for more in the Loaded group, the total average incidence of VTs, on the other hand, was not significantly different between the groups (2.0 ± 1.1 in the Loaded group *versus* none in the Unloaded group and 0.5 ± 0.4 in the Non-contracting group).

A statistical correlation between the ischemic volume in the hearts and arrhythmia incidence has shown no clear relationship between the two variables.

3.2.3 Origin of ischemia-induced PVE in the Loaded isolated rabbit heart

Spatio-temporally resolved recordings of surface activation in the contracting heart were made possible by our voltage optical mapping.

Figure 3.13 depicts normal atrially paced activation across the left ventricular wall in a Loaded heart, as well as activation due to a PVE. As can be seen, activation normally progresses rapidly and relatively homogeneously across the epicardial surface. In contrast, PVEs for which we captured a focal origin showed a focus of activation near the ischemic border, which then progressed more slowly through the myocardium.

Our optical recordings were taken for 15 sec of every min during the 60 min ischemia (i.e. 25% of our experiment was optically recorded). We observed numerous ectopies

originating from the ischemic border, but did not calculate the incidence. Coronel et al. calculated that 26.4% of the arrhythmias observed during 60 min of regional ischemia had a focal origin at the ischemic border (Coronel et al. 2002).

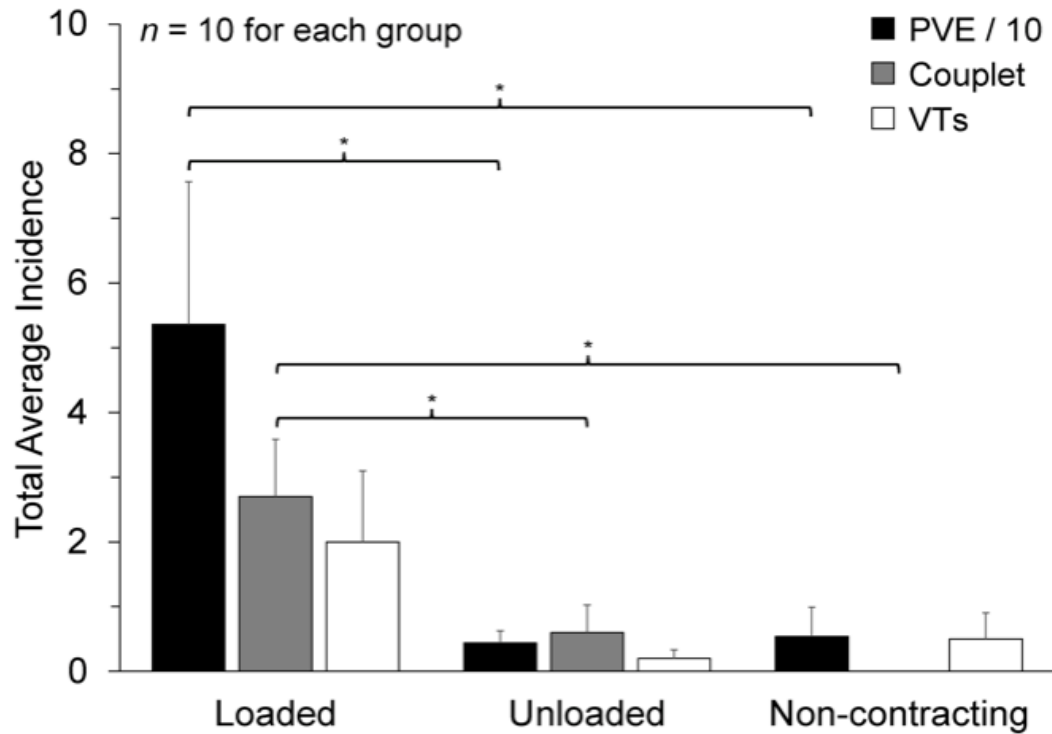
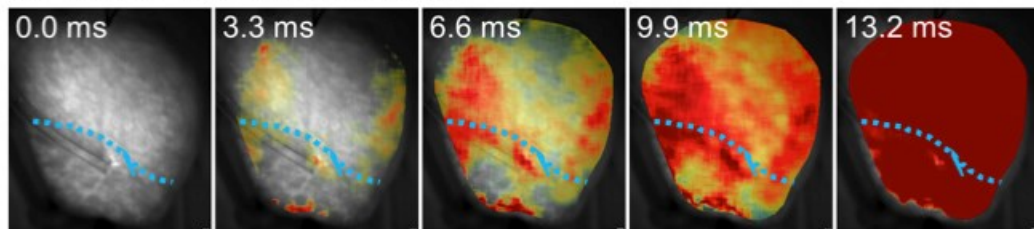


Figure 3.12. Total average incidence of arrhythmias during 60 min of regional ischemia across groups. A comparison of the total incidence of arrhythmias during 60 min of ischemia in the three groups. PVE/10 (black bars; premature ventricular excitations divided by ten); couplet (grey bars; two successive PVEs); VTs (white bars; ventricular tachycardia defined as three or more PVEs). * indicates $p < 0.05$ by one-way ANOVA with Tukey *post-hoc* tests.

A Normal Ventricular Excitation



B Premature Ventricular Excitation

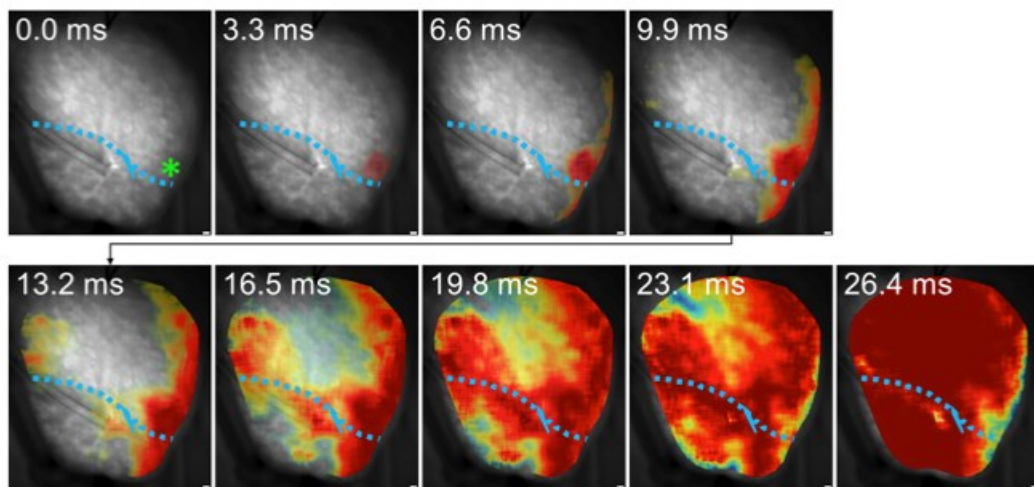


Figure 3.13. *Voltage optical mapping of epicardial activation sequence.* Optical mapping recordings of (A) normal ventricular excitation driven by right atrial pacing and (B) premature ventricular excitation after 25 min of regional ischemia in a *Loaded* heart. Blue line indicates ischemic border; green asterisk indicates PVE origin.

3.3. Aim 3: Effects of Independent Changes in Regional Mechanical Activity

Figure 3.14 shows a representative example of the epicardial distribution of fluorescent microspheres perfused through the cannulated anterior branch of the left circumflex coronary artery, demonstrating the effectiveness of this technique for locally perfusing a region of the myocardium, as well as the effect of local perfusion of 8 μ M blebbistatin on left ventricular pressure and activation. Local blebbistatin perfusion generally caused a decrease in peak left ventricular pressure and an increase in left ventricular end-diastolic pressure, indicating an effect on mechanics similar to that seen during acute regional ischemia. This, however, did not result in a change in the pattern of ventricular activation or in the induction of arrhythmias.

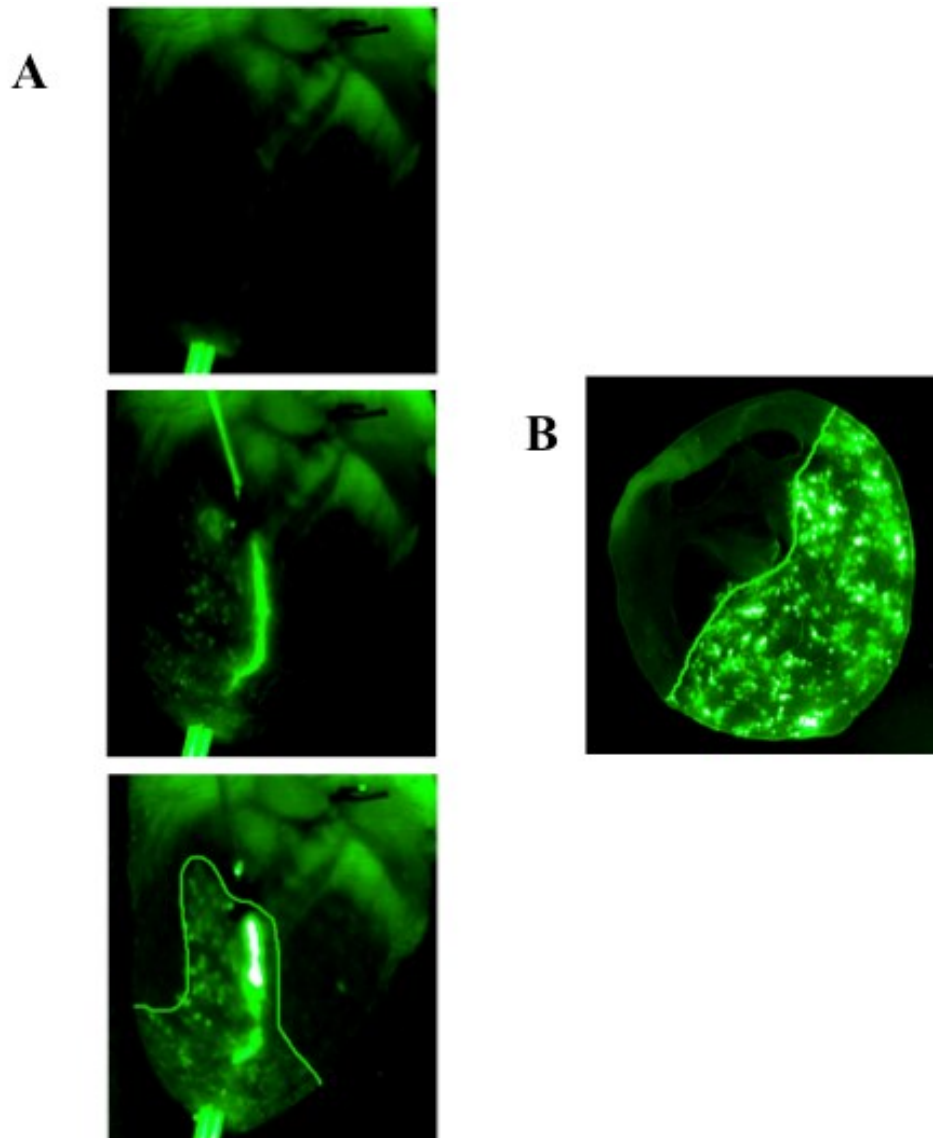


Figure 3.14. *Assessing locally-perfused area using fluorescent microspheres.* **Panel A** shows local perfusion of green microspheres through the cannulated left branch of the circumflex. **Panel B** shows the transmural microsphere distribution in a transverse section of the ventricles, demarcating the locally-perfused region (green microspheres).

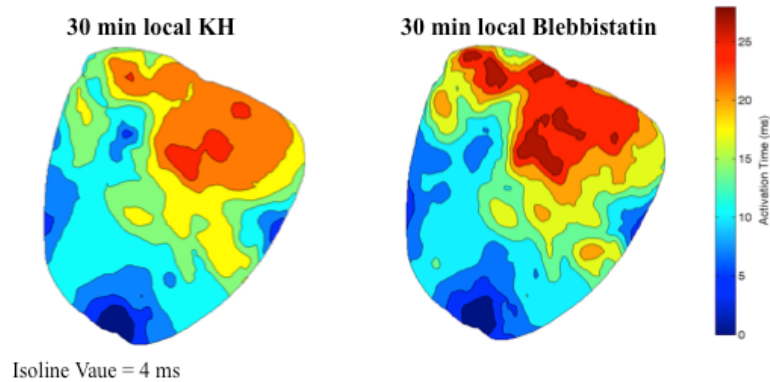
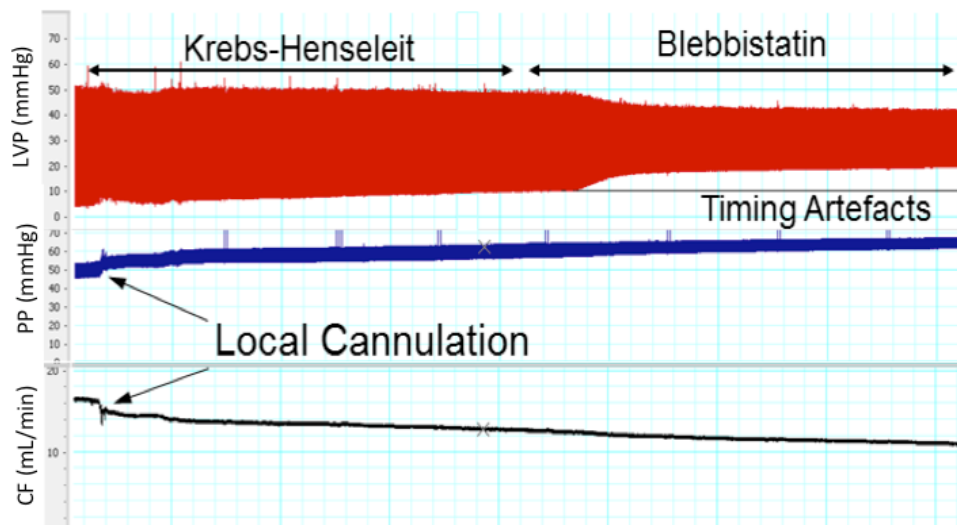
A**B**

Figure 3.15. Activation maps example of ventricular pressures and hemodynamics in locally-perfused heart. (A) Representative optical mapping-derived epicardial activation maps were made to assess altered patterns of conduction after 30 min local perfusion of Krebs-Heinseleit (KH; physiologic buffer) and after 30 min local perfusion of blebbistatin (excitation-contraction uncoupler). 0 ms represents earliest activation (deep blue). Isochrones represent 4 ms steps. (B) Example of experimental tracing of left ventricular pressure (LVP), total perfusion pressure (PP) and total coronary flow (CF) in a locally-perfused heart. Cannulation of the left branch of the circumflex is indicated in the PP and CF tracing by arrows. Timing artefacts (indicated by arrow) are to synchronize our optical recordings. During the first portion of the experiment, Krebs-Henseleit physiologic buffer is locally-perfused (indicated by double-ended arrow). During the second portion, a solution of blebbistatin (double-ended arrow) is locally-perfused.

CHAPTER 4

Discussion

Previous studies have demonstrated a potential role of mechanical effects in arrhythmogenesis during acute regional ischemia. Coronel et al. investigated the nature of ischemia-induced arrhythmias in the swine heart and their results suggest a necessary contribution of ventricular load (Coronel *et al.* 2002). Computational modeling studies using three-dimensional simulations have supported these experimental findings and suggest that activation of cation non-specific stretch-activated channels by altered regional contraction are involved (Jie *et al.* 2010). Yet experimental verification of this, or other potential mechanisms remain outstanding. For this, a small animal model showing a similar importance of mechanics for ventricular arrhythmias during acute regional ischemia is needed.

Thus, the goals of our study were to: (i) develop a physiologically-relevant small animal isolated heart model of acute regional ischemia; (ii) in this model establish the importance of ventricular load and contraction for the induction of arrhythmias; and (iii) determine whether changes in regional mechanical activity alone are sufficient for the induction of arrhythmias.

4.1. Overview of Key Findings

Our first investigation was conducted in Langendorff-perfused isolated rabbit hearts using three experimental groups: Loaded (physiologically-loaded balloon in the left ventricle), Unloaded (empty balloon in the left ventricle) and Non-contracting (excitation-contraction uncoupled left ventricle).

Upon ligation of the anterior branch of the left circumflex coronary artery for 60 min, we observed:

- (i) A significant decrease in APD_{80} and dF_n/dt_{max} in the ischemic region, which stabilized after 30 min (Figures 6 and 7);
- (ii) A significantly higher incidence of PVEs and couplets in the Loaded group than in either the Unloaded or Non-contracting groups, which peaked between 30-35 min (Figures 10 and 11);
- (iii) That PVEs of focal origin occurred at the ischemic border (Figure 12).

Our second investigation was conducted in Loaded Langendorff-perfused isolated rabbit hearts in which the anterior branch of the left circumflex coronary artery was locally perfused with blebbistatin, to regionally affect mechanics. It was found that local excitation-contraction uncoupling affected mechanics, but did not result in the induction of arrhythmias.

4.2. Choice of Experimental Model

4.2.1 Rabbit versus other small animal models

For our investigation, we used isolated hearts from female New Zealand white rabbits.

More and more, mice and rats are becoming the primary experimental model to study human disease. However, the use of rabbits for cardiovascular research has many advantages as a physiologically relevant model.

One advantage of the rabbit is that its cardiac electrophysiology is more comparable to human than other small animals (Nattel *et al.* 2008; Bers 2002; Nerbonne 2000). The

main repolarizing currents in mice flow through channels that are not found in human (Nerbonne 2004). Rabbits express the same repolarizing currents as found in human, namely I_{Kr} and I_{Ks} (Vermeulen *et al.* 1994). Thus, the repolarization phase of the action potential is more comparable in rabbit than it is in rodent. In addition, the small size of rodent hearts can affect the pattern of myocardial excitation. The rabbit heart's effective size allows for wave patterns during arrhythmogenesis to more closely mimic those seen in human myocardium (Panfilov 2006).

Another advantage of the rabbit relates to differences in the composition of sarcomeric proteins between humans and mice (Swynghedauw 1986). Mice predominantly express the *alpha* isoform of the myosin heavy chain (alpha-MHC), whereas the *beta* isoform (beta-MHC) dominates in human (Swynghedauw 1986). In rabbit myocardium, beta-MHC is the major myosin isoform (Kavinsky *et al.* 1984). Our investigation concerns the contribution of cardiac mechanics to the induction of arrhythmias, so an animal model with similar sarcomeric structure as in human may be important.

Rabbit also has similar overall coronary anatomy to human (Burton *et al.* 2011), while having negligible collateral circulation (Maxwell *et al.* 2000), which allows for consistently well-defined areas of ischemia upon ligation of the coronary artery (Toyooka *et al.* 1984). At the same time, myocardial responses to ischemia and pharmacological intervention are more similar to human in rabbit than in rodent (Harken *et al.* 1981).

The rabbit, thus, represents a more relevant model system to study arrhythmias that occur during acute regional ischemia.

4.2.2 Physiological pacing rate and ischemic volume-based exclusion criteria

Throughout all experiments, heart rate was maintained at 4 Hz by atrial pacing. Baseline heart rate varies in Langendorff-perfused rabbit heart preparations (2.5 – 3.5 Hz); therefore, we aimed to control rate across all hearts.

It is well known that arrhythmogenic vulnerability is dependent on heart rate. Heart rate is an important source of variation (Curtis 1998). The onset of ischemia-induced ventricular arrhythmias is delayed by bradycardia (Bernier *et al.* 1989). Moreover, the incidence of arrhythmias becomes very low if heart rate is slow (Bernier *et al.* 1989). Sinus rate in isolated Langendorff-perfused hearts is generally less than *in vivo*, even when temperature and other sources of variation are controlled (Curtis 1998). Thus, in order to avoid bradycardia and to control across all animals and groups, we paced all hearts at 4 Hz, which is in the physiological range.

Another important source of variation for arrhythmogenic vulnerability is size of the ischemic region (Curtis 1998). The incidence of ventricular arrhythmias occurring during acute regional ischemia is reported to exhibit a bell-shaped relationship with ischemic area, with maximum susceptibility occurring when approximately 50% of the left and right ventricles are ischemic (Ridley *et al.* 1992). The reason for this bell-shaped relationship is not known and may indicate that ischemia-induced arrhythmias occur due to an interaction between ischemic and non-ischemic tissue (Ridley *et al.* 1992).

Consequently, we aimed for an average ischemic volume of 40% of the left and right ventricles and excluded any subjects with an ischemic volume of less than 25%.

4.3. Electrophysiological Effects of Regional Ischemia

We observed significant shortening of APD₈₀ and a reduction in dF_n/dt_{max} (which represents reduced dV/dt_{max}) in the ischemic tissue. There was a graded response, as both variables gradually decreased across the ischemic border into the ischemic zone.

Ischemia inducing a significant shortening of the action potential (AP) and a reduction in dF_n/dt_{max} in the affected zone is a hallmark effect of ischemia on action potential morphology (Liu *et al.* 2004). In fact, during acute regional ischemia, the myocardium is generally divided into three zones based on APD: an area of uniformly shortened APD (ischemic zone), an area of normal APD (non-ischemic zone), and a graded area in between (ischemic border zone) (Liu *et al.* 2004). The similarity of our findings compared to past results gave us confidence in the relevance and utility of our acute regional ischemia isolated heart model.

As can be seen in our APD analysis, APs slightly shorten even in the healthy regions of interest closest to the ischemic border. This may be due to an ischemic injury current that electrotonically propagates from the ischemic zone to alter the electrophysiology in the healthy myocardium. This could also be due to altered mechano-electric coupling in the healthy myocardium caused by a changed mechanical environment during ischemia.

It should also be noted that the effect of ischemia on upstroke velocity was much more rapid than it was on APD. Upstroke velocity was immediately slowed after 5 min of ischemia and stabilized at this value for the rest of ischemia. This is much unlike APDs, which gradually shortened and stabilized only after 15-30 min of ischemia. A clear

explanation of why upstroke velocity is impacted faster than APD during ischemia remains elusive.

4.4. Incidence of Arrhythmias

In the present study, there were significantly more arrhythmias (PVEs and couplets) in the Loaded group than in the Unloaded or Non-contracting groups. The highest incidence of arrhythmias in the Loaded group occurred between 30-35 min, a phase of ischemia associated with arrhythmias known as phase 1b.

This result corroborates the findings of Coronel et al., who showed that more arrhythmias occurred in their loaded pig hearts than in their unloaded hearts (Coronel et al. 2002). In addition to ventricular load, the inclusion of the Non-contracting group in our study suggests a more general importance of mechanical activity for arrhythmias, thus providing further support for the hypothesis that changes in ventricular mechanics are necessary for the induction of arrhythmias during acute regional ischemia. The Coronel et al. study also demonstrated that the severity of arrhythmias was significantly greater in loaded hearts. While the difference in VTs between the groups was not significant in our study, there was a trend towards a higher incidence of VTs in the Loaded group. This may represent a feedback of mechanics on the substrate for arrhythmias, or may be a consequence of the occurrence of more ectopic triggers for VTs.

4.5. Origin of Arrhythmias

Our optical mapping recordings show that some arrhythmias occurring in the Loaded group have a focal origin near the ischemic border. This is an intriguing observation since it is known that coronary occlusion results in non-uniform contraction between healthy

and ischemic tissue, resulting in increased tension and stretch in the ischemic region, especially at the ischemic border (Theroux *et al.* 1974; Barrabes *et al.* 1996; Lopex *et al.* 2010). Further, increased arrhythmogenicity at the ischemic border has been previously described (Coronel *et al.* 2002; Jie *et al.* 2010). Thus stretch of ischemic border zone tissue has been hypothesized as a potential contributor to arrhythmias during acute regional ischemia (Coronel *et al.* 2002), acting through mechano-electric coupling mechanisms (Lab 1982; Lerman *et al.* 1985; Reiter *et al.* 1988; Trapero *et al.* 2008).

The notion that myocardial stretch causes arrhythmias during acute regional ischemia is supported by experimental and clinical evidence. For instance, experimental studies have demonstrated that the inducibility of VF is directly related to the increase in end-diastolic length of the ischemic zone (Barrabes *et al.* 2013) and that arrhythmias are more easily induced in isolated hearts by rapid intraventricular volume pulses in acutely ischemic hearts (Parker *et al.* 2004). Stretch-induced arrhythmias have been clinically implicated as cardiac wall motion abnormalities are a strong predictor for arrhythmias (Hansen *et al.* 1990; Lerman *et al.* 1985). By observing an origin of arrhythmias near the ischemic border, our results further support a potential contribution of ischemic border zone stretch as an arrhythmogenic trigger.

Using a stimulation protocol, we also investigated the potential for programmed left ventricular excitations to act as arrhythmic triggers. Additionally, we investigated the incidence of arrhythmias for 30 min of reperfusion after 60 min of acute regional ischemia. However, neither intervention led to an obvious effect on arrhythmogenesis, so we focused on acute regional ischemia and spontaneous ventricular arrhythmias only. Still, these two interventions are of potential interest for future work.

4.6. Necessity versus Sufficiency of Mechanical Effects in Arrhythmia Induction

In our local perfusion experiments, we observed a marked reduction in LV systolic pressure and an increase in LV diastolic pressure with regional administration of blebbistatin. These changes in LV pressure mimic those observed after coronary artery ligation in our acute regional ischemia experiments, suggesting there was a similar effect on regional mechanics. At the same time, activation time was not affected, suggesting that these effects were not due to changes in electrical activity.

Despite this localized alteration of mechanical activity, however, we did not observe arrhythmias in these hearts. This negative result suggests that myocardial mechanical effects are not sufficient for the induction of ventricular arrhythmias. This agrees in part with the simulation studies conducted by Jie et al. in a three-dimensional computational model of the regionally ischemic rabbit heart (Jie *et al.* 2010). Jie et al. showed that ischemia-induced changes in both cardiac mechanics and subcellular ion handling were necessary to sustain ventricular arrhythmias, but that neither were alone sufficient.

However, they also showed that alterations in mechanics associated with ischemia alone can induce PVEs in their model, which was not the case on our experimental model. This difference may reflect that our local mechanical intervention did not affect contraction to the same degree as that which occurs in ischemia, or that the computational model needs refinement. The lack of arrhythmias in our local perfusion experiments may also be explained by the insufficient stretch effects of regional non-contraction. During regional ischemia, the affected area firstly suffers depressed contractility and then becomes stiffened. Since our local perfusion experiments only studied regional non-contraction, we neglected regional stiffening which may have acted as a strong arrhythmic trigger. In

the future, it would be intriguing to regionally *stiffen* myocardium and study the effect on arrhythmogenesis.

4.7. Mechanisms Underlying the Mechanical Contribution to Arrhythmias during Acute Regional Ischemia

In this study we have established an experimental small animal isolated heart model of acute regional ischemia in which mechanical effects make a necessary contribution to ventricular arrhythmias. Future studies using this model will enable the elucidation of underlying mechanisms. There are numerous MEC pathways that may be involved.

4.7.1 SAC_{NS}

In general, cardiac stretch-activated channels are specific mechanosensitive ion channels whose gating completely depends on sarcolemmal stretch (Reed *et al.* 2014). Stretch-activated channels were first discovered in non-myocytes in 1984 (Guharay & Sachs 1984), and shortly thereafter, two types of cardiac stretch-activated channels were identified in myocytes: SAC_{NS} and SAC_K (Craelius *et al.* 1988; Kim 1992). As SAC_{NS} cause membrane depolarization (as opposed to repolarization for SAC_K) in most phases of the cardiac action potential, they are a potential candidate in the context of stretch-induced arrhythmias.

SAC_{NS} opening depolarizes the membrane through Na⁺ and possibly Ca²⁺ influx (Reed *et al.* 2014). There are several pharmacological inhibitors of SAC_{NS} that have been identified. For instance, Zeng *et al.* have demonstrated a strong inhibition of SAC_{NS} using gadolinium ions (Gd³⁺) (Zeng *et al.* 2000), while Sachs *et al.* have identified the GsMTx-4 peptide isolated from Chilean tarantula venom as a powerful inhibitor of SAC_{NS}

(Bowman *et al.* 2007). These have both been employed to test for a contribution of SAC_{NS} in arrhythmias during acute regional ischemia.

To test for the involvement of SAC_{NS} in arrhythmia during acute regional ischemia, Barrabes *et al.* infused 40 μM Gd^{3+} directly into the ischemic area post-coronary occlusion in the open-chest pig (Barrabes *et al.* 2006). They found that intracoronary infusion of Gd^{3+} failed to reduce the incidence of arrhythmias (ventricular tachycardia or fibrillation) as compared to untreated pigs. However, while stretch-induced arrhythmias can be suppressed *in vitro* by Gd^{3+} (Bode *et al.* 2000; Hansen *et al.* 1991; Kiseleva *et al.* 2000; Yang & Sachs 1989; Zeng *et al.* 2000), a major limitation of its use *in vivo* is that this ion has a strong binding affinity to anions present in the blood, thereby hindering its utility to test SAC_{NS} in normal physiological settings (Caldwell *et al.* 1998). Thus, plasma concentration may have been too low for adequate block of SAC_{NS}, especially as it was infused for only 2 min, which may account for the negative result.

This work was followed by the use of GsMTx-4 in the same experimental model (Barrabes *et al.* 2015), which is favourable as it is a more potent blocker of SAC_{NS} and has better bioavailability than Gd^{3+} . In this study, global intravenous infusion of GsMTx-4 also did not suppress ventricular arrhythmias (PVEs, ventricular tachycardia or fibrillation) following coronary occlusion in the open-chest pig. This study was also potentially limited, however, as the optimal dosage for *in vivo* administration of GsMTx-4 has not been established and the administered dose (57 $\mu\text{g}/\text{kg}$ bolus and 3.8 $\mu\text{g}/\text{kg}/\text{min}$ infusion) and resulting plasma concentration (170 nM) may have been inadequate (in the isolated rabbit heart 200 nM is necessary to reduce stretch-induced atrial fibrillation

(Bode *et al.* 2001), while 500 nm is needed for the suppression of local mechanically-induced ventricular excitation (Quinn *et al.* 2011)).

Nonetheless, these findings may argue against a major role for SAC_{NS} in the induction of ventricular arrhythmias during acute regional ischemia, so it is pertinent to consider other potential mechanisms.

4.7.2 Stretch-induced changes of intracellular Ca²⁺ handling

Stretch-induced changes in intracellular Ca²⁺ handling may also contribute to arrhythmogenesis during acute regional ischemia. Stretch of myocardium has been shown to increase Ca²⁺ release from the SR, which directly increases cytoplasmic [Ca²⁺].

Specifically, myocardial stretch increases the open probability of the ryanodine receptor, through which Ca²⁺ is extruded from the SR into the cytoplasm (Iribe & Kohl 2008; Gamble *et al.* 1992; Iribe *et al.* 2009 Prosser *et al.* 2011; Prosser *et al.* 2013).

Additionally, stretch potentiates troponin-C binding affinity for Ca²⁺, so that more Ca²⁺ ions are bound upon increased stretch (Allen & Kentish 1988; Allen & Kurihara 1982).

Subsequently, more Ca²⁺ is released upon relaxation of the stretched myocardium, thereby increasing cytoplasmic [Ca²⁺] (Wakayama *et al.* 2005). This increased release of Ca²⁺ from troponin-C is explained by a rapid reduction of its affinity for calcium upon muscular relaxation, owing to a reduction in the number of calcium-activated cross-bridges (Allen & Kentish 1988). Therefore, stretch can cause an increased cytoplasmic [Ca²⁺] during contraction and relaxation. This, on top of the already elevated intracellular and SR [Ca²⁺] during ischemia (Lee *et al.* 1988), may lead to further Ca²⁺-induced Ca²⁺ release from the SR, resulting in calcium waves that can depolarize the sarcolemma through electrogenic extrusion of Ca²⁺ *via* the Na⁺/Ca²⁺-exchanger (Miura *et al.* 2008; ter

Keurs & Boyden 2007) and act as an arrhythmic trigger (ter Keurs & Boyden 2007). This hypothesis is supported by numerous experimental studies in different model systems.

(A) Non-uniform contraction and Ca^{2+} waves

The effect of non-uniform contraction on Ca^{2+} handling has been investigated in isolated rat cardiac trabeculae muscle (Wakayama *et al.* 2005; Miura *et al.* 2010; Miura *et al.* 2013). In this model, contractile heterogeneity of the trabecular muscle is generated by exposing a segment of the preparation to a small jet of solution with a composition that reduces excitation-contraction coupling and contractile force.

For instance, by exposing a segment of trabecular muscle to a jet solution containing 2,3-butanedione monoxime (BDM; an excitation-contraction uncoupler), Wakayama *et al.* reduced local contraction, so that there was non-uniformity in contraction similar to that seen during acute regional ischemia (Wakayama *et al.* 2005). Cytoplasmic $[Ca^{2+}]$ increased during jet solution treatment, and frequent Ca^{2+} waves were elicited from the contractile border zone, a region in which contraction was partially suppressed. They showed that Ca^{2+} waves were caused by non-uniformity of sarcomere force generation and the resulting surge of Ca^{2+} during relaxation of border zone muscle stretched during contraction. This was followed by studies in which they demonstrated that sustained arrhythmias could be induced by programmed stimulation only in non-uniformly contracting muscle (induced with a jet of blebbistatin) in which Ca^{2+} surges preceded synchronous increases in intracellular $[Ca^{2+}]$ (Miura *et al.* 2010), as well as in muscle with local increases in $[K^+]_o$ (as occurs in ischemia) (Miura *et al.* 2013), thus implicating non-uniform contraction and stretch at the border between healthy and non-contracting muscle in the induction of arrhythmias during ischemia.

(B) Stretch and reactive oxygen species-induced Ca^{2+} release

The ability of stretch to cause spontaneous SR Ca^{2+} release has been studied in isolated cardiac myocytes (Iribe & Kohl 2008; Prosser *et al.* 2011; Prosser *et al.* 2013). Ca^{2+} sparks, the elementary unit of excitation-contraction coupling (Williams *et al.* 2011; Cheng & Lederer 2008; Cheng *et al.* 2010), occur at a low rate during diastole in ventricular myocytes (Prosser *et al.* 2013). If a myocyte is stretched within a physiological range, the rate of calcium sparks increases rapidly and reversibly (Prosser *et al.* 2011; Iribe *et al.* 2009). This has been shown by Prosser *et al.* to depend on a stretch-induced increase in production of reactive oxygen species (ROS) (Prosser *et al.* 2010), chemically reactive molecules containing oxygen ions and peroxides that are naturally formed during metabolism, and whose production is increased with ischemia (Carmeliet 1999). In the isolated ventricular myocyte, cell stretch activates local ROS production through *NADPH oxidase 2* (Nox2), by a process requiring an intact microtubule network (Prosser *et al.* 2013). The resulting stretch-induced ROS surge leads to post-translational modification of ryanodine receptors, increasing their sensitivity to cytoplasmic Ca^{2+} , thus promoting Ca^{2+} -induced Ca^{2+} release from the SR, cytoplasmic Ca^{2+} overload, and subsequent effects on cellular electrophysiology. This work has been followed by studies in isolated trabeculae muscle by Miura *et al.*, which have shown that stretch-induced ROS production also increases Ca^{2+} wave velocity, also through the microtubule network, in a stretch-magnitude dependent manner (Miura *et al.* 2013; Miura *et al.* 2015). Especially relevant for border zone stretch in ischemia, stretch-induced ROS production is enhanced by increased amplitude and frequency of stretch (Prosser *et al.* 2013), and the resulting increase in diastolic Ca^{2+} spark frequency may contribute to the

increase in cytosolic and SR Ca^{2+} that occurs with ischemia (Mattiuzzi *et al.* 2015), creating a positive, highly arrhythmogenic, feedback loop.

(C) Inhibition of arrhythmias by Ca^{2+} chelators

Further evidence for a role of Ca^{2+} in acute ischemia-induced arrhythmias comes from studies using chelators of intracellular Ca^{2+} . It has been reported by Xing *et al.* that Ca^{2+} -induced DADs and triggered activity may underlie a majority of focal VTs in ischemic endocardium (Xing & Martins 2004). This is supported by a study from Wu *et al.* demonstrating that pretreatment with BAPTA-AM (a potent Ca^{2+} chelator) attenuates the occurrence of ventricular arrhythmias in globally ischemic hearts (Wu *et al.* 2011).

(D) Inhibition of arrhythmias by $\text{Na}^+/\text{Ca}^{2+}$ -exchanger antagonists

Alterations in Ca^{2+} handling have been implicated in the induction of VTs in other cardiac conditions in which mechano-electric heterogeneity have been implicated in arrhythmias, such as long-QT syndrome-induced *Torsade de Pointes* (a form of polymorphic VT characterized by a gradual change in the amplitude and twisting of the QRS complexes around the isoelectric line) (ter Bekke & Volders 2012). For instance, there is strong evidence that Ca^{2+} -induced EADs may be the most important trigger of *Torsade de Pointes* (Volders *et al.* 2000).

While the cellular mechanisms for EADs are not fully understood, the $\text{Na}^+/\text{Ca}^{2+}$ -exchanger has been implicated in their generation (Milberg *et al.* 2008). Due to its stoichiometry, the $\text{Na}^+/\text{Ca}^{2+}$ -exchanger works electrogenically, producing an inward electrical current during sarcoplasmic reticulum Ca^{2+} release. It is thought that the precipitator of EADs is a spontaneous release of Ca^{2+} from the SR, causing a sudden

increase in cytosolic Ca^{2+} , which leads to $\text{Na}^+/\text{Ca}^{2+}$ -exchanger activation, depolarizing the membrane such that a PVE is triggered (Sipido *et al.* 2006). To support this, Milberg *et al.* demonstrated that the $\text{Na}^+/\text{Ca}^{2+}$ -exchanger blocker SEA0400 suppressed EADs, reduced dispersion of repolarization, and ultimately reduced the incidence of *Torsade de Pointes* in an isolated rabbit heart model (Milberg *et al.* 2008), thus demonstrating that release of Ca^{2+} can indeed lead to ventricular arrhythmias *via* activation of the $\text{Na}^+/\text{Ca}^{2+}$ -exchanger. Interestingly in this context, it has also been shown that in established ventricular fibrillation in the rabbit heart, acceleration of wave speed by stretch is reduced by the $\text{Na}^+/\text{Ca}^{2+}$ -exchanger blocker KB-R7943 (Chorro *et al.* 2009), which may be related to stretch-induced Ca^{2+} wave acceleration seen with increased ROS (Miura *et al.* 2013).

4.7.3 Effects on metabolism

Another possible contributor to the differences in arrhythmogenicity seen between the groups in our study might be differences in metabolic demand between Loaded, Unloaded, and Non-contracting hearts. Oxygen and energy requirements have been shown to vary widely between these three modes of isolated heart preparation (Kuzmiak-Glancy *et al.* 2015), and differences in the imbalance of oxygen supply and energy demand could cause large differences in ATP synthesis, NADH production, and pH levels between the groups.

A recent study by Wengrowski *et al.* utilized fluorescent imaging of epicardial NADH (fNADH) to gain insight into the oxidative state of cardiac tissue between different isolated heart preparations (Wengrowski *et al.* 2014). An increased mismatch in oxygen supply and demand causes NADH levels to increase and this translates into a stronger fNADH signal. In their study, they compared fNADH signals in Loaded (working heart

mode), Unloaded (with no balloon insertion), and Non-contracting (blebbistatin treated) hearts during global no-flow ischemia. They found that ATP and oxygen demands were highest in Loaded and lowest in Non-contracting hearts. In the Non-contracting hearts, NADH levels rose much slower and took three times longer to reach a plateau during ischemia than the other two groups. This indicates a significantly lower energy utilization in the Non-contracting heart.

While this might be of concern for our study, despite this difference in energy demand NADH levels reached a similar plateau in all three groups by 5 min of no-flow ischemia. This suggests that after the initial phase of ischemia, all oxygen has been depleted in the ischemic tissue and the metabolic state is similar. In our experiments, the highest incidence of arrhythmias, and those which we are primarily interested in, occurred between 25 – 35 min after coronary artery occlusion and at this time point the metabolic state may not significantly differ across the groups.

4.8. Conclusion & Future Directions

In conclusion, we have now established an experimental small animal isolated heart model of acute regional ischemia in which the mechanical contribution to arrhythmias can be assessed. Our findings suggest that there is a necessary contribution of both ventricular load and contraction for arrhythmogenesis in the context of acute regional ischemia. Our research suggests that altered cardiac mechanics *alone* are not sufficient for the induction and sustenance of ventricular arrhythmias.

Going forward, our future work will focus on elucidating the underlying mechanisms involved in these mechanically-induced arrhythmias. Based on the potential mechanisms discussed above, this will include:

- (i) Optical measurement of changes in myocardial deformation during acute regional ischemia and with local mechanical interventions, using epicardial surface markers;
- (ii) Pharmacological interventions to assess potential MEC mechanisms, such as SAC_{NS} block, block of ROS production, Ca²⁺ chelation, and RyR stabilization;
- (iii) Comparison of metabolism between the three groups; by HPLC measurement of ATP;
- (iv) Investigation of possible interactions between altered mechanics and components of ischemia (such as activation of mechano-sensitive $I_{K(ATP)}$ or increased $[K^+]_o$) by their independent variation using our local perfusion model.

This work had addressed certain shortcomings in our understanding of ischemia-induced ventricular arrhythmias. This is an essential step in the journey for improved therapeutic and preventative innovations. A more thorough understanding of the contribution of mechano-electric feedback may lead us to novel mechano-sensitive pharmacological and therapeutic targets.

The ultimate hope is that further basic science research in the field of mechanically-induced arrhythmias will help reduce the incidence of arrhythmia-related death in disease. Seeing as this is still the leading cause of death in our nation this area of research touches many lives. Still, much work is to be done if we are to fully understand the etiology of cardiovascular disease and death.

REFERENCES

- Allen, D. G., Morris, P. G., Orchard, C. H., & Pirolo, J. S. (1985). A nuclear magnetic resonance study of metabolism in the ferret heart during hypoxia and inhibition of glycolysis. *The Journal of Physiology*, 361(1), 185-204.
- Allen, D. G., & Kentish, J. C. (1988). Calcium concentration in the myoplasm of skinned ferret ventricular muscle following changes in muscle length. *The Journal of Physiology*, 407(1), 489-503.
- Allen, D. G., & Kurihara, S. (1982). The effects of muscle length on intracellular calcium transients in mammalian cardiac muscle. *The Journal of Physiology*, 327(1), 79-94.
- Anderson, S. E., Cala, P. M., Steenbergen, C., London, R. E., & Murphy, E. (1991). Effects of Hypoxia and Acidification on Myocardial Na and Ca. *Annals of the New York Academy of Sciences*, 639(1), 453-455.
- Allen, D. G., & Orchard, C. H. (1987). Myocardial contractile function during ischemia and hypoxia. *Circulation Research*, 60(2), 153-168.

Ambrosi, P., Habib, G., Kreitmann, B., Faugere, G., & Metras, D. (1995). Valsalva manoeuvre for supraventricular tachycardia in transplanted heart recipient. *The Lancet*, 346(8976), 713.

Allessie, M. A., Bonke, F. I., & Schopman, F. J. (1977). Circus movement in rabbit atrial muscle as a mechanism of tachycardia. III. The "leading circle" concept: a new model of circus movement in cardiac tissue without the involvement of an anatomical obstacle. *Circulation research*, 41(1), 9.

Bode, F., Katchman, A., Woosley, R. L., & Franz, M. R. (2000). Gadolinium decreases stretch-induced vulnerability to atrial fibrillation. *Circulation*, 101(18), 2200-2205.

Bode, F., Franz, M. R., Wilke, I., Bonnemeier, H., Schunkert, H., & Wiegand, U. K. (2006). Ventricular fibrillation induced by stretch pulse: implications for sudden death due to commotio cordis. *Journal of cardiovascular electrophysiology*, 17(9), 1011-1017.

Bode, F., Sachs, F., & Franz, M. R. (2001). Tarantula peptide inhibits atrial fibrillation. *Nature*, 409(6816), 35-36.

Bowman, C. L., Gottlieb, P. A., Suchyna, T. M., Murphy, Y. K., & Sachs, F. (2007). Mechanosensitive ion channels and the peptide inhibitor GsMTx-4: history, properties, mechanisms and pharmacology. *Toxicon*, 49(2), 249-270.

Burton, R. A., Quinn, T. A., & Kohl, P. (2011). Rediscovering the third coronary artery: A second right coronary artery is not at all unusual, as described here from Oxford, England. *European heart journal*, 32(12), 1435-1437.

Bers, D. M. (2002). Cardiac Na/Ca exchange function in rabbit, mouse and man: what's the difference?. *Journal of molecular and cellular cardiology*, 34(4), 369-373.

Barrabés, J. A., Garcia-Dorado, D., Ruiz-Meana, M., Piper, H. M., Solares, J., González, M. A., & Soler, J. S. (1996). Myocardial segment shrinkage during coronary reperfusion in situ. *Pflügers Archiv*, 431(4), 519-526.

Barrabés, J. A., Garcia-Dorado, D., Padilla, F., Agulló, L., Trobo, L., Carballo, J., & Soler-Soler, J. (2002). Ventricular fibrillation during acute coronary occlusion is related to the dilation of the ischemic region. *Basic research in cardiology*, 97(6), 445-451.

Barrabés, J. A., Figueras, J., Candell-Riera, J., Agulló, L., Inserte, J., & Garcia-Dorado, D. (2013). Distension of the ischemic region predicts increased ventricular fibrillation inducibility following coronary occlusion in swine. *Revista Española de Cardiología (English Edition)*, 66(3), 171-176.

Barrabés, J. A., Garcia-Dorado, D., Agulló, L., Rodríguez-Sinovas, A., Padilla, F., Trobo, L., & Soler-Soler, J. (2006). Intracoronary infusion of Gd³⁺ into ischemic region does not suppress phase Ib ventricular arrhythmias after coronary occlusion in swine. *American Journal of Physiology-Heart and Circulatory Physiology*, 290(6), H2344-H2350.

Barrabés, J. A., Inserte, J., Agulló, L., Rodríguez-Sinovas, A., Albuquerque-Béjar, J. J., & Garcia-Dorado, D. (2015). Effects of the Selective Stretch-Activated Channel Blocker GsMtx4 on Stretch-Induced Changes in Refractoriness in Isolated Rat Hearts and on Ventricular Premature Beats and Arrhythmias after Coronary Occlusion in Swine.

Böhm, A., Pintér, A., & Préda, I. (2002). Ventricular tachycardia induced by a pacemaker lead. *Acta cardiologica*, 57(1), 23-24.

Bainbridge, F. A. (1915). The influence of venous filling upon the rate of the heart. *The Journal of physiology*, 50(2), 65-84.

Bell, R. M., Mocanu, M. M., & Yellon, D. M. (2011). Retrograde heart perfusion: the Langendorff technique of isolated heart perfusion. *Journal of molecular and cellular cardiology*, 50(6), 940-950.

Bernier, M., Curtis, M. J., & Hearse, D. J. (1989). Ischemia-induced and reperfusion-induced arrhythmias: importance of heart rate. *American Journal of Physiology-Heart and Circulatory Physiology*, 256(1), H21-H31.

Chorro, F. J., Trapero, I., Such-Miquel, L., Pelechano, F., Mainar, L., Canoves, J., & Such, L. (2009). Pharmacological modifications of the stretch-induced effects on ventricular fibrillation in perfused rabbit hearts. *American Journal of Physiology-Heart and Circulatory Physiology*, 297(5), H1860-H1869.

Cheng, H., & Lederer, W. J. (2008). Calcium sparks. *Physiological reviews*, 88(4), 1491-1545.

Cheng, H., Lederer, W. J., & Cannell, M. B. (1993). Calcium sparks: elementary events underlying excitation-contraction coupling in heart muscle. *Science*, 262(5134), 740-744.

Caldwell, R. A., Clemo, H. F., & Baumgarten, C. M. (1998). Using gadolinium to identify stretch-activated channels: technical considerations. *American Journal of Physiology-Cell Physiology*, 275(2), C619-C621.

Cobb, L. A., Fahrenbruch, C. E., Olsufka, M., & Copass, M. K. (2002). Changing incidence of out-of-hospital ventricular fibrillation, 1980-2000. *Jama*, 288(23), 3008-3013.

Carmeliet, E. (1999). Cardiac ionic currents and acute ischemia: from channels to arrhythmias. *Physiological reviews*, 79(3), 917-1017.

Clarke, K., Stewart, L. C., Neubauer, S., Balschi, J. A., Smith, T. W., Ingwall, J. S., & Springer, C. S. (1993). Extracellular volume and transsarcolemmal proton movement during ischemia and reperfusion: a ³¹P NMR spectroscopic study of the isovolumic rat heart. *NMR in biomedicine*, 6(4), 278-286.

Coraboeuf, E., Deroubaix, E., & Coulombe, A. (1980). Acidosis-induced abnormal repolarization and repetitive activity in isolated dog Purkinje fibers. *Journal de physiologie*, 76(2), 97.

Craelius, W., Chen, V., & El-Sherif, N. (1988). Stretch activated ion channels in ventricular myocytes. *Bioscience reports*, 8(5), 407-414.

Colquhoun, D., Neher, E., Reuter, H., & Stevens, C. F. (1981). Inward current channels activated by intracellular Ca in cultured cardiac cells.

Callewaert, G., Carmeliet, E., & Vereecke, J. (1984). Single cardiac Purkinje cells: general electrophysiology and voltage-clamp analysis of the pace-maker current. *The Journal of Physiology*, 349, 643.

Carmeliet, E. & Vereecke, J. (2002). Arrhythmias. In *Cardiac Cellular Electrophysiology* (pp. 279 – 305). Norwell, MA: Kluwer Academic Publishers.

Coronel, R., Wilms-Schopman, F. J., Opthof, T., Van Capelle, F. J., & Janse, M. J. (1991). Injury current and gradients of diastolic stimulation threshold, TQ potential, and extracellular potassium concentration during acute regional ischemia in the isolated perfused pig heart. *Circulation Research*, 68(5), 1241-1249.

Craelius, W., Chen, V., & El-Sherif, N. (1988). Stretch activated ion channels in ventricular myocytes. *Bioscience reports*, 8(5), 407-414.

Coste, B., Mathur, J., Schmidt, M., Earley, T. J., Ranade, S., Petrus, M. J., & Patapoutian, A. (2010). Piezo1 and Piezo2 are essential components of distinct mechanically activated cation channels. *Science*, 330(6000), 55-60.

Cayla, G., Macia, J. C., & Pasquie, J. L. (2007). Images in cardiovascular medicine. Precordial thump in the catheterization laboratory experimental evidence for Commotio cordis. *Circulation*, 115(11), e332.

Coronel, R., Trayanova, N.A., Jie X. & Janse, M.J. (2011) Stretch-induced arrhythmias in ischaemia. In *Cardiac Mechano-Electric Coupling and Arrhythmias* (pp. 352 – 358). New York, NY: Oxford University Press Inc.

Califf, R. M., Burks, J. M., Behar, V. S., Margolis, J. R., & Wagner, G. S. (1978). Relationships among ventricular arrhythmias, coronary artery disease, and angiographic and electrocardiographic indicators of myocardial fibrosis. *Circulation*, 57(4), 725-732.

Dosdall, D.J. and Ideker, R.E. (2014). Mechanisms of ventricular tachycardia and fibrillation. In *Cardiac Electrophysiology: From Cell to Bedside* (pp. 475 – 482). Philadelphia, PA: Elsevier.

De Mello, W. C. (1975). Effect of intracellular injection of calcium and strontium on cell communication in heart. *The Journal of Physiology*, 250(2), 231-245.

Deck, K. A. (1964). Dehnungseffekte am spontanschlagenden, isolierten Sinusknoten. *Pflügers Archiv European Journal of Physiology*, 280(2), 120-130.

Diaz, M. E., Cook, S. J., Chamunorwa, J. P., Trafford, A. W., Lancaster, M. K., O'Neill, S. C., & Eisner, D. A. (1996). Variability of spontaneous Ca²⁺ release between different rat ventricular myocytes is correlated with Na⁺-Ca²⁺ exchange and [Na⁺]_i. *Circulation Research*, 78(5), 857-862.

Donoso, P., Mill, J. G., O'Neill, S. C., & Eisner, D. A. (1992). Fluorescence measurements of cytoplasmic and mitochondrial sodium concentration in rat ventricular myocytes. *The Journal of physiology*, 448(1), 493-509.

de Vreede-Swagemakers, J. J., Gorgels, A. P., Dubois-Arbouw, W. I., Van Ree, J. W., Daemen, M. J., Houben, L. G., & Wellens, H. J. (1997). Out-of-hospital cardiac arrest in the 1990s: a population-based study in the Maastricht area on incidence, characteristics and survival. *Journal of the American College of Cardiology*, 30(6), 1500-1505.

Ehara, T., Noma, A., & Ono, K. (1988). Calcium-activated non-selective cation channel in ventricular cells isolated from adult guinea-pig hearts. *The Journal of Physiology*, 403, 117.

Franz, M. R., Burkhoff, D., Yue, D., & Sagawa, K. (1989). Mechanically induced action potential changes and arrhythmia in isolated and in situ canine hearts. *Cardiovascular research*, 23(3), 213-223.

Friel, D. D., & Bean, B. P. (1988). Two ATP-activated conductances in bullfrog atrial cells. *The Journal of general physiology*, 91(1), 1-27.

Friedrich, M., Benndorf, K., Schwalb, M., & Hirche, H. J. (1990). Effects of anoxia on K and Ca currents in isolated guinea pig cardiocytes. *Pflügers Archiv*, 416(1-2), 207-209.

Gamble, J., Taylor, P. B., & Kenno, K. A. (1992). Myocardial stretch alters twitch characteristics and Ca²⁺ loading of sarcoplasmic reticulum in rat ventricular muscle. *Cardiovascular research*, 26(9), 865-870.

Glitsch, H. G., & Tappe, A. (1995). Change of Na⁺ pump current reversal potential in sheep cardiac Purkinje cells with varying free energy of ATP hydrolysis. *The Journal of Physiology*, 484(3), 605-616.

Gambassi, G., Hansford, R. G., Sollott, S. J., Hogue, B. A., Lakatta, E. G., & Capogrossi, M. C. (1993). Effects of acidosis on resting cytosolic and mitochondrial Ca²⁺ in mammalian myocardium. *The Journal of general physiology*, 102(3), 575-597.

Griese, M., Perlitz, V., Jüngling, E., & Kammermeier, H. (1988). Myocardial performance and free energy of ATP-hydrolysis in isolated rat hearts during graded hypoxia, reoxygenation and high K⁺-perfusion. *Journal of molecular and cellular cardiology*, 20(12), 1189-1201.

Guharay, F., & Sachs, F. (1984). Stretch-activated single ion channel currents in tissue-cultured embryonic chick skeletal muscle. *The Journal of physiology*, 352(1), 685-701.

Hansen, D. E., Craig, C. S., & Hondeghem, L. M. (1990). Stretch-induced arrhythmias in the isolated canine ventricle. Evidence for the importance of mechanoelectrical feedback. *Circulation*, 81(3), 1094-1105.

Hansen, D. E., Borganelli, M., Stacy, G. P., & Taylor, L. K. (1991). Dose-dependent inhibition of stretch-induced arrhythmias by gadolinium in isolated canine ventricles. Evidence for a unique mode of antiarrhythmic action. *Circulation Research*, 69(3), 820-831.

Harken, A. H., Simson, M. B., Haselgrove, J., Wetstein, L., Harden, W. R., & Barlow, C. H. (1981). Early ischemia after complete coronary ligation in the rabbit, dog, pig, and monkey. *American Journal of Physiology-Heart and Circulatory Physiology*, 241(2), H202-H210.

Hirche, H., Hoehner, M., & Risse, J. H. (1987). Inotropic changes in ischaemic and non-ischaemic myocardium and arrhythmias within the first 120 minutes of coronary occlusion in pigs. In *Cardiac Energetics* (pp. 301-310). Steinkopff.

Han, X., & Ferrier, G. R. (1995). Contribution of Na⁺-Ca²⁺ exchange to stimulation of transient inward current by isoproterenol in rabbit cardiac Purkinje fibers. *Circulation research*, 76(4), 664-674.

Haigney, M. C., Lakatta, E. G., Stern, M. D., & Silverman, H. S. (1994). Sodium channel blockade reduces hypoxic sodium loading and sodium-dependent calcium loading. *Circulation*, 90(1), 391-399.

Haldón, J. L., Quero, M. F., Mancha, F., Urbano, J. A., Guisado, A., Villa, M., & Martínez, Á. M. (2010). NT-proBNP y variables ecocardiográficas en el infarto con elevación del ST tratado con angioplastia primaria: relación entre ambos y utilidad como predictores de remodelado ventricular. *Revista española de cardiología*, 63(9), 1019-1027.

Iribe, G., & Kohl, P. (2008). Axial stretch enhances sarcoplasmic reticulum Ca²⁺ leak and cellular Ca²⁺ reuptake in guinea pig ventricular myocytes: experiments and models. *Progress in biophysics and molecular biology*, 97(2), 298-311.

Iribe, G., Ward, C. W., Camelliti, P., Bollensdorff, C., Mason, F., Burton, R. A., & Kohl, P. (2009). Axial stretch of rat single ventricular cardiomyocytes causes an acute and transient increase in Ca²⁺ spark rate. *Circulation research*, 104(6), 787-795.

Janse, M. J., & Wit, A. L. (1989). Electrophysiological mechanisms of ventricular arrhythmias resulting from myocardial ischemia and infarction. *Physiol Rev*, 69(4), 1049-1169.

Jabr, R. I., & Cole, W. C. (1993). Alterations in electrical activity and membrane currents induced by intracellular oxygen-derived free radical stress in guinea pig ventricular myocytes. *Circulation research*, 72(6), 1229-1244.

Jabr, R. I., & Cole, W. C. (1995). Oxygen-derived free radical stress activates nonselective cation current in guinea pig ventricular myocytes role of sulfhydryl groups. *Circulation research*, 76(5), 812-824.

Janse, M. J. (2003). A brief history of sudden cardiac death and its therapy. *Pharmacology & therapeutics*, 100(1), 89-99.

Jie, X., Gurev, V., & Trayanova, N. (2010). Mechanisms of mechanically induced spontaneous arrhythmias in acute regional ischemia. *Circulation research*, 106(1), 185-192.

Janse, M. J., Opthof, T., & Kléber, A. G. (1998). Animal models of cardiac arrhythmias. *Cardiovascular research*, 39(1), 165-177.

Kohl, P. (2009). Cardiac stretch-activated channels and mechano-electric transduction. In D. P. Zipes & J. Jalife (Eds.), *Cardiac electrophysiology: From cell to bedside* (pp. 115–126). Philadelphia: Saunders.

Kohl, P., Sachs, F., & Franz, M. R. (Eds.). (2011). *Cardiac mechano-electric coupling and arrhythmias*. Oxford University Press.

Kuzmiak-Glancy, S., Jaimes, R., Wengrowski, A. M., & Kay, M. W. (2015). Oxygen demand of perfused heart preparations: How electromechanical function and inadequate oxygenation affect physiology and optical measurements. *Experimental physiology*.

Kamkin, A., Kiseleva, I., & Isenberg, G. (2000). Stretch-activated currents in ventricular myocytes: amplitude and arrhythmogenic effects increase with hypertrophy. *Cardiovascular research*, 48(3), 409-420.

Kim, D. (1992). A mechanosensitive K⁺ channel in heart cells. Activation by arachidonic acid. *The Journal of General Physiology*, 100(6), 1021-1040.

Kleber, A. G. (1983). Resting membrane potential, extracellular potassium activity, and intracellular sodium activity during acute global ischemia in isolated perfused guinea pig hearts. *Circulation Research*, 52(4), 442-450.

Kaila, K., & Vaughan-Jones, R. D. (1987). Influence of sodium-hydrogen exchange on intracellular pH, sodium and tension in sheep cardiac Purkinje fibres. *The Journal of Physiology*, 390(1), 93-118.

Kihara, Y., Grossman, W., & Morgan, J. P. (1989). Direct measurement of changes in intracellular calcium transients during hypoxia, ischemia, and reperfusion of the intact mammalian heart. *Circulation Research*, 65(4), 1029-1044.

Knopf, H., McDonald, F. M., Bischoff, A., Hirche, H., & Addicks, K. (1988). Effect of propranolol on early postischemia arrhythmias and noradrenaline and potassium release of ischemic myocardium in anesthetized pigs. *Journal of cardiovascular pharmacology*, 12, S41-47.

Kiyosue, T., Aomine, M., & Aritam M. (1984). Lysophosphatidylcholine decreases single channel conductance of inward rectifier K channel in mammalian ventricular myocytes. *The Japanese journal of physiology*, 34(2), 369-373.

Kleber, A. G. (1983). Resting membrane potential, extracellular potassium activity, and intracellular sodium activity during acute global ischemia in isolated perfused guinea pig hearts. *Circulation Research*, 52(4), 442-450.

Kavinsky, C. J., Umeda, P. K., Levin, J. E., Sinha, A. M., Nigro, J. M., Jakovcic, S., & Rabinowitz, M. (1984). Analysis of cloned mRNA sequences encoding subfragment 2 and part of subfragment 1 of alpha-and beta-myosin heavy chains of rabbit heart. *Journal of Biological Chemistry*, 259(5), 2775-2781.

Kaplinsky, E., Ogawa, S., Balke, C. W., & Dreifus, L. S. (1979). Two periods of early ventricular arrhythmia in the canine acute myocardial infarction model. *Circulation*, *60*(2), 397-403.

Kohl, P., Hunter, P., & Noble, D. (1999). Stretch-induced changes in heart rate and rhythm: clinical observations, experiments and mathematical models. *Progress in biophysics and molecular biology*, *71*(1), 91-138.

Kleber, A. G., Janse, M. J., Wilms-Schopmann, F. J., Wilde, A. A., & Coronel, R. (1986). Changes in conduction velocity during acute ischemia in ventricular myocardium of the isolated porcine heart. *Circulation*, *73*(1), 189-198.

Lab, M. J. (1982). Contraction-excitation feedback in myocardium. Physiological basis and clinical relevance. *Circulation research*, *50*(6), 757.

Lee, P., Bollensdorff, C., Quinn, T. A., Wuskell, J. P., Loew, L. M., & Kohl, P. (2011). Single-sensor system for spatially resolved, continuous, and multiparametric optical mapping of cardiac tissue. *Heart Rhythm*, *8*(9), 1482-1491.

Lerman, B. B., Burkhoff, D., Yue, D. T., Franz, M. R., & Sagawa, K. (1985). Mechanoelectrical feedback: independent role of preload and contractility in modulation of canine ventricular excitability. *Journal of Clinical Investigation*, 76(5), 1843.

Langendorff, O. (1895). Untersuchungen am überlebenden Säugethierherzen. *Pflügers Archiv European Journal of Physiology*, 61(6), 291-332.

Lawrence, C. L., Pollard, C. E., Hammond, T. G., & Valentin, J. P. (2008). In vitro models of proarrhythmia. *British journal of pharmacology*, 154(7), 1516-1522.

Lee, J. C., Epstein, L. M., Huffer, L. L., Stevenson, W. G., Koplan, B. A., & Tedrow, U. B. (2009). ICD lead proarrhythmia cured by lead extraction. *Heart Rhythm*, 6(5), 613-618.

Lindsay, A. C., Wong, T., Segal, O., & Peters, N. S. (2006). An unusual twist: ventricular tachycardia induced by a loop in a right ventricular pacing wire. *QJM*, 99(5), 347-348.

Levine, J. H., Guarnieri, T. H. O. M. A. S., Kadish, A. H., White, R. I., Calkins, H. U. G. H., & Kan, J. S. (1988). Changes in myocardial repolarization in patients undergoing balloon valvuloplasty for congenital pulmonary stenosis: evidence for contraction-excitation feedback in humans. *Circulation*, 77(1), 70-77.

Langer, F., Rodriguez, F., Cheng, A., Ortiz, S., Harrington, K. B., Zasio, M. K., & Miller, D. C. (2007). Alterations in lateral left ventricular wall transmural strains during acute circumflex and anterior descending coronary occlusion. *The Annals of thoracic surgery*, 84(1), 51-60.

Lamont, C., & Eisner, D. A. (1996). The sarcolemmal mechanisms involved in the control of diastolic intracellular calcium in isolated rat cardiac trabeculae. *Pflügers Archiv*, 432(6), 961-969.

Liu, Y. B., Pak, H. N., Lamp, S. T., Okuyama, Y., Hayashi, H., Wu, T. J., & Lin, S. F. (2004). Coexistence of two types of ventricular fibrillation during acute regional ischemia in rabbit ventricle. *Journal of cardiovascular electrophysiology*, 15(12), 1433-1440.

Lee, H. C., Mohabir, R., Smith, N., Franz, M. R., & Clusin, W. T. (1988). Effect of ischemia on calcium-dependent fluorescence transients in rabbit hearts containing indo 1. Correlation with monophasic action potentials and contraction. *Circulation*, 78(4), 1047-1059.

Myerburg, R.J. (2014). Sudden Cardiac Death in Adults. In *Cardiac Electrophysiology: From Cell to Bedside* (pp. 981 - 991). Philadelphia, PA: Elsevier.

McDonald, T. F., Pelzer, S., Trautwein, W., & Pelzer, D. J. (1994). Regulation and modulation of calcium channels in cardiac, skeletal, and smooth muscle cells. *Physiological Reviews*, 74(2), 365.

Ming, Z., Nordin, C., & Aronson, R. S. (1994). Role of L-Type Calcium Channel Window Current in Generating Current-Induced Early Afterdepolarizations. *Journal of cardiovascular electrophysiology*, 5(4), 323-334.

Maroto, R., Raso, A., Wood, T. G., Kurosky, A., Martinac, B., & Hamill, O. P. (2005). TRPC1 forms the stretch-activated cation channel in vertebrate cells. *Nature cell biology*, 7(2), 179-185.

Maxwell, M. P., Hearse, D. J., & Yellon, D. M. (1987). Species variation in the coronary collateral circulation during regional myocardial ischaemia: a critical determinant of the rate of evolution and extent of myocardial infarction. *Cardiovascular research*, 21(10), 737-746.

Matiukas, A., Mitrea, B. G., Qin, M., Pertsov, A. M., Shvedko, A. G., Warren, M. D., & Loew, L. M. (2007). Near-infrared voltage-sensitive fluorescent dyes optimized for optical mapping in blood-perfused myocardium. *Heart Rhythm*, 4(11), 1441-1451.

Miura, M., Wakayama, Y., Endoh, H., Nakano, M., Sugai, Y., Hirose, M., & Shimokawa, H. (2008). Spatial non-uniformity of excitation–contraction coupling can enhance arrhythmogenic-delayed afterdepolarizations in rat cardiac muscle. *Cardiovascular research*.

Mattiazzi, A., Bassani, R. A., Escobar, A. L., Palomeque, J., Valverde, C. A., Petroff, M. V., & Bers, D. M. (2015). Chasing cardiac physiology and pathology down the CaMKII cascade. *American Journal of Physiology-Heart and Circulatory Physiology*, *308*(10), H1177-H1191.

Miura, M., Nishio, T., Hattori, T., Murai, N., Stuyvers, B. D., Shindoh, C., & Boyden, P. A. (2010). Effect of nonuniform muscle contraction on sustainability and frequency of triggered arrhythmias in rat cardiac muscle. *Circulation*, *121*(25), 2711-2717.

Milberg, P., Pott, C., Fink, M., Frommeyer, G., Matsuda, T., Baba, A., ... & Eckardt, L. (2008). Inhibition of the Na⁺/Ca²⁺ exchanger suppresses torsades de pointes in an intact heart model of long QT syndrome-2 and long QT syndrome-3. *Heart Rhythm*, *5*(10), 1444-1452.

Noma, A., & Tsuboi, N. (1987). Dependence of junctional conductance on proton, calcium and magnesium ions in cardiac paired cells of guinea-pig. *The Journal of Physiology*, 382(1), 193-211.

Nakano, A., Heusch, G., Cohen, M. V., & Downey, J. M. (2002). Preconditioning one myocardial region does not necessarily precondition the whole rabbit heart. *Basic research in cardiology*, 97(1), 35-39.

Nerbonne, J. M. (2000). Molecular basis of functional voltage-gated K⁺ channel diversity in the mammalian myocardium. *The Journal of Physiology*, 525(2), 285-298.

Nerbonne, J. M. (2004). Studying cardiac arrhythmias in the mouse—a reasonable model for probing mechanisms?. *Trends in cardiovascular medicine*, 14(3), 83-93.

Nattel, S., Duker, G., & Carlsson, L. (2008). Model systems for the discovery and development of antiarrhythmic drugs. *Progress in biophysics and molecular biology*, 98(2), 328-339.

Nakagawa, A., Arita, M., Shimada, T., & Shirabe, J. (1988). Effects of mechanical stretch on the membrane potential of guinea pig ventricular muscles. *The Japanese journal of physiology*, 38(6), 819-838.

Opthof, T., Sutton, P., Coronel, R., Wright, S., Kallis, P., & Taggart, P. (2012). The association of abnormal ventricular wall motion and increased dispersion of repolarization in humans is independent of the presence of myocardial infarction. *Frontiers in physiology*, 3.

Opthof, T. (2007). Embryological development of pacemaker hierarchy and membrane currents related to the function of the adult sinus node: implications for autonomic modulation of biopacemakers. In *Biopacemaking* (pp. 6-26). Springer Berlin Heidelberg.

Parker, K. K., Lavelle, J. A., Taylor, L. K., Wang, Z., & Hansen, D. E. (2004). Stretch-induced ventricular arrhythmias during acute ischemia and reperfusion. *Journal of Applied Physiology*, 97(1), 377-383.

Pogwizd, S. M., & Corr, P. B. (1987). Reentrant and nonreentrant mechanisms contribute to arrhythmogenesis during early myocardial ischemia: results using three-dimensional mapping. *Circulation Research*, 61(3), 352-371.

Piper, H. M., Siegmund, B., Ladilov, Y. V., & Schlüter, K. D. (1993). Calcium and sodium control in hypoxic-reoxygenated cardiomyocytes. *Basic research in cardiology*, 88(5), 471-482.

Pike, M. M., Luo, C. S., Clark, M. D., Kirk, K. A., Kitakaze, M., Madden, M. C., & Pohost, G. M. (1993). NMR measurements of Na⁺ and cellular energy in ischemic rat heart: role of Na⁺-H⁺ exchange. *American Journal of Physiology-Heart and Circulatory Physiology*, 265(6), H2017-H2026.

Philipson, K. D., Bersohn, M. M., & Nishimoto, A. Y. (1982). Effects of pH on Na⁺-Ca²⁺ exchange in canine cardiac sarcolemmal vesicles. *Circulation Research*, 50(2), 287-293.

Prod'hom, B., Pietrobon, D., & Hess, P. (1989). Interactions of protons with single open L-type calcium channels. Location of protonation site and dependence of proton-induced current fluctuations on concentration and species of permeant ion. *The Journal of general physiology*, 94(1), 23-42.

Panfilov, A. V. (2006). Is heart size a factor in ventricular fibrillation? Or how close are rabbit and human hearts?. *Heart Rhythm*, 3(7), 862-864.

Prosser, B. L., Ward, C. W., & Lederer, W. J. (2010). Subcellular Ca²⁺ signaling in the heart: the role of ryanodine receptor sensitivity. *The Journal of general physiology*, 136(2), 135-142.

Prosser, B. L., Ward, C. W., & Lederer, W. J. (2011). X-ROS signaling: rapid mechano-chemo transduction in heart. *Science*, 333(6048), 1440-1445.

Prosser, B. L., Ward, C. W., & Lederer, W. J. (2013). X-ROS signalling is enhanced and graded by cyclic cardiomyocyte stretch. *Cardiovascular research*, 98(2), 307-314.

Quinn, T. A. (2014). The importance of non-uniformities in mechano-electric coupling for ventricular arrhythmias. *Journal of Interventional Cardiac Electrophysiology*, 39(1), 25-35.

Quinn, T. A., & Kohl, P. (2011). Systems biology of the heart: hype or hope?. *Annals of the New York Academy of Sciences*, 1245(1), 40-43.

Quinn, T. A., Jin, H., & Kohl, P. (2011). Mechanically-induced premature ventricular excitation is mediated by cation non-selective stretch-activated channels and depends on the extent of local tissue deformation in isolated rabbit heart. *Circulation*, 124(21 Supplement), A13098.

Quan, W., & Rudy, Y. (1990). Unidirectional block and reentry of cardiac excitation: a model study. *Circulation research*, 66(2), 367-382.

Reed, A., Kohl, P., & Peyronnet, R. (2014). Molecular candidates for cardiac stretch-activated ion channels. *Global cardiology science & practice*, 2014(2), 9.

Rubart, M., & Zipes, D. P. (2005). Mechanisms of sudden cardiac death. *Journal of Clinical Investigation*, 115(9), 2305.

Ruknudin, A., Sachs, F., & Bustamante, J. O. (1993). Stretch-activated ion channels in tissue-cultured chick heart. *American Journal of Physiology-Heart and Circulatory Physiology*, 264(3), H960-H972.

Ridley, P. D., Yacoub, M. H., & Curtis, M. J. (1992). A modified model of global ischaemia: application to the study of syncytial mechanisms of arrhythmogenesis. *Cardiovasc Res*, 26(4), 309-315.

Reiter, M. J., Synhorst, D. P., & Mann, D. E. (1988). Electrophysiological effects of acute ventricular dilatation in the isolated rabbit heart. *Circulation Research*, 62(3), 554-562.

Sipido, K. R., Varro, A., & Eisner, D. (2006). Sodium calcium exchange as a target for antiarrhythmic therapy. In *Basis and Treatment of Cardiac Arrhythmias* (pp. 159-199). Springer Berlin Heidelberg.

Siogas, K., Pappas, S., Graekas, G., Goudevenos, J., Liapi, G., & Sideris, D. A. (1998). Segmental wall motion abnormalities alter vulnerability to ventricular ectopic beats associated with acute increases in aortic pressure in patients with underlying coronary artery disease. *Heart*, 79(3), 268-273.

Silverman, H. S. (1994). Ionic basis of ischaemic cardiac injury: insights from cellular studies. *Cardiovascular Research*, 28(5), 581-597.

Sukharev, S. I., Blount, P., Martinac, B., Blattner, F. R., & Kung, C. (1994). A large-conductance mechanosensitive channel in *E. coli* encoded by *mscL* alone. *Nature*, 368(6468), 265-268.

Smith, W. T., Fleet, W. F., Johnson, T. A., Engle, C. L., & Cascio, W. E. (1995). The Ib phase of ventricular arrhythmias in ischemic in situ porcine heart is related to changes in cell-to-cell electrical coupling. *Circulation*, 92(10), 3051-3060.

Shattock, M. J., & Matsuura, H. (1993). Measurement of Na⁺-K⁺ pump current in isolated rabbit ventricular myocytes using the whole-cell voltage-clamp technique. Inhibition of the pump by oxidant stress. *Circulation Research*, 72(1), 91-101.

Schaapherder, A. F. M., Schumacher, C. A., Coronel, R., & Fiolet, J. W. T. (1990). Transmural inhomogeneity of extracellular [K⁺] and pH and myocardial energy metabolism in the isolated rat heart during acute global ischemia; dependence on gaseous environment. *Basic research in cardiology*, 85(1), 33-44.

Statistics Canada. (2011c, October). Mortality, summary list of causes 2008.

Swynghedauw, B. (1986). Developmental and functional adaptation of contractile proteins in cardiac and skeletal muscles. *Physiol Rev*, 66(3), 710-771.

Stacy, G. P., Jobe, R. L., Taylor, L. K., & Hansen, D. E. (1992). Stretch-induced depolarizations as a trigger of arrhythmias in isolated canine left ventricles. *American Journal of Physiology-Heart and Circulatory Physiology*, 263(2), H613-H621.

Seo, K., Inagaki, M., Nishimura, S., Hidaka, I., Sugimachi, M., Hisada, T., & Sugiura, S. (2010). Structural heterogeneity in the ventricular wall plays a significant role in the initiation of stretch-induced arrhythmias in perfused rabbit right ventricular tissues and whole heart preparations. *Circulation research*, 106(1), 176-184.

Taggart, P., & Sutton, P. (2011). Termination of arrhythmias by haemodynamic unloading. *Cardiac Mechano-Electric Coupling and Arrhythmias*, 369.

ter Bekke, R. M., & Volders, P. G. (2012). Arrhythmogenic mechano-electric heterogeneity in the long-QT syndrome. *Progress in biophysics and molecular biology*, 110(2), 347-358.

Trapero, I., Chorro, F. J., Such-Miquel, L., Cánoves, J., Tormos, Á., Pelechano, F., ... & Such, L. (2008). Efectos de la estreptomicina en las modificaciones de la activación miocárdica durante la fibrilación ventricular inducidas por el estiramiento. *Revista española de cardiología*, 61(2), 201-205.

Theroux, P., Franklin, D., ROSS, J., & Kemper, W. S. (1974). Regional myocardial function during acute coronary artery occlusion and its modification by pharmacologic agents in the dog. *Circulation Research*, 35(6), 896-908.

Tranum-Jensen, J., Janse, M. J., Fiolet, W. T., Krieger, W. J., d'Alnoncourt, C. N., & Durrer, D. I. R. K. (1981). Tissue osmolality, cell swelling, and reperfusion in acute regional myocardial ischemia in the isolated porcine heart. *Circulation Research*, 49(2), 364-381.

Trafford, A. W., Diaz, M. E., Negretti, N., & Eisner, D. A. (1997). Enhanced Ca^{2+} current and decreased Ca^{2+} efflux restore sarcoplasmic reticulum Ca^{2+} content after depletion. *Circulation research*, 81(4), 477-484.

Tan, R. C., Osaka, T., & Joyner, R. W. (1991). Experimental model of effects on normal tissue of injury current from ischemic region. *Circulation research*, 69(4), 965-974.

Taggart, P., Sutton, P. M., Treasure, T., O'Brien, W., Runnalls, M., Swanton, R. H., & Emanuel, R. W. (1988). Monophasic action potentials at discontinuation of cardiopulmonary bypass: evidence for contraction-excitation feedback in man. *Circulation*, 77(6), 1266-1275.

ter Keurs, H. E., Shinozaki, T., Zhang, Y. M., Wakayama, Y., Sugai, Y., Kagaya, Y., ... & Landesberg, A. (2008). Sarcomere Mechanics in Uniform and Nonuniform Cardiac Muscle. *Annals of the New York Academy of Sciences*, 1123(1), 79-95.

Taggart, P., Sutton, P., John, R., & Swanton, H. (1992). Monophasic action potential recordings during acute changes in ventricular loading induced by the Valsalva manoeuvre. *British heart journal*, 67(3), 221-229.

Taggart, P., & Sutton, P. M. (1999). Cardiac mechano-electric feedback in man: clinical relevance. *Progress in biophysics and molecular biology*, 71(1), 139-154.

Toyo-oka, T., Kamishiro, T., Fumino, H., Masaki, T., & Hosoda, S. (1984). Rabbit hearts for the critical evaluation of drugs to reduce the size of experimentally produced acute myocardial infarction. *Japanese heart journal*, 25(4), 623-632.

ter Keurs, H. E., & Boyden, P. A. (2007). Calcium and arrhythmogenesis. *Physiological reviews*, 87(2), 457-506.

ter Keurs, H. E. (2011). Electromechanical coupling in the cardiac myocyte; stretch-arrhythmia feedback. *Pflügers Archiv-European Journal of Physiology*, 462(1), 165-175.

vanWagoner, D. R. (1993). Mechanosensitive gating of atrial ATP-sensitive potassium channels. *Circulation Research*, 72(5), 973-983.

Vermeulen, J. T., Mcguire, M. A., Opthof, T., Coronel, R., De Bakker, J. M., Klöpping, C., & Janse, M. J. (1994). Triggered activity and automaticity in ventricular trabeculae of failing human and rabbit hearts. *Cardiovascular research*, 28(10), 1547-1554.

Volders, P. G., Vos, M. A., Szabo, B., Sipido, K. R., de Groot, S. M., Gorgels, A. P., & Lazzara, R. (2000). Progress in the understanding of cardiac early afterdepolarizations and torsades de pointes: time to revise current concepts. *Cardiovascular research*, 46(3), 376-392.

Williams, G. S., Chikando, A. C., Tuan, H. T. M., Sobie, E. A., Lederer, W. J., & Jafri, M. S. (2011). Dynamics of calcium sparks and calcium leak in the heart. *Biophysical journal*, 101(6), 1287-1296.

White, E., Le Guennec, J. Y., Nigretto, J. M., Gannier, F., Argibay, J. A., & Garnier, D. (1993). The effects of increasing cell length on auxotonic contractions; membrane potential and intracellular calcium transients in single guinea-pig ventricular myocytes. *Experimental Physiology*, 78(1), 65-78.

Watson, R. M., Markle, D. R., Ro, Y. M., Goldstein, S. R., McGuire, D. A., Peterson, J. I., & Patterson, R. E. (1984). Transmural pH gradient in canine myocardial ischemia. *American Journal of Physiology-Heart and Circulatory Physiology*, 246(2), H232-H238.

Wilde, A. A., & Aksnes, G. (1995). Myocardial potassium loss and cell depolarisation in ischaemia and hypoxia. *Cardiovascular research*, 29(1), 1-15.

Wakayama, Y., Miura, M., Stuyvers, B. D., Boyden, P. A., & ter Keurs, H. E. (2005). Spatial nonuniformity of excitation–contraction coupling causes arrhythmogenic Ca²⁺ waves in rat cardiac muscle. *Circulation research*, 96(12), 1266-1273.

Wu, T. J., Lin, S. F., Hsieh, Y. C., Lin, T. C., Lin, J. C., & Ting, C. T. (2011). Pretreatment of BAPTA-AM Suppresses the Genesis of Repetitive Endocardial Focal Discharges and Pacing-Induced Ventricular Arrhythmia During Global Ischemia. *Journal of cardiovascular electrophysiology*, 22(10), 1154-1162.

Wengrowski, A. M., Kuzmiak-Glancy, S., Jaimes, R., & Kay, M. W. (2014). NADH changes during hypoxia, ischemia, and increased work differ between isolated heart preparations. *American Journal of Physiology-Heart and Circulatory Physiology*, 306(4), H529-H537.

Xiao, Y. F., Kang, J. X., Morgan, J. P., & Leaf, A. (1995). Blocking effects of polyunsaturated fatty acids on Na⁺ channels of neonatal rat ventricular myocytes. *Proceedings of the National Academy of Sciences*, 92(24), 11000-11004.

Xing, D., & Martins, J. B. (2004). Triggered activity due to delayed afterdepolarizations in sites of focal origin of ischemic ventricular tachycardia. *American Journal of Physiology-Heart and Circulatory Physiology*, 287(5), H2078-H2084.

Ytrehus, K., Liu, Y., Tsuchida, A., Miura, T., Liu, G. S., Yang, X. M., & Downey, J. M. (1994). Rat and rabbit heart infarction: effects of anesthesia, perfusate, risk zone, and method of infarct sizing. *American Journal of Physiology-Heart and Circulatory Physiology*, 267(6), H2383-H2390.

Yang, X. C., & Sachs, F. (1989). Block of stretch-activated ion channels in *Xenopus* oocytes by gadolinium and calcium ions. *Science*, 243(4894), 1068-1071.

Zeng, T., Bett, G. C., & Sachs, F. (2000). Stretch-activated whole cell currents in adult rat cardiac myocytes. *American Journal of Physiology-Heart and Circulatory Physiology*, 278(2), H548-H557.

APPENDIX: COPYRIGHT PERMISSIONS

6/28/2015

Rightslink Printable License

SPRINGER LICENSE TERMS AND CONDITIONS

Jun 28, 2015

This is a License Agreement between Tarek Lawen ("You") and Springer ("Springer") provided by Copyright Clearance Center ("CCC"). The license consists of your order details, the terms and conditions provided by Springer, and the payment terms and conditions.

All payments must be made in full to CCC. For payment instructions, please see information listed at the bottom of this form.

License Number	3657780600382
License date	Jun 28, 2015
Licensed content publisher	Springer
Licensed content publication	Journal of Interventional Cardiac Electrophysiology
Licensed content title	The importance of non-uniformities in mechano-electric coupling for ventricular arrhythmias
Licensed content author	T. Alexander Quinn
Licensed content date	Jan 1, 2013
Volume number	39
Issue number	1
Type of Use	Thesis/Dissertation
Portion	Figures
Author of this Springer article	No
Order reference number	None
Original figure numbers	Figure 1
Title of your thesis / dissertation	Mechanical Effects Contribute to Ventricular Arrhythmias during Acute Regional Ischemia in the Isolated Rabbit Heart
Expected completion date	Jul 2015
Estimated size(pages)	100
Total	0.00 USD

Terms and Conditions

Introduction

The publisher for this copyrighted material is Springer Science + Business Media. By clicking "accept" in connection with completing this licensing transaction, you agree that the following terms and conditions apply to this transaction (along with the Billing and Payment terms and conditions established by Copyright Clearance Center, Inc. ("CCC"), at the time that you opened your Rightslink account and that are available at any time at <http://myaccount.copyright.com>).

Limited License

With reference to your request to reprint in your thesis material on which Springer Science

<https://s100.copyright.com/App/PrintableLicenseFrame.jsp?publisherID=62&publisherName=Springer&publication=1383-875X&publicationID=6613&rightID=1...> 1/3

and Business Media control the copyright, permission is granted, free of charge, for the use indicated in your enquiry.

Licenses are for one-time use only with a maximum distribution equal to the number that you identified in the licensing process.

This License includes use in an electronic form, provided its password protected or on the university's intranet or repository, including UMI (according to the definition at the Sherpa website: <http://www.sherpa.ac.uk/romeo/>). For any other electronic use, please contact Springer at (permissions.dordrecht@springer.com or permissions.heidelberg@springer.com).

The material can only be used for the purpose of defending your thesis limited to university-use only. If the thesis is going to be published, permission needs to be re-obtained (selecting "book/textbook" as the type of use).

Although Springer holds copyright to the material and is entitled to negotiate on rights, this license is only valid, subject to a courtesy information to the author (address is given with the article/chapter) and provided it concerns original material which does not carry references to other sources (if material in question appears with credit to another source, authorization from that source is required as well).

Permission free of charge on this occasion does not prejudice any rights we might have to charge for reproduction of our copyrighted material in the future.

Altering/Modifying Material: Not Permitted

You may not alter or modify the material in any manner. Abbreviations, additions, deletions and/or any other alterations shall be made only with prior written authorization of the author(s) and/or Springer Science + Business Media. (Please contact Springer at (permissions.dordrecht@springer.com or permissions.heidelberg@springer.com))

Reservation of Rights

Springer Science + Business Media reserves all rights not specifically granted in the combination of (i) the license details provided by you and accepted in the course of this licensing transaction, (ii) these terms and conditions and (iii) CCC's Billing and Payment terms and conditions.

Copyright Notice:Disclaimer

You must include the following copyright and permission notice in connection with any reproduction of the licensed material: "Springer and the original publisher /journal title, volume, year of publication, page, chapter/article title, name(s) of author(s), figure number(s), original copyright notice) is given to the publication in which the material was originally published, by adding: with kind permission from Springer Science and Business Media"

Warranties: None

Example 1: Springer Science + Business Media makes no representations or warranties with respect to the licensed material.

Example 2: Springer Science + Business Media makes no representations or warranties with respect to the licensed material and adopts on its own behalf the limitations and disclaimers

established by CCC on its behalf in its Billing and Payment terms and conditions for this licensing transaction.

Indemnity

You hereby indemnify and agree to hold harmless Springer Science + Business Media and CCC, and their respective officers, directors, employees and agents, from and against any and all claims arising out of your use of the licensed material other than as specifically authorized pursuant to this license.

No Transfer of License

This license is personal to you and may not be sublicensed, assigned, or transferred by you to any other person without Springer Science + Business Media's written permission.

No Amendment Except in Writing

This license may not be amended except in a writing signed by both parties (or, in the case of Springer Science + Business Media, by CCC on Springer Science + Business Media's behalf).

Objection to Contrary Terms

Springer Science + Business Media hereby objects to any terms contained in any purchase order, acknowledgment, check endorsement or other writing prepared by you, which terms are inconsistent with these terms and conditions or CCC's Billing and Payment terms and conditions. These terms and conditions, together with CCC's Billing and Payment terms and conditions (which are incorporated herein), comprise the entire agreement between you and Springer Science + Business Media (and CCC) concerning this licensing transaction. In the event of any conflict between your obligations established by these terms and conditions and those established by CCC's Billing and Payment terms and conditions, these terms and conditions shall control.

Jurisdiction

All disputes that may arise in connection with this present License, or the breach thereof, shall be settled exclusively by arbitration, to be held in The Netherlands, in accordance with Dutch law, and to be conducted under the Rules of the 'Netherlands Arbitrage Instituut' (Netherlands Institute of Arbitration). *OR:*

All disputes that may arise in connection with this present License, or the breach thereof, shall be settled exclusively by arbitration, to be held in the Federal Republic of Germany, in accordance with German law.

Other terms and conditions:

v1.3

Questions? customercare@copyright.com or +1-855-239-3415 (toll free in the US) or +1-978-646-2777.

**ELSEVIER LICENSE
TERMS AND CONDITIONS**

Jun 29, 2015

This is a License Agreement between Tarek Lawen ("You") and Elsevier ("Elsevier") provided by Copyright Clearance Center ("CCC"). The license consists of your order details, the terms and conditions provided by Elsevier, and the payment terms and conditions.

All payments must be made in full to CCC. For payment instructions, please see information listed at the bottom of this form.

Supplier	Elsevier Limited The Boulevard, Langford Lane Kidlington, Oxford, OX5 1GB, UK
Registered Company Number	1982084
Customer name	Tarek Lawen
Customer address	5956 Bilton Lane Halifax, NS B3H4M3
License number	3658181372769
License date	Jun 28, 2015
Licensed content publisher	Elsevier
Licensed content publication	Journal of the American College of Cardiology
Licensed content title	Origin of ischemia-induced phase 1b ventricular arrhythmias in pig hearts
Licensed content author	Ruben Coronel, Francien J.G Wilms-Schopman, Joris R deGroot
Licensed content date	2 January 2002
Licensed content volume number	39
Licensed content issue number	1
Number of pages	11
Start Page	166
End Page	176
Type of Use	reuse in a thesis/dissertation
Portion	figures/tables/illustrations
Number of figures/tables/illustrations	All
Actual number of figures/tables/illustrations	11
Format	both print and electronic
Are you the author of this	No

Elsevier article?	
Will you be translating?	No
Original figure numbers	Figure 1, Figure 4
Title of your thesis/dissertation	Mechanical Effects Contribute to Ventricular Arrhythmias during Acute Regional Ischemia in the Isolated Rabbit Heart
Expected completion date	Jul 2015
Estimated size (number of pages)	
Elsevier VAT number	GB 494 6272 12
Permissions price	0.00 USD
VAT/Local Sales Tax	0.00 USD / 0.00 GBP
Total	0.00 USD
Terms and Conditions	

INTRODUCTION

1. The publisher for this copyrighted material is Elsevier. By clicking "accept" in connection with completing this licensing transaction, you agree that the following terms and conditions apply to this transaction (along with the Billing and Payment terms and conditions established by Copyright Clearance Center, Inc. ("CCC"), at the time that you opened your Rightslink account and that are available at any time at <http://myaccount.copyright.com>).

GENERAL TERMS

2. Elsevier hereby grants you permission to reproduce the aforementioned material subject to the terms and conditions indicated.

3. Acknowledgement: If any part of the material to be used (for example, figures) has appeared in our publication with credit or acknowledgement to another source, permission must also be sought from that source. If such permission is not obtained then that material may not be included in your publication/copies. Suitable acknowledgement to the source must be made, either as a footnote or in a reference list at the end of your publication, as follows:

"Reprinted from Publication title, Vol /edition number, Author(s), Title of article / title of chapter, Pages No., Copyright (Year), with permission from Elsevier [OR APPLICABLE SOCIETY COPYRIGHT OWNER]." Also Lancet special credit - "Reprinted from The Lancet, Vol. number, Author(s), Title of article, Pages No., Copyright (Year), with permission from Elsevier."

4. Reproduction of this material is confined to the purpose and/or media for which permission is hereby given.

5. Altering/Modifying Material: Not Permitted. However figures and illustrations may be altered/adapted minimally to serve your work. Any other abbreviations, additions, deletions and/or any other alterations shall be made only with prior written authorization of Elsevier Ltd. (Please contact Elsevier at permissions@elsevier.com)

6. If the permission fee for the requested use of our material is waived in this instance, please be advised that your future requests for Elsevier materials may attract a fee.
7. **Reservation of Rights:** Publisher reserves all rights not specifically granted in the combination of (i) the license details provided by you and accepted in the course of this licensing transaction, (ii) these terms and conditions and (iii) CCC's Billing and Payment terms and conditions.
8. **License Contingent Upon Payment:** While you may exercise the rights licensed immediately upon issuance of the license at the end of the licensing process for the transaction, provided that you have disclosed complete and accurate details of your proposed use, no license is finally effective unless and until full payment is received from you (either by publisher or by CCC) as provided in CCC's Billing and Payment terms and conditions. If full payment is not received on a timely basis, then any license preliminarily granted shall be deemed automatically revoked and shall be void as if never granted. Further, in the event that you breach any of these terms and conditions or any of CCC's Billing and Payment terms and conditions, the license is automatically revoked and shall be void as if never granted. Use of materials as described in a revoked license, as well as any use of the materials beyond the scope of an unrevoked license, may constitute copyright infringement and publisher reserves the right to take any and all action to protect its copyright in the materials.
9. **Warranties:** Publisher makes no representations or warranties with respect to the licensed material.
10. **Indemnity:** You hereby indemnify and agree to hold harmless publisher and CCC, and their respective officers, directors, employees and agents, from and against any and all claims arising out of your use of the licensed material other than as specifically authorized pursuant to this license.
11. **No Transfer of License:** This license is personal to you and may not be sublicensed, assigned, or transferred by you to any other person without publisher's written permission.
12. **No Amendment Except in Writing:** This license may not be amended except in a writing signed by both parties (or, in the case of publisher, by CCC on publisher's behalf).
13. **Objection to Contrary Terms:** Publisher hereby objects to any terms contained in any purchase order, acknowledgment, check endorsement or other writing prepared by you, which terms are inconsistent with these terms and conditions or CCC's Billing and Payment terms and conditions. These terms and conditions, together with CCC's Billing and Payment terms and conditions (which are incorporated herein), comprise the entire agreement between you and publisher (and CCC) concerning this licensing transaction. In the event of any conflict between your obligations established by these terms and conditions and those established by CCC's Billing and Payment terms and conditions, these terms and conditions shall control.
14. **Revocation:** Elsevier or Copyright Clearance Center may deny the permissions described in this License at their sole discretion, for any reason or no reason, with a full refund payable to you. Notice of such denial will be made using the contact information provided by you. Failure to receive such notice will not alter or invalidate the denial. In no event will Elsevier or Copyright Clearance Center be responsible or liable for any costs, expenses or damage incurred by you as a result of a denial of your permission request, other than a refund of the

amount(s) paid by you to Elsevier and/or Copyright Clearance Center for denied permissions.

LIMITED LICENSE

The following terms and conditions apply only to specific license types:

15. Translation: This permission is granted for non-exclusive world **English** rights only unless your license was granted for translation rights. If you licensed translation rights you may only translate this content into the languages you requested. A professional translator must perform all translations and reproduce the content word for word preserving the integrity of the article. If this license is to re-use 1 or 2 figures then permission is granted for non-exclusive world rights in all languages.

16. Posting licensed content on any Website: The following terms and conditions apply as follows: Licensing material from an Elsevier journal: All content posted to the web site must maintain the copyright information line on the bottom of each image; A hyper-text must be included to the Homepage of the journal from which you are licensing at <http://www.sciencedirect.com/science/journal/xxxxx> or the Elsevier homepage for books at <http://www.elsevier.com>; Central Storage: This license does not include permission for a scanned version of the material to be stored in a central repository such as that provided by Heron/XanEdu.

Licensing material from an Elsevier book: A hyper-text link must be included to the Elsevier homepage at <http://www.elsevier.com>. All content posted to the web site must maintain the copyright information line on the bottom of each image.

Posting licensed content on Electronic reserve: In addition to the above the following clauses are applicable: The web site must be password-protected and made available only to bona fide students registered on a relevant course. This permission is granted for 1 year only. You may obtain a new license for future website posting.

17. For journal authors: the following clauses are applicable in addition to the above:

Preprints:

A preprint is an author's own write-up of research results and analysis, it has not been peer-reviewed, nor has it had any other value added to it by a publisher (such as formatting, copyright, technical enhancement etc.).

Authors can share their preprints anywhere at any time. Preprints should not be added to or enhanced in any way in order to appear more like, or to substitute for, the final versions of articles however authors can update their preprints on arXiv or RePEc with their Accepted Author Manuscript (see below).

If accepted for publication, we encourage authors to link from the preprint to their formal publication via its DOI. Millions of researchers have access to the formal publications on ScienceDirect, and so links will help users to find, access, cite and use the best available version. Please note that Cell Press, The Lancet and some society-owned have different preprint policies. Information on these policies is available on the journal homepage.

Accepted Author Manuscripts: An accepted author manuscript is the manuscript of an article that has been accepted for publication and which typically includes author-incorporated changes suggested during submission, peer review and editor-author communications.

Authors can share their accepted author manuscript:

- immediately
 - o via their non-commercial person homepage or blog
 - o by updating a preprint in arXiv or RePEc with the accepted manuscript
 - o via their research institute or institutional repository for internal institutional uses or as part of an invitation-only research collaboration work-group
 - o directly by providing copies to their students or to research collaborators for their personal use
 - o for private scholarly sharing as part of an invitation-only work group on commercial sites with which Elsevier has an agreement
- after the embargo period
 - o via non-commercial hosting platforms such as their institutional repository
 - o via commercial sites with which Elsevier has an agreement

In all cases accepted manuscripts should:

- link to the formal publication via its DOI
- bear a CC-BY-NC-ND license - this is easy to do
- if aggregated with other manuscripts, for example in a repository or other site, be shared in alignment with our hosting policy not be added to or enhanced in any way to appear more like, or to substitute for, the published journal article.

Published journal article (JPA): A published journal article (PJA) is the definitive final record of published research that appears or will appear in the journal and embodies all value-adding publishing activities including peer review co-ordination, copy-editing, formatting, (if relevant) pagination and online enrichment.

Policies for sharing publishing journal articles differ for subscription and gold open access articles:

Subscription Articles: If you are an author, please share a link to your article rather than the full-text. Millions of researchers have access to the formal publications on ScienceDirect, and so links will help your users to find, access, cite, and use the best available version.

Theses and dissertations which contain embedded PJAs as part of the formal submission can be posted publicly by the awarding institution with DOI links back to the formal

publications on ScienceDirect.

If you are affiliated with a library that subscribes to ScienceDirect you have additional private sharing rights for others' research accessed under that agreement. This includes use for classroom teaching and internal training at the institution (including use in course packs and courseware programs), and inclusion of the article for grant funding purposes.

Gold Open Access Articles: May be shared according to the author-selected end-user license and should contain a [CrossMark logo](#), the end user license, and a DOI link to the formal publication on ScienceDirect.

Please refer to Elsevier's [posting policy](#) for further information.

18. For book authors the following clauses are applicable in addition to the above: Authors are permitted to place a brief summary of their work online only. You are not allowed to download and post the published electronic version of your chapter, nor may you scan the printed edition to create an electronic version. **Posting to a repository:** Authors are permitted to post a summary of their chapter only in their institution's repository.

19. Thesis/Dissertation: If your license is for use in a thesis/dissertation your thesis may be submitted to your institution in either print or electronic form. Should your thesis be published commercially, please reapply for permission. These requirements include permission for the Library and Archives of Canada to supply single copies, on demand, of the complete thesis and include permission for Proquest/UMI to supply single copies, on demand, of the complete thesis. Should your thesis be published commercially, please reapply for permission. Theses and dissertations which contain embedded PJAs as part of the formal submission can be posted publicly by the awarding institution with DOI links back to the formal publications on ScienceDirect.

Elsevier Open Access Terms and Conditions

You can publish open access with Elsevier in hundreds of open access journals or in nearly 2000 established subscription journals that support open access publishing. Permitted third party re-use of these open access articles is defined by the author's choice of Creative Commons user license. See our [open access license policy](#) for more information.

Terms & Conditions applicable to all Open Access articles published with Elsevier:

Any reuse of the article must not represent the author as endorsing the adaptation of the article nor should the article be modified in such a way as to damage the author's honour or reputation. If any changes have been made, such changes must be clearly indicated.

The author(s) must be appropriately credited and we ask that you include the end user license and a DOI link to the formal publication on ScienceDirect.

If any part of the material to be used (for example, figures) has appeared in our publication with credit or acknowledgement to another source it is the responsibility of the user to ensure their reuse complies with the terms and conditions determined by the rights holder.

Additional Terms & Conditions applicable to each Creative Commons user license:

CC BY: The CC-BY license allows users to copy, to create extracts, abstracts and new works from the Article, to alter and revise the Article and to make commercial use of the Article (including reuse and/or resale of the Article by commercial entities), provided the user gives appropriate credit (with a link to the formal publication through the relevant DOI), provides a link to the license, indicates if changes were made and the licensor is not represented as endorsing the use made of the work. The full details of the license are available at <http://creativecommons.org/licenses/by/4.0>.

CC BY NC SA: The CC BY-NC-SA license allows users to copy, to create extracts, abstracts and new works from the Article, to alter and revise the Article, provided this is not done for commercial purposes, and that the user gives appropriate credit (with a link to the formal publication through the relevant DOI), provides a link to the license, indicates if changes were made and the licensor is not represented as endorsing the use made of the work. Further, any new works must be made available on the same conditions. The full details of the license are available at <http://creativecommons.org/licenses/by-nc-sa/4.0>.

CC BY NC ND: The CC BY-NC-ND license allows users to copy and distribute the Article, provided this is not done for commercial purposes and further does not permit distribution of the Article if it is changed or edited in any way, and provided the user gives appropriate credit (with a link to the formal publication through the relevant DOI), provides a link to the license, and that the licensor is not represented as endorsing the use made of the work. The full details of the license are available at <http://creativecommons.org/licenses/by-nc-nd/4.0>. Any commercial reuse of Open Access articles published with a CC BY NC SA or CC BY NC ND license requires permission from Elsevier and will be subject to a fee.

Commercial reuse includes:

- Associating advertising with the full text of the Article
- Charging fees for document delivery or access
- Article aggregation
- Systematic distribution via e-mail lists or share buttons

Posting or linking by commercial companies for use by customers of those companies.

20. Other Conditions:

v1.7

Questions? customercare@copyright.com or +1-855-239-3415 (toll free in the US) or +1-978-646-2777.

**WOLTERS KLUWER HEALTH, INC. LICENSE
TERMS AND CONDITIONS**

Jun 28, 2015

This Agreement between Tarek Lawen ("You") and Wolters Kluwer Health, Inc. ("Wolters Kluwer Health, Inc.") consists of your license details and the terms and conditions provided by Wolters Kluwer Health, Inc. and Copyright Clearance Center.

License Number	3657780509681
License date	Jun 28, 2015
Licensed Content Publisher	Wolters Kluwer Health, Inc.
Licensed Content Publication	Circulation Research
Licensed Content Title	Mechanisms of Mechanically Induced Spontaneous Arrhythmias in Acute Regional Ischemia
Licensed Content Author	Xiao Jie, Viatcheslav Gurev, Natalia Trayanova
Licensed Content Date	Jan 8, 2010
Licensed Content Volume Number	106
Licensed Content Issue Number	1
Type of Use	Dissertation/Thesis
Requestor type	Individual
Portion	Figures/table/illustration
Number of figures/tables/illustrations	1
Figures/tables/illustrations used	Figure 7
Author of this Wolters Kluwer article	No
Title of your thesis / dissertation	Mechanical Effects Contribute to Ventricular Arrhythmias during Acute Regional Ischemia in the Isolated Rabbit Heart
Expected completion date	Jul 2015
Estimated size(pages)	100
Requestor Location	Tarek Lawen 5956 Bilton Lane Halifax, NS B3H4M3 Canada Attn: Tarek Lawen
Billing Type	Invoice
Billing Address	Tarek Lawen 5956 Bilton Lane

<https://s100.copyright.com/App/PrintableLicenseFrame.jsp?publisherID=130&publisherName=WoltersKluwer&publication=circresaha&publicationID=29511&r...> 1/4

Halifax, NS B3H4M3
 Canada
 Attn: Tarek Lawen

Total 0.00 USD

[Terms and Conditions](#)

Terms and conditions Wolters Kluwer Health

1. **Transfer of License:** Wolters Kluwer hereby grants you a non-exclusive license to reproduce this material for this purpose, and for no other use, subject to the conditions herein
2. **Credit Line:** A credit line will be prominently placed, wherever the material is reused and include: the author(s), title of article, title of journal, volume number, issue number and inclusive pages.
Where a journal is being published by a learned society, the details of that society must be included in the credit line.
 - i. **for Open access journals:**The following statement needs to be added when reprinting the material in Open Access journals only: "promotional and commercial use of the material in print, digital or mobile device format is prohibited without the permission from the publisher Wolters Kluwer Health. Please contact lwjournalpermissions@wolterskluwer.com for further information
3. **Exceptions:** In case of *Disease Colon Rectum, Plastic Reconstructive Surgery, The Green Journal, Critical care Medicine, Pediatric Critical Care Medicine, the American Heart Publications, the American Academy of Neurology* the following guideline applies: no drug/ trade name or logo can be included in the same page as the material re-used.
4. **Translations:** When requesting a permission to translate a full text article, Wolters Kluwer/ Lippincott Williams & Wilkins request to receive the pdf of the translated document. This disclaimer should be added at all times:
Wolters Kluwer Health and its Societies take no responsibility for the accuracy of the translation from the published English original and are not liable for any errors which may occur.
5. **Warranties** The requestor warrants that the material shall not be used in any manner which may be considered derogatory to the title, content, or authors of the material, or to Wolters Kluwer
6. **Indemnity:** You hereby indemnify and hold harmless Wolters Kluwer and their respective officers, directors, employees and agents, from and against any and all claims, costs, proceeding or demands arising out of your unauthorised use of the Licensed Material.
7. **Geographical Scope:** Permission granted is valid worldwide in the English language and the languages specified in your original request
8. Wolters Kluwer cannot supply the requestor with the original artwork or a "clean copy."
9. Permission is valid if the borrowed material is original to a Wolters Kluwer imprint (Lippincott-Raven Publishers, Williams & Wilkins, Lea & Febiger, Harwal, Rapid Science, Little Brown & Company, Harper & Row Medical, American Journal of Nursing Co, and Urban & Schwarzenberg)
10. **Termination of contract:** If you opt not to use the material requested above please notify RightsLink or Wolters Kluwer Health/ Lippincott Williams & Wilkins within 90 days of the original invoice date.
11. This permission does not apply to **images** that are credited to publications other than Wolters Kluwer journals. For images credited to non-Wolters Kluwer Health journal publications, you will need to obtain permission from the journal referenced in the figure or table legend or credit line before making any use of image(s) or table(s)
12. **Third party material:** Adaptations are protected by copyright, so if you would like to reuse material that we have adapted from another source, you will need not only our permission, but the permission of the rights holder of the original material. Similarly, if you want to reuse an adaptation of original LWW content that appears in another publishers work, you will need our permission and that of the next publisher. The adaptation should be credited as follows: Adapted with permission from Wolters Kluwer Health: Book author, title, year of

- publication or Journal name, article author, title, reference citation, year of publication.
13. **Altering or modifying material:** Please note that modification of text within figures or full-text article is strictly forbidden.
 14. Please note that articles in the **ahead-of-print stage** of publication can be cited and the content may be re-used by including the date of access and the unique DOI number. Any final changes in manuscripts will be made at the time of print publication and will be reflected in the final electronic issue. Disclaimer: Articles appearing in the Published Ahead-of-Print section have been peer-reviewed and accepted for publication in the relevant journal and posted online before print publication. Articles appearing as publish ahead-of-print may contain statements, opinions, and information that have errors in facts, figures, or interpretation. Accordingly, Lippincott Williams & Wilkins, the editors and authors and their respective employees are not responsible or liable for the use of any such inaccurate or misleading data, opinion or information contained in the articles in this section.
 15. **Duration of the license:**
 - i. Permission is granted for a one-time use only within 12 months from the date of this invoice. Rights herein do not apply to future reproductions, editors, revisions, or other derivative works. Once the 12-month term has expired, permission to renew must be submitted in writing.
 - ii. For content reused in another journal or book, in print or electronic format, the license is one-time use and lasts for the 1st edition of a book or for the life of the edition in case of journals.
 - iii. If your Permission Request is for use on a website (which is not a journal or a book), internet, intranet, or any publicly accessible site, you agree to remove the material from such site after 12 months or else renew your permission request.
 16. **Contingent on payment:** *While you may exercise the rights licensed immediately upon issuance of the license at the end of the licensing process for the transaction, provided that you have disclosed complete and accurate details of your proposed use, no license is finally effective unless and until full payment is received from you (either by publisher or by CCC) as provided in CCC's Billing and Payment terms and conditions. If full payment is not received on a timely basis, then any license preliminarily granted shall be deemed automatically revoked and shall be void as if never granted. Further, in the event that you breach any of these terms and conditions or any of CCC's Billing and Payment terms and conditions, the license is automatically revoked and shall be void as if never granted. Use of materials as described in a revoked license, as well as any use of the materials beyond the scope of an unrevoked license, may constitute copyright infringement and publisher reserves the right to take any and all action to protect its copyright in the materials.*
 17. **Waived permission fee:** If the permission fee for the requested use of our material has been waived in this instance, please be advised that your future requests for Wolters Kluwer materials may attract a fee on another occasion. Please always check with the Wolters Kluwer Permissions Team if in doubt lwjournalpermissions@wolterskluwer.com

For Books only:

18. 1. Permission is granted for a one time use only. Rights herein do not apply to future reproductions, editions, revisions, or other derivative works.

SPECIAL CASES:

1. **For STM Signatories only, as agreed as part of the STM Guidelines**

Any permission granted for a particular edition will apply also to subsequent editions and for editions in other languages, provided such editions are for the work as a whole in situ and does not involve the separate exploitation of the permitted illustrations or excerpts.

Please click [here](#) to view the STM guidelines.

v1.11

Questions? customercare@copyright.com or +1-855-239-3415 (toll free in the US) or +1-978-646-2777.

